

INSTITUTE OF SEISMOLOGY  
UNIVERSITY OF HELSINKI  
REPORT S-56

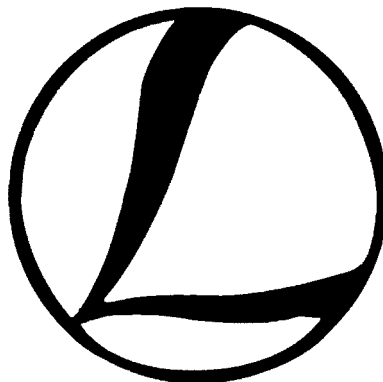
# LITHOSPHERE 2012

SEVENTH SYMPOSIUM ON  
THE STRUCTURE, COMPOSITION AND EVOLUTION  
OF THE LITHOSPHERE IN FINLAND

*PROGRAMME AND EXTENDED ABSTRACTS*

edited by

Ilmo Kukkonen, Emilia Kosonen, Kati Oinonen, Olav Eklund, Annakaisa Korja, Toivo Korja,  
Raimo Lahtinen, Juha Pekka Lunkka and Markku Poutanen



Geological Survey of Finland  
Espoo, November 6-8, 2012

Helsinki 2012

Editor-in-Chief: Pekka Heikkinen  
Guest Editors: Ilmo Kukkonen, Emilia Kosonen, Kati Oinonen, Olav Eklund,  
Annakaisa Korja, Toivo Korja, Raimo Lahtinen, Juha Pekka Lunkka  
and Markku Poutanen

Publisher: Institute of Seismology  
P.O. Box 68  
FI-00014 University of Helsinki  
Finland  
Phone: +358-9-1911 (switchboard)  
Fax: +358-9-191 51698  
<http://www.helsinki.fi/geo/seismo/>

ISSN 0357-3060  
ISBN 978-952-10-5066-4 (Paperback)  
Helsinki University Print  
Helsinki 2012  
ISBN 978-952-10-5067-1 (PDF)

# LITHOSPHERE 2012

## SEVENTH SYMPOSIUM ON THE STRUCTURE, COMPOSITION AND EVOLUTION OF THE LITHOSPHERE IN FINLAND

### *PROGRAMME AND EXTENDED ABSTRACTS*

Geological Survey of Finland,  
Espoo,  
November 6-8, 2012

#### **CONTRIBUTING ORGANIZATIONS**

Finnish National Committee of the International Lithosphere Programme (ILP)  
Finnish Geodetic Institute  
Geological Survey of Finland  
University of Helsinki  
University of Oulu  
Åbo Akademi University

#### **ORGANIZING COMMITTEE AND EDITORS**

Ilmo Kukkonen	Geological Survey of Finland P.O. B. 96, FI-02151 Espoo, Finland E-mail: ilmo.kukkonen [at] gtk.fi
Olav Eklund	Geology and mineralogy, Åbo Akademi University Domkyrkotorget 1, FI-20500 Åbo/Turku, Finland E-mail: olav eklund [at] abo.fi
Annakaisa Korja	Institute of Seismology, Dept. of Geosciences and Geography P.O.B. 68, FI-00014 University of Helsinki, Finland E-mail: annakaisa.korja [at] helsinki.fi
Toivo Korja	Department of Physics, University of Oulu P.O.B 3000, FI-90014 University of Oulu, Finland E-mail: toivo.korja [at] oulu.fi
Emilia Kosonen	Institute of Seismology, Dept. of Geosciences and Geography P.O.B. 68, FI-00014 University of Helsinki, Finland E-mail: emilia.kosonen [at] helsinki.fi
Raimo Lahtinen	Geological Survey of Finland P.O. B. 96, FI-02151 Espoo, Finland E-mail: raimo.lahtinen [at] gtk.fi
Juha Pekka Lunkka	Department of Geosciences P.O. Box 3000, FI-90014, University of Oulu E-mail: juha.pekka.lunkka [at] oulu.fi
Kati Oinonen	Institute of Seismology, Dept. of Geosciences and Geography P.O.B. 68, FI-00014 University of Helsinki, Finland E-mail: kati.oinonen [at] helsinki.fi
Markku Poutanen	Finnish Geodetic Institute Geodeetinrinne 2, FI-02430 Masala, Finland E-mail: markku.poutanen [at] fgi.fi

## References of Lithosphere Symposia Publications

- Pesonen, L.J., Korja, A. and Hjelt, S.-E., 2000 (Eds.).* Lithosphere 2000 - A Symposium on the Structure, Composition and Evolution of the Lithosphere in Finland. Programme and Extended Abstracts, Espoo, Finland, October 4-5, 2000. Institute of Seismology, University of Helsinki, Report S-41, 192 pages.
- Lahtinen, R., Korja, A., Arhe, K., Eklund, O., Hjelt, S.-E. and Pesonen, L.J., 2002 (Eds.).* Lithosphere 2002 – Second Symposium on the Structure, Composition and Evolution of the Lithosphere in Finland. Programme and Extended Abstracts, Espoo, Finland, November 12-13, 2002. Institute of Seismology, University of Helsinki, Report S-42, 146 pages.
- Ehlers, C., Korja A., Kruuna, A., Lahtinen, R. and Pesonen, L.J., 2004 (Eds.).* Lithosphere 2004 – Third Symposium on the Structure, Composition and Evolution of the Lithosphere in Finland. Programme and Extended Abstracts, November 10-11, 2004, Turku, Finland. Institute of Seismology, University of Helsinki, Report S-45, 131 pages.
- Kukkonen, I.T., Eklund, O., Korja, A., Korja, T., Pesonen, L.J. and Poutanen, M., 2006 (Eds.).* Lithosphere 2006 – Fourth Symposium on the Structure, Composition and Evolution of the Lithosphere in Finland. Programme and Extended Abstracts, Espoo, Finland, November 9-10, 2006. Institute of Seismology, University of Helsinki, Report S-46, 233 pages.
- Korja, T., Arhe, K., Kaikkonen, P., Korja, A., Lahtinen, R. and Lunkka, J.P., 2008 (Eds.).* Lithosphere 2008 – Fifth Symposium on the Structure, Composition and Evolution of the Lithosphere in Finland. Programme and Extended Abstracts, Oulu, Finland, November 5-6, 2008. Institute of Seismology, University of Helsinki, Report S-53, 132 pages.
- Heikkinen, P., Arhe, K., Korja, T., Lahtinen, R., Pesonen, L.J. and Rämö, T., 2010 (Eds.).* Lithosphere 2010 – Sixth Symposium on the Structure, Composition and Evolution of the Lithosphere in Finland. Programme and Extended Abstracts, Helsinki, Finland, October 27-28, 2010. Institute of Seismology, University of Helsinki, Report S-55, 154 pages.
- Kukkonen, I.T., Kosonen E.M., Oinonen, K., Eklund, O., Korja, A., Korja, T., Lahtinen, R., Lunkka, J.P. and Poutanen, M., 2012 (Eds.).* Lithosphere 2012 – Seventh Symposium on the Structure, Composition and Evolution of the Lithosphere in Finland. Programme and Extended Abstracts, Espoo, Finland, November 6-8, 2012. Institute of Seismology, University of Helsinki, S-56, 116 pages.

**Keywords** (GeoRef Thesaurus, AGI): lithosphere, crust, upper mantle, Fennoscandia, Finland, Precambrian, Baltic Shield, symposia

## TABLE OF CONTENTS

<b>PREFACE</b>	<b>ix</b>
<b>PROGRAMME</b>	<b>xi</b>
<b>EXTENDED ABSTRACTS</b>	<b>xv</b>
<i>R. Alviola.</i> Distribution of rare element pegmatites in Finland	1
<i>F. Chopin, A. Korja and P. Hölttä.</i> Tectonometamorphic evolution of the Bothian belt within the Svecofennian orogen - a case study for the building of a large dome in the Paleoproterozoic	5
<i>P. Eilu and K. Rasilainen.</i> Fennoscandian Neoarchaean–Palaeoproterozoic Ni and PGE metallogeny and supercontinent cycles	9
<i>O. Eklund and S. Fröjdö.</i> Petrology of an enriched gabbro in the Bothnian core complex	13
<i>J. Engström, A. Kärki and S. Paulamäki.</i> The polyphase ductile deformation at Olkiluoto, SW Finland	17
<i>S. Gradmann, J. Ebbing and J. Fullea.</i> Juxtaposed Lithospheres of Norway and Sweden – insights from 3D integrated geophysical modelling	21
<i>S. Heinonen, E. Koivisto, M. Heinonen and P. Heikkinen.</i> Seismic 3D modelling: case studies from Pyhäsalmi and Kevitsa, Finland	25
<i>N. Juhojuntti, S. Bergman and S. Olsson.</i> Crustal structure in the Kiruna district, northern Sweden: Preliminary results from a seismic reflection study	29
<i>J.V. Korhonen.</i> Indications of neotectonic movements at Swan Water (Joutenvesi) of the Saimaa Lake system	33
<i>A. Korja, P. Heikkinen, Y. Roslov and S. Mertanen.</i> North European Transect (NET) – Growth of Northern Europe in Supercontinent Cycles	35
<i>A. Korja, O.T. Rämö, O. Eklund, T. Korja, A. Kärki and P. Hölttä.</i> Evolution of the middle crust in Central Fennoscandia - MIDCRUST	39
<i>E. Kozlovskaya, L. Vinnik, G. Kosarev, S. Oreshin and POLENET/LAPNET Working Group.</i> Structure of the upper mantle in the northern Fennoscandian Shield obtained by joint inversion of POLENET/LAPNET P- and S- receiver functions	43
<i>I. Kukkonen, S. Heinonen, P. Heikkinen and P. Sorjonen-Ward.</i> Delineating ophiolite-derived host rocks of massive sulfide Cu-Co-Zn deposits with 2D high-resolution seismic reflection data in Outokumpu, Finland	45

<b>M. Kurhila, E. Suikkanen and A. Kotilainen.</b> Geochronology and isotopic characterization of the Vaasa complex in western Finland	47
<b>Y. Kähkönen and H. Huhma.</b> Revised U-Pb zircon ages of supracrustal rocks of the Paleoproterozoic Tampere Schist Belt, southern Finland	51
<b>A. Kärki, T. Korja, M. Mahmoud, M. Pirttijärvi, J. Tirronniemi, P. Tuisku and J. Woodard.</b> Structure of the Raahe –Ladoga Shear Complex	55
<b>E. Lanne.</b> Coda waves of local earthquakes: A case history from northern Finland	59
<b>E. Lehtonen, T. Halkoaho, P. Hölttä, H. Huhma, E. Luukkonen, E. Heilimo and A. Käpyaho.</b> Constraining the age and evolution of Archean greenstone belts in the Kuhmo and Suomussalmi areas, Finland	63
<b>K. Moisio and P. Kaikkonen.</b> Effective elastic thickness of the lithosphere in the seismic POLAR profile, Northern Finland	67
<b>K. Nikkilä and A. Korja.</b> Shearing in the northern part of the Central Finland granitoid complex	71
<b>K. Nikkilä, H. Koyi, A. Korja and O. Eklund.</b> Lateral flow in the middle crust– Experiments from the Svecofennian orogen	75
<b>T. F. Redfield, P.T. Osmundsen and B.W.H. Hendriks.</b> From the Gneiss Age to the Ice Age: Lithosphere, landscape, and the shaping of Fennoscandia	79
<b>O.T. Rämö, A. Kotilainen, M.A. Barnes, R. Michallik and C.G. Barnes.</b> Magmatic evolution of the Vaasa granite complex, western Finland: Preliminary constraints from <i>in situ</i> geochemistry of alkali feldspar megacrysts	83
<b>J. Salminen, S. Mertanen, D. Evans, and Z. Wang.</b> Paleomagnetic and geochemical studies of the Subjotnian Satakunta diabase dykes – implications to Mesoproterozoic supercontinent Nuna	87
<b>H. Silvennoinen, E. Kozlovskaya, E. Kissling and POLENET/LAPNET Working Group.</b> Structure of the upper mantle beneath the northern Fennoscandian Shield revealed by high-resolution teleseismic P-wave travelttime tomography	91
<b>D.B. Snyder, M. Hillier and B.A. Kjarsgaard.</b> 3-D structural model of the Slave craton mantle lithosphere, Northwest Territories, Canada	93
<b>A. Soesoo and S. Hade.</b> Geochemistry and age of some A-type granitoid rocks of Estonia	97
<b>M.B. Stephens and J. Andersson.</b> Contrasting orogenic systems in the Fennoscandian Shield, southern Sweden	101

- K. Vaittinen, T. Korja, M. Mahmoud, M. Pirttijärvi, M. Smirnov, I. Lahti and P. Kaikkonen.*** Vintage and retro conductivity models of the Bothnian Bay region: implications for the crustal structure and processes of the Svecofennian orogen 105
- I. Virshylo, G. Prodaivoda and E. Kozlovskaya.*** Method of joint inversion of velocity model and gravity data based on mineralogical composition 109
- D. M. Whipp, Jr., C. Beaumont and J. Braun.*** Feeding the ‘aneurysm’: Orogen-parallel mass transport into Nanga Parbat and the western Himalayan syntaxis 113



## PREFACE

The Finnish National committee of the International Lithosphere Programme (ILP) organises every second year the LITHOSPHERE symposium, which provides a forum for lithosphere researchers to present results and reviews as well as to inspire interdisciplinary discussions. The seventh symposium – LITHOSPHERE 2012 – comprises 38 presentations. The extended abstracts (in this volume) provide a good overview on current research on structure and processes of solid Earth. This time the symposium is intended also for contributions from neighboring countries, and we are very happy to receive a good number of colleagues from Sweden, Norway, Estonia, Ukraine and Canada.

The three-day symposium is hosted by the Geological Survey of Finland (GTK) and it will take place in Espoo at the Southern Finland Office of GTK in November 6-8, 2012. The participants will present their results in oral and poster sessions. Posters prepared by graduate or postgraduate students will be evaluated and the best one will be awarded. The invited talk is given by Dr. Tim Redfield from the Geological Survey of Norway.

This special volume “*LITHOSPHERE 2012*” contains the programme and extended abstracts of the symposium in alphabetical order.

Helsinki, October 19, 2012

Ilmo Kukkonen, Olav Eklund, Annakaisa Korja, Toivo Korja, Raimo Lahtinen,  
Juha Pekka Lunkka and Markku Poutanen

Lithosphere 2012 Organizing Committee



# LITHOSPHERE 2012 Symposium Programme

## Tuesday, November 6

- 09:00 - 10:00 Registration at the Geological Survey of Finland, Espoo, Sederholm Auditorium
- 10:00 - 10:05 Opening
- 10:05 - 11:50 Session 1: Lithosphere structure and evolution from upper crust to asthenosphere**  
Chair: Ilmo Kukkonen
- 10:05 - 10:50 **T. F. Redfield, P.T. Osmundsen and B.W.H. Hendriks [Invited]**  
From the Gneiss Age to the Ice Age: Lithosphere, landscape, and the shaping of Fennoscandia
- 10:50 - 11:20 **K. Vaittinen, T. Korja, M. Mahmoud, M. Pirttijärvi, M. Smirnov, I. Lahti and P. Kaikkonen**  
Vintage and retro conductivity models of the Bothnian Bay region: implications for the crustal structure and processes of the Svecofennian orogen
- 11:20 - 11:50 **D. M. Whipp, Jr., C. Beaumont and J. Braun**  
Feeding the 'aneurysm': Orogen - parallel mass transport into Nanga Parbat and the western Himalayan syntaxis
- 11:50 - 13:00 Lunch**
- 13:00 - 14:30 Session 2: Lithosphere structure and evolution from upper crust to asthenosphere (cont.)**  
Chair: Pekka Heikkinen
- 13:00 - 13:30 **E. Kozlovskaya, L. Vinnik, G. Kosarev, S. Oreshin and POLENET/LAPNET Working Group**  
Structure of the upper mantle in the northern Fennoscandian Shield obtained by joint inversion of POLENET/LAPNET P- and S- receiver functions
- 13:30 - 14:00 **K. Moisio and P. Kaikkonen**  
Effective elastic thickness of the lithosphere in the seismic POLAR profile, Northern Finland
- 14:00 - 14:30 **E. Lanne**  
Coda waves of local earthquakes: A case history from northern Finland
- 14:30 - 15:00 Coffee/Tea**

**15:00 - 16:30 Session 3: Lithosphere evolution, structures and mineral resources**

Chair: Raimo Lahtinen

- 15:00 - 15:30 **A. Kärki, T. Korja, M. Mahmoud, M. Pirttijärvi, J. Tirronniemi, P. Tuisku and J. Woodard**  
Structure of the Raahe –Ladoga Shear Complex
- 15:30 - 16:00 **J. Salminen, S. Mertanen, D. Evans, and Z. Wang**  
Paleomagnetic and geochemical studies of the Subjotnian Satakunta diabase dykes – implications to Mesoproterozoic supercontinent Nuna
- 16:00 - 16:30 **R. Alviola**  
Distribution of rare element pegmatites in Finland
- 16:30 - 17:00 **I. Kukkonen, S. Heinonen, P. Heikkinen and P. Sorjonen-Ward**  
Delineating ophiolite-derived host rocks of massive sulfide Cu-Co-Zn deposits with 2D high-resolution seismic reflection data in Outokumpu, Finland

**Wednesday, November 7****09:20 - 12:20 Session 4: Archaean and Proterozoic lithosphere evolution**

Chair: O. Eklund

- 09:20 - 09:50 **M.B. Stephens and J. Andersson**  
Contrasting orogenic systems in the Fennoscandian Shield, southern Sweden
- 09:50 - 10:20 **A. Korja, O.T. Rämö, O. Eklund, T. Korja, A. Kärki and P. Hölttä**  
Evolution of the middle crust in Central Fennoscandia - MIDCRUST
- 10:20 - 10:50 **K. Nikkilä, H. Koyi, A. Korja and O. Eklund**  
Lateral flow in the middle crust– Experiments from the Svecofennian orogen

**10:50- 11:20 Coffee/Tea**

- 11:20 - 11:50 **F. Chopin, A. Korja and P. Hölttä**  
Tectonometamorphic evolution of the Bothian belt within the Svecofennian orogen - a case study for the building of a large dome in the Paleoproterozoic
- 11:50 - 12:20 **M. Kurhila, E. Suikkanen and A. Kotilainen**  
Geochronology and isotopic characterization of the Vaasa complex in western Finland

**12:20 - 13:30 Lunch****13.30 - 17:00 Session 5: 3D and 4D modeling of lithosphere structures and evolution**

Chair: A. Korja

- 13:30 - 14:00 **S. Gradmann, J. Ebbing and J. Fullea**  
Juxtaposed Lithospheres of Norway and Sweden – insights from 3D integrated geophysical modelling
- 14:00 - 14:30 **S. Heinonen, E. Koivisto, M. Heinonen and P. Heikkinen**  
Seismic 3D modelling: case studies from Pyhäsalmi and Kevitsa, Finland

14:30 - 15:00 **N. Juhojuntti, S. Bergman and S. Olsson**  
Crustal structure in the Kiruna district, northern Sweden: Preliminary results from a seismic reflection study

**15:00 - 15:30 Coffee/tea**

15:30 - 16:00 **D.B. Snyder, M. Hillier and B.A. Kjarsgaard**  
3-D structural model of the Slave craton mantle lithosphere, Northwest Territories, Canada

16:00 - 16:30 **R. Lahtinen**  
Evolution history of the Norrbotten-Lapland boundary: preliminary results

**16:30 - 16:45 Session 6: Poster introductions**

Chair: M. Poutanen  
(2 min talks with two slides in the auditorium)

**16:45 - 19:30 Poster viewing and networking with refreshments**

- P01 **P. Eilu and K. Rasilainen**  
Fennoscandian Neoproterozoic–Palaeoproterozoic Ni and PGE metallogeny and supercontinent cycles
- P02 **J. V. Korhonen**  
Indications of neotectonic movements at Swan Water (Joutenvesi) of the Saimaa Lake system
- P03 **A. Korja, P. Heikkinen, Y. Roslov and S. Mertanen**  
North European Transect (NET) – Growth of Northern Europe in Supercontinent Cycles
- P04 **E. Lehtonen, T. Halkoaho, P. Hölttä, H. Huhma, E. Luukkonen, E. Heilimo and A. Käpyaho**  
Constraining the age and evolution of Archean greenstone belts in the Kuhmo and Suomussalmi areas, Finland
- P05 **K. Nikkilä and A. Korja**  
Shearing in the northern part of the Central Finland granitoid complex
- P06 **H. Silvennoinen, E. Kozlovskaya, E. Kissling and POLENET/LAPNET Working Group**  
Structure of the upper mantle beneath the northern Fennoscandian Shield revealed by high-resolution teleseismic P-wave traveltimes tomography
- P07 **I. Virshylo, G. Prodaivoda and E. Kozlovskaya**  
Method of joint inversion of velocity model and gravity data based on mineralogical composition

## Thursday, November 8

### 9:20 - 12:20 Session 7: Archaean and Proterozoic lithosphere evolution (cont.)

Chair: I. Kukkonen

9:20 - 9:50 **O.T. Rämö, A. Kotilainen, M.A. Barnes, R. Michallik and C.G. Barnes**  
Magmatic evolution of the Vaasa granite complex, western Finland:  
Preliminary constraints from *in situ* geochemistry of alkali feldspar megacrysts

9:50 - 10:20 **O. Eklund and S. Fröjdö**  
Petrology of an enriched gabbro in the Bothnian core complex

10:20 - 10:50 **J. Engström, A. Kärki and S. Paulamäki**  
The polyphase ductile deformation at Olkiluoto, SW Finland

### 10:50- 11:20 Coffee/Tea

11:20 - 11:50 **Y. Kähkönen and H. Huhma**  
Revised U-Pb zircon ages of supracrustal rocks of the Paleoproterozoic  
Tampere Schist Belt, southern Finland

11:50 - 12:20 **A. Soesoo and S. Hade**  
Geochemistry and age of some A-type granitoid rocks of Estonia

### 12:20 - 13:20 Lunch

### 13:20 - 15:30 Session 8: Other lithospheric topics: Neotectonics, scientific drilling projects, short communications

Chair: J.P. Lunkka

13:20 - 13:50 **I. Kukkonen and R. Sutinen**  
Ruokojärvi postglacial fault, northern Finland – A recent trenching study

13:50 - 14:05 **J. V. Korhonen**  
Indications of neotectonic movements at Swan Water (Joutenvesi) of the  
Saimaa Lake system

14:05 - 14:20 **M. Poutanen**  
Future of DYNAQLIM

14:20 - 14:35 **T. Rämö**  
Short communication on a new project "Magma dynamics and crystallization  
of A-type granite magma chambers as revealed by *in situ* isotopic and  
elemental geochemical analysis of feldspar megacrysts"

14:35 - 14:50 **J. Virtasalo**  
IODP Expedition 347 - Baltic Sea Paleoenvironment

14:50 - 15:05 **I. Kukkonen, M.V.S. Ask and O. Olesen**  
Current status of the ICPD drilling proposal DAFNE – Drilling Active Faults  
in Northern Europe

### 15:05- 15:30 Final discussions and poster award

Chair: Ilmo Kukkonen

## **EXTENDED ABSTRACTS**



## Distribution of rare element pegmatites in Finland

R. Alviola

E-mail: reijo.alviola [at] kolumbus.fi

About 50 rare element pegmatite groups are known in Finland. Most of them are pegmatites of LCT family, 10 of them belong to NYF family and 6 of them are classified as mixed family pegmatites. LCT pegmatites are located two major schist areas, in the schist belts of Southern Finland and in the Pohjanmaa schist belt to Kainuu belt. The NYF pegmatites are hosted by rapakivi granites or the Central Finland Granitoid Complex. Northern Finland is very poor in pegmatites.

**Keywords:** rare element pegmatites, distribution, Finland

### 1. Basics terms

**Pegmatite** is an essentially igneous rock and commonly granitic in composition. It is usually coarse-grained or very coarse-grained, but the grain-size is often very variable. Pegmatites occur as dykes, lenticular nodes and bulbous or irregular bodies, usually with sharp contacts to their igneous or metamorphic host-rocks.

According to Vlasov (1966) abundance of the **rare-elements** in Earth's crust is only 0.126 %. Six most common rare-elements make altogether 76 % of the rare elements leaving only 24 % for the remaining thirty one rare elements.

### 2. Main geological classes of granitic pegmatites

Based on P-T conditions that characterize the host-rock suites and represent the maximal estimates during pegmatite emplacement four main **classes** of granitic pegmatites are distinguished (Fig. 1).

Pegmatites of the **abyssal class** are according to Černý (1991) most commonly segregations of anatectic leucosome. Mineralization is commonly sparse.

Pegmatites of **muscovite class** are usually generated directly by partial melting, Černý and Ercit (2005). These pegmatites are typically barren, but some discordant pegmatites may show minor REE-type or Li-type mineralization.

**Rare-element class** pegmatites are generated by differentiation from granitic plutons and emplaced at intermediate to shallow depth, Černý and Ercit (2005). This class is most investigated, best known and economically most important class of pegmatites. These pegmatites include economically interesting REE- or Li-, Be-, Nb, Ta- and Sn- mineralizations.

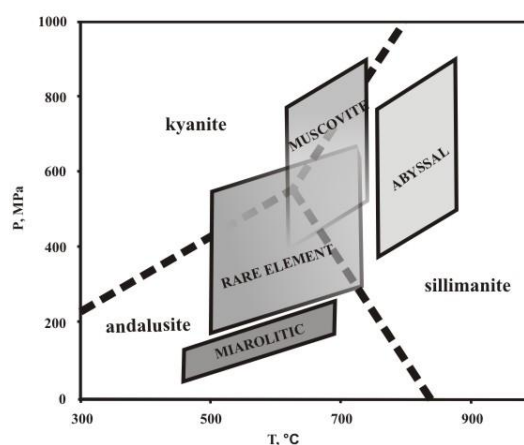


**Figure 1.** P-T diagram showing the fields of the four main classes of granitic pegmatites. Simplified from London (2008).

Pegmatites of **miarolitic class** are shallow seated with elevated contents of primary cavities. Geochemical signature is similar to rare-element class, but more diversified and the pegmatites are often of pocket size. Miarolitic pegmatites are important sources of gem material.

### 3. Petrogenetic families of granitic pegmatites

The concept of **pegmatite families** deals not only with the pegmatites, but with their parental granites. Therefore it is currently applicable only to pegmatites of rare-element and miarolitic classes. According to Černý and Ercit (2005) there are three pegmatite families:

- **NYF family** is marked with typical elements **Nb>Ta, Ti, Y, Sc, REE, Zr, U, Th and F**. The parent granites are mainly subaluminous ( $A/CNK=1$ ) to metaluminous ( $A/CNK<1, A/NK>1$ ) A- to I-types.
- **LCT family** typically carries, and gets progressively enriched in, **Li, Rb, Cs, Be, Sn, Ta, Nb (Ta>Nb)**. The parent granites are peraluminous of S, I or mixed S+I-type.
- **Mixed NYF+LCT** family granites and pegmatites show mixed geochemical and mineralogical characteristics.

### 4. Distribution of rare element pegmatites in Finland

About 50 rare element pegmatite groups are currently known in Finland (Fig. 2). Ten of them are supposed to belong to the NYF family. Majority of the pegmatite groups, 37, are LCT pegmatites and perhaps 6 groups are of mixed LCT+NYF family.

Five NYF pegmatite groups are hosted by rapakivi granites of Wiborg, Vehmaa or Fjälskär intrusion. Three NYF pegmatite groups are located inside the Central Finland Granitoid Complex and one NYF group is inside or in the vicinity of Otanmäki granite.

Majority of the LCT and mixed pegmatite groups (19 groups) in Southern Finland are located in the schist belt of Southern Finland Granitoid Zone, and its continuation, reaching from Kemiö to Tohmajärvi. Another accumulation of LCT pegmatite groups (14 groups) is going along and across schist belts between Haapaluoma and Puolanka/Kajaani. In Northern Finland very few rare element pegmatites are known. Pello and Posio seem to be of a mixed family nature.

**Age distribution** of Finnish rare element pegmatites seems to be so far rather simple:

- NYF pegmatites in the Central Finland Granitoid Complex are about 1865 Ma (Töysä) of age
- based on about ten radiometric U-Pb datings the LCT pegmatites in Southern Finland and Ostrobothnia-Kajaani area are 1789-1813 Ma of age
- pegmatites hosted in rapakivi granites are the youngest ones, eg. Luumäki dike in Wiborg area is about 1628 Ma of age.

### References:

- Černý, P., 1991. Rare-element granitic pegmatites. Part I, Anatomy and internal evolution of pegmatite deposits. *Geoscience Canada* 18, 49-67.
- Černý, P. and Ercit, T.S., 2005. The classification of granitic pegmatites revisited. *Canadian Mineralogist*, 43, 2005-2026.
- London, D., 2008. Pegmatites. *Canadian Mineralogist*, Special Publication 10, 347 p.
- Vlasov, K.A., editor, 1964. Geochemistry and mineralogy of rare elements and genetic types of their deposits. Vol. 1, Translated from Russia by Israel Program for Scientific translations, Jerusalem, 688 p.

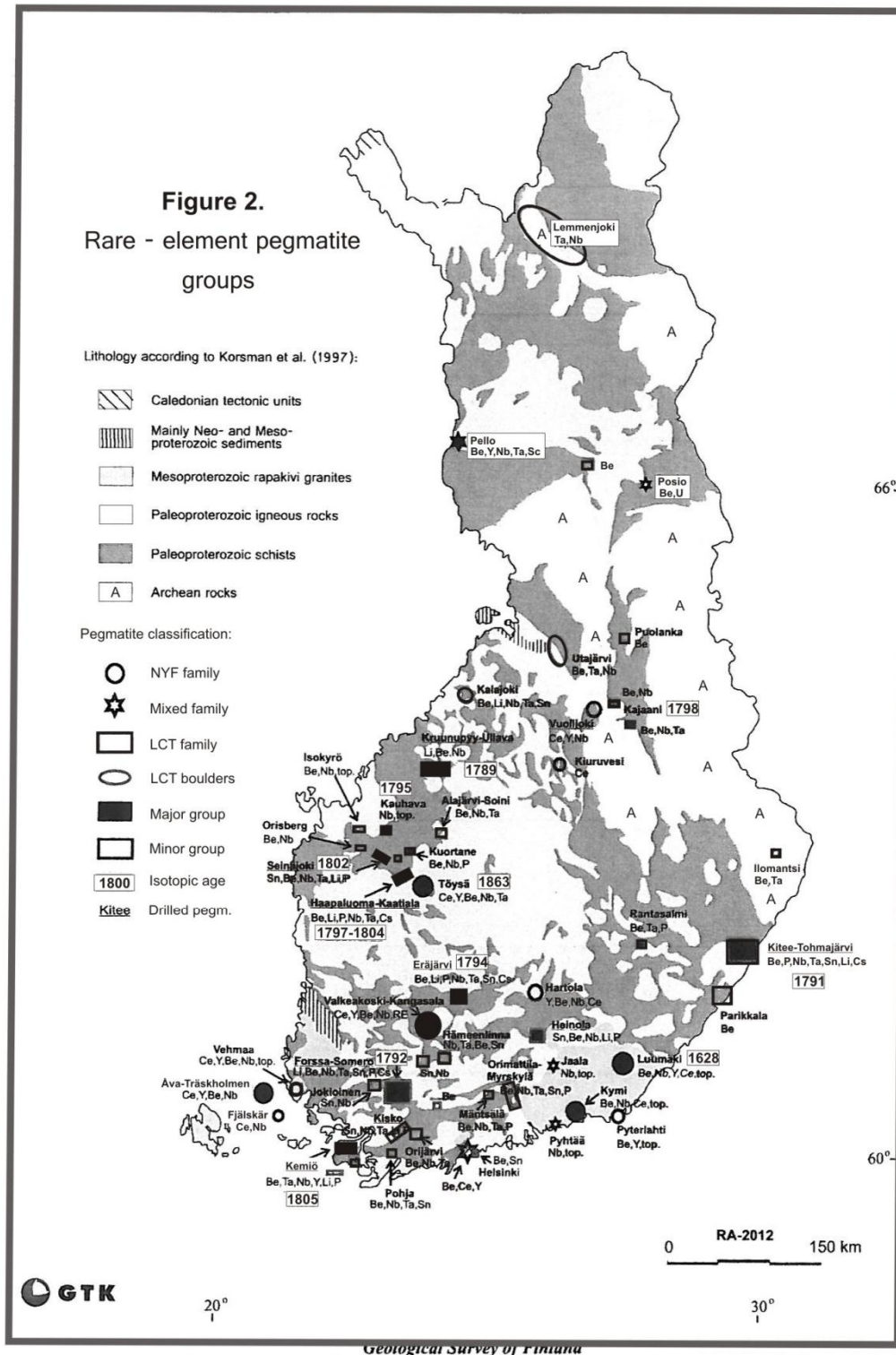


Figure 2. Rare element pegmatite groups in Finland.



# Tectonometamorphic evolution of the Bothian belt within the Svecofennian orogen - a case study for the building of a large dome in the Paleoproterozoic

F. Chopin<sup>1</sup>, A. Korja<sup>1</sup> and P. Hölttä<sup>2</sup>

<sup>1</sup> Department of Geosciences and Geography, University of Helsinki, Finland

<sup>2</sup> Geological Survey of Finland, Finland

E-mail: francis.chopin [at] helsinki.fi

We present here our first results about the tectonometamorphic evolution of the Bothian belt forming the mantle of the Vaasa Dome in the Svecofennian orogeny. In the eastern mantle part of the dome, a general N-S shortening, associated with HT metamorphism increasing toward its core is describe whereas N-S trending shear zones delimiting this mantle zone are discussed.

**Keywords:** middle crust, high grade metamorphism, orogenic dome, Vaasa Dome, Svecofennian orogen, Paleoproterozoic, Northern Europe

## 1. Introduction

Dome structures are present in most orogenies from Archean to Phanerozoic time. They are cored by granitoids to high-grade rocks and mantled by lower grade metamorphic rocks. The evolution of this kind of structure displays the thermal evolution of the orogenic continental crust and its complex rheological behavior in various tectonic setting (e.g. Burg et al., 2004; Witney et al., 2004; Rey et al., 2009). Their study permit to understand the complex relation between orogenic supra- and infrastructure levels (Culshaw et al., 2006). This study focuses on the tectonometamorphic evolution of the Paleoproterozoic Bothian Belt situated in the central part of the Svecofennian orogen, Fennoscandian Shield (e.g. Korja et al, 2009).

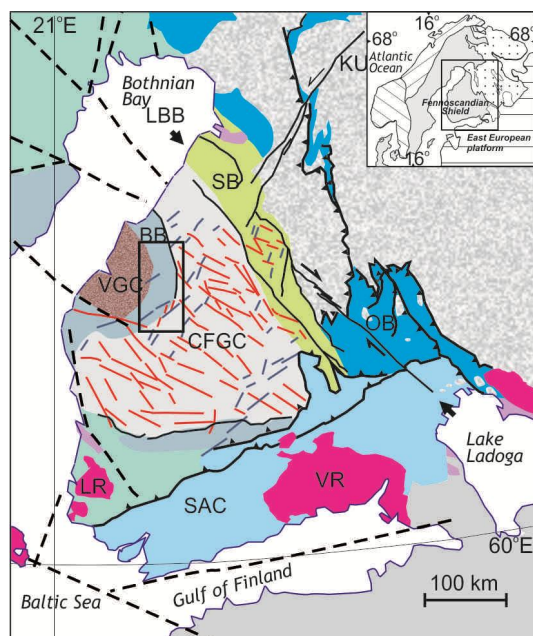


**Figure 1.** Bothnian Belt and Vaasa Granitoid Complex is situated in the Central part of the Svecofennian orogen, Fennoscandian Shield, Northern Europe. Tectonic map is after Korja et al., 2009. The major tectonic units are: VGC, Vaasa Granitoid Complex; BB, Bothnian Belt; CFGC; OB, Outokumpu Belt; SAC, Southern Finland Arc Complex; SB, Savo Belt; TB, Tampere Belt.

## **2. Geological background**

The Vaasa Dome is made of a granitoid core (the Vaasa Granitoid Complex), which is mantled by the metamorphic Bothnian Belt (Korsman et al., 1997; Vaarma and Pipping, 1997, 2003; Mäkitie, 2001; Lehtonen et al., 2005; Sipilä et al., 2008). It is in contact with the Central Finland Granitoid Complex to east. Metamorphic ages from the Bothnian Belt (c. 1.88–1.86 Ga, e.g. Williams et al., 2008) shows younger ages compared to the granitoid rocks from the Central Finland Granitoid Complex. The Bouguer and aeromagnetic data as well as the seismic profiles are in agreement with a domal architecture (Korja et al., 2009, Valtonen et al., 2011).

## **3. Preliminary studies of the tectonometamorphic evolution of the Bothnian belt**

This study focused on the western part of the the Vaasa Dome. In the mantle zone, the Bothian Belt exposes HT metamorphic rocks with increasing metamorphic grade from low amphibolite facies to high grade diatexite (metasediments, metavolcanites) towards the core of the dome. They are intruded by numerous syn- to late stage granitoids/pegmatites. The core of the Vaasa Dome exposes mainly granitoids with few relics of metamorphic rocks in its eastern parts similar to those present within the Bothian Belt.

A detailed field study has revealed complex tectonometamorphic evolution of the dome. The tectonic contact between the Vaasa Dome and the Central Finland Granitoid Complex is a N–S directed steeply dipping shear zone whose kinematics is uncertain. Nevertheless, we suggest a general uplift of the whole western Vaasa Dome. Close to the tectonic contact/shear zone, the Bothian Belt (mantle zone) suffered a first tectonometamorphic event increasing from east to west. Where preserved, the first metamorphic foliation is roughly moderately to flat lying. It records generally only low amphibolites facies metamorphism in eastern most part, whereas a first stage of melting is present closer to the western core.

The second tectonometamorphic event is causing N–S to NNW–SSE directed shortening and results in the formation of E–W to WSW–ENE trending steep axial planar cleavage to pervasive, subvertical new foliation. The intensity of this deformation seems to increase as we approach granitoid dome core in the west. At first order, the grade of metamorphism increases also in the same direction: i.e. from low amphibolites facies to metatexite/diatexite with more syn-tectonic granitoids within the Bothian Belt as closer to the core.

Late deformation has localized at the boundary between the Bothian Belt and the granitic core of the dome. Within the boundary zone, the intense deformation of soft high-grade metatexite to diatexite produces a NNW–SSE striking sub-vertical shear zone. In the core of the dome, some syntectonic intrusions show sub-horizontal direction of flow close to this contact, but a minor vertical component could be also present. A careful study is warranted for a better understanding of their kinematics.

Late to post- tectonic pegmatites and granitoids are widespread in the whole massif.

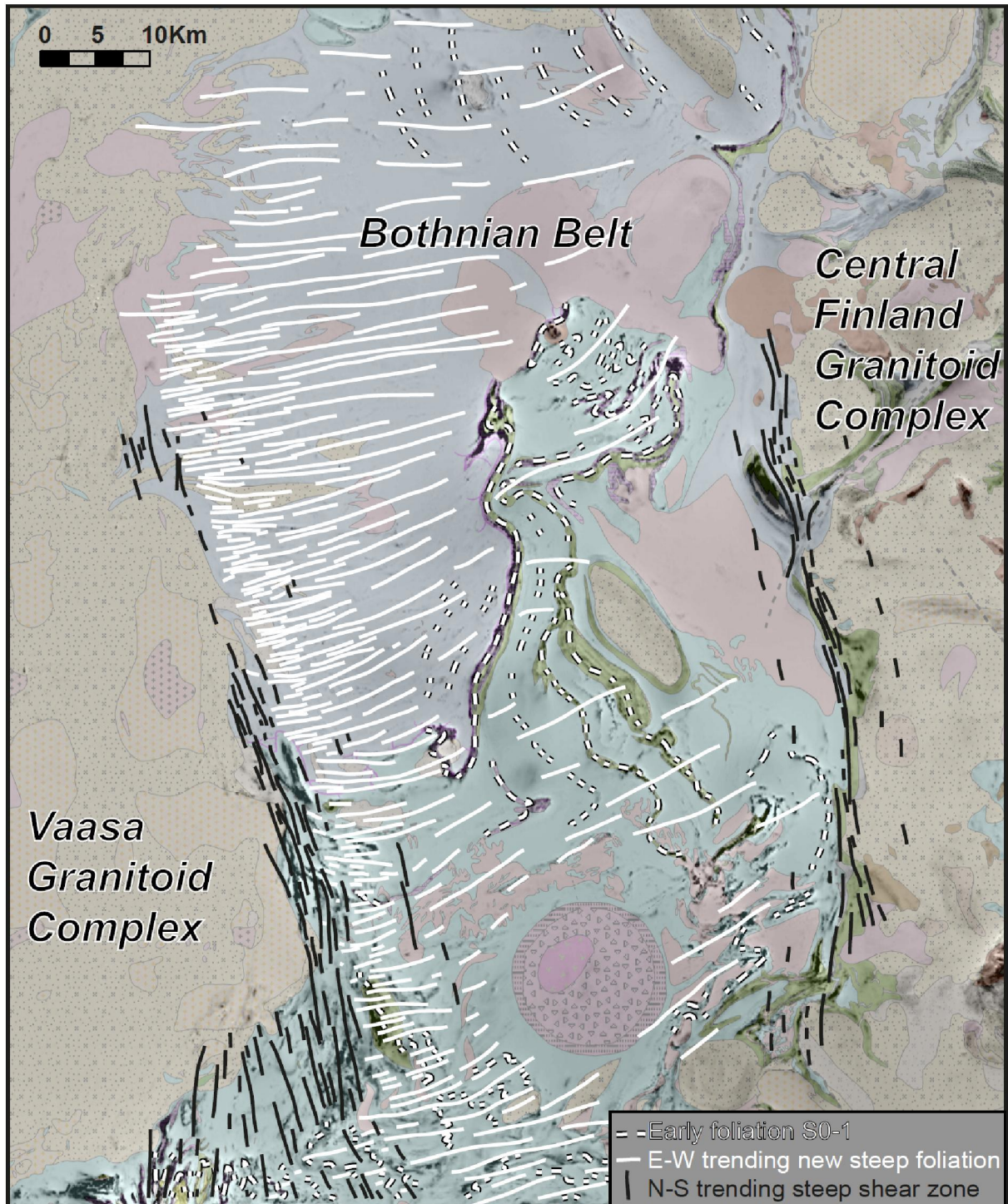


**Figure 2.** First order structural map of the Bothnian Belt. See location in Figure 1. Background: 1:200000 bedrock maps compiled by the Geological Survey of Finland and aeromagnetic map (courtesy to GTK).

#### 4. Discussion

We suggest to use the core and mantle terminology for this dome, which is neutral regarding the tectonic interpretation, rather than core complex which means dome made by extension. This core and mantle structure could reflect contrasting orogenic infra- to suprastructure exposure.

In the future we will propose a geodynamic model to the formation of this Paleoproterozoic dome based on additional field studies, quantitative microstructural and metamorphic petrology that will be combined with other ongoing MIDCRUST studies (e.g. magmatic petrology, geochronology, geophysics). It will give a new opportunity to understand flow of infrastructure in large hot orogen (Vanderhaeghe and Teyssier 2001; Andersen and Rämö, 2007; Chardon et al., 2009; Maierová et al., 2012).

#### References:

- Andersen, T. and Rämö, O.T., 2007. Granites and Crustal Anatexis, Special Issue. *Lithos*, 93(3–4), 215–339.
- Burg, J.-P., Kaus, B. J. P. and Podladchikov, Y. Y., 2004. Dome structures in collision orogens: Mechanical investigation of the gravity/compression interplay. *Geological Society of America Special Papers*, 380, 47–66.
- Chardon, D., Gapais, D. and Cagnard, F., 2009. Flow of ultra-hot orogens: A view from the Precambrian, clues for the Phanerozoic. *Tectonophysics*, 477, 105–118.
- Culshaw, N. G., Beaumont, C. and Jamieson, R. A., 2006. The orogenic superstructure-infrastructure concept; revisited, quantified, and revived. *Geology*, 34, 733–736.
- Korja, A., Kosunen, P. and Heikkinen, P.J., 2009. A Case Study of Lateral Spreading the Precambrian Svecofennian Orogen In: Ring, U. and Wernicke, B. *Extending a Continent: Architecture, Rheology and Heat Budget*. Geological Society of London, Special Paper, 321, 225–251. DOI: 10.1144/SP321.11
- Korsman, K., Koistinen, T., Kohonen, J., Wennerström, M., Ekdahl, E., Honkano, M., Idman, H. and Pekkula, Y. (Eds.), 1997. *Bedrock map of Finland, 1:1 000 000*. Geological Survey of Finland, Espoo, Finland.
- Lehtonen, M.I., Kujala, H., Kärkkäinen, N., Lehtonen, A., Mäkitie, H., Mänttari, I., Virransalo, P. and Vuokko, J., 2005. Pre-Quaternary rocks of the South Ostrobothnian Schist Belt. Geological Survey of Finland, Rep. 158. 155 p. + 1 app. map
- Maierová, P., Lexa, O., Schulmann, K. and Štípská, P., 2012. Contrasting tectonic and metamorphic evolution of orogenic lower crust in the Bohemian Massif: A numerical model, *Gondwana Research*, in press, DOI: 10.1016/j.gr.2012.08.020
- Mäkitie, H., 2001. Eastern margin of the Vaasa Migmatite Complex, Kauhava, western Finland: preliminary petrography and geochemistry of the diatexites. *Bulletin of the Geological Society of Finland*, 73(1–2), 35–46.
- Rey, P.F., Teyssier, C. and Whitney, D.L., 2009. Extension rates, crustal melting, and core complex dynamics. *Geology*, 37(5), 391–394.
- Sipilä, P., Kujala, H., Torssonen, M., Mäkitie, H. and Väisänen, M., 2008. *Bedrock map of the Oravainen-Lapua-Alahärmä area*. Geological Survey of Finland. Electronic publication.
- Vaarma, M. and Pipping, F., 1997. Pre-Quaternary rocks of the Alajärvi and Evijärvi map-sheet areas. 2313 ja 2314. 1:100 000. Geological Survey of Finland, 83 p.
- Vaarma, M. and Pipping, F., 2003. Pre-Quaternary rocks of the Kyyjärvi and Perho map-sheet areas. 2331 ja 2332. 1:100 000. Geological Survey of Finland, 54 p.
- Vanderhaeghe, O. and Teyssier, C., 2001. Partial melting and flow of orogens: *Tectonophysics*, 342, 451–472.
- Whitney, D. L., Teyssier, C. and Vanderhaeghe, O., 2004. Gneiss domes and crustal flow. *Geological Society of America Special Papers*, 380, 15–33.
- Williams, I.S., Rutland, R.W.R., Kousa, J., 2008. A regional 1.92 Ga tectonothermal episode in Ostrobothnia, Finland : implications for models of Svecofennian accretion. *Precambrian Research*, 165(1–2), 15–36.

# Fennoscandian Neoproterozoic–Palaeoproterozoic Ni and PGE metallogeny and supercontinent cycles

P. Eilu<sup>1</sup> and K. Rasilainen<sup>1</sup>

<sup>1</sup>Geological Survey of Finland, PO Box 96, 02151 Espoo, Finland  
E-mail: pasi.eilu [at] gtk.fi

Known and estimated undiscovered nickel and PGE resources of the Fennoscandian shield are mostly related to major stages of supercontinent evolution. Archaean komatiite-hosted nickel deposits may predate the *Kenorland* assembly. Major PGE and Ni deposits in ca. 2.45 Ga layered intrusions are related to the initial breakup of the Kenorland, whereas the large Talvivaara, Pechenga and Kevitsa deposits, and komatiite-hosted Ni deposits in Central Lapland, are closely related to the final Kenorland breakup at ca. 2.1–1.98 Ga. Finally, the initial assembly of the *Columbia* created the numerous orogenic, mafic to ultramafic intrusion-hosted, Ni deposits across the Svecofennian domain.

**Keywords:** Nickel, platinum, palladium, ores, undiscovered resources, komatiites, intrusions, supercontinents, Kenorland, Columbia, Fennoscandia

## 1. Introduction

Major mineral deposit formation is, for many deposit types, related to distinct stages of supercontinent cycles (e.g., Groves and Bierlein 2007). This relationship can be used both for exploring certain genetic types of mineral deposits (especially in target region selection) and as an indication of a certain type of crustal evolution and stage of supercontinent cycle. The timing and formation Ni and PGE deposits in the Archaean and Palaeoproterozoic parts of the Fennoscandian shield are here described in relation to supercontinent cycles. We also summarise the recent assessments of undiscovered Ni and PGE resources in the region. These assessments, in combination with the pre-mining resources of the known deposits, show how nearly all the Ni and PGE endowment within the Fennoscandian shield is related to supercontinent cycles.

## 2. Known Ni and PGE deposits and metallogenic belts in Archaean and Palaeoproterozoic Fennoscandia

Nickel deposits and occurrences are known from pre-*Kenorland* assembly komatiites (2.9–2.75 Ga?) in some of the Meso- to Neoproterozoic greenstone belts in Finland and Russia (Fig. 1). The assembly of Kenorland (2.75–2.60 Ga?), accretion and deformation, caused partial remobilisation of the deposits and locally produced Ni-Cu ore bodies, with significantly upgraded metal concentrations, in structurally-controlled locations. Most of the known Archaean Ni deposits of the shield are small; very few larger ones have been discovered.

The by far most significant PGE mineralisation stage within the Fennoscandian shield took place at ca. 2.45 Ga, with the initial breakup of the Kenorland, when a rifting event possibly related to a major mantle plume (Mertanen and Pesonen 2012) produced reef- and contact-type PGE-Ni-Cu deposits in layered intrusions across the Archaean parts of the shield. As some of the deposits are potentially very large, also their Ni endowment is significant.

The final breakup of the Kenorland took place during 2.2–1.98 Ga. This included formation of extensive intracontinental basins which were filled by clastic sedimentary and komatiitic to tholeiitic volcanic sequences, and by mafic-ultramafic intrusions. This stage produced the enormous black shale-hosted Talvivaara Ni-Cu-Zn-Co deposit in eastern

Finland, and the mafic-ultramafic intrusion-hosted Pechenga and Kevitsa Ni-Cu±PGE deposits in the northern part of Finland and the Kola Peninsula. Also the ca. 2.1–2.0 Ga komatiite-hosted Ni deposits in Central Lapland were formed in this stage. The recently discovered Sakatti Ni-Cu deposit, near Kevitsa, may relate to this stage of supercontinent evolution. (Mutanen 1997, Papunen 1998, Lahtinen et al. 2008)

Assembly of the supercontinent *Columbia* begun sometime during 1.95–1.89 Ga, and lasted at least until 1.63 Ga (Mertanen and Pesonen 2012). The initial supercontinent assembly, with accretion of magmatic arcs and microcontinents with the Archaean craton, produced tens of orogenic mafic-ultramafic intrusion-hosted Ni-Cu deposits across the Svecofennian domain in Finland and in Northern Sweden (Peltonen 2005, Hallberg et al. 2012). These deposits are small to medium-sized; so far, no large deposits have been detected, but a number has been mined in Finland.

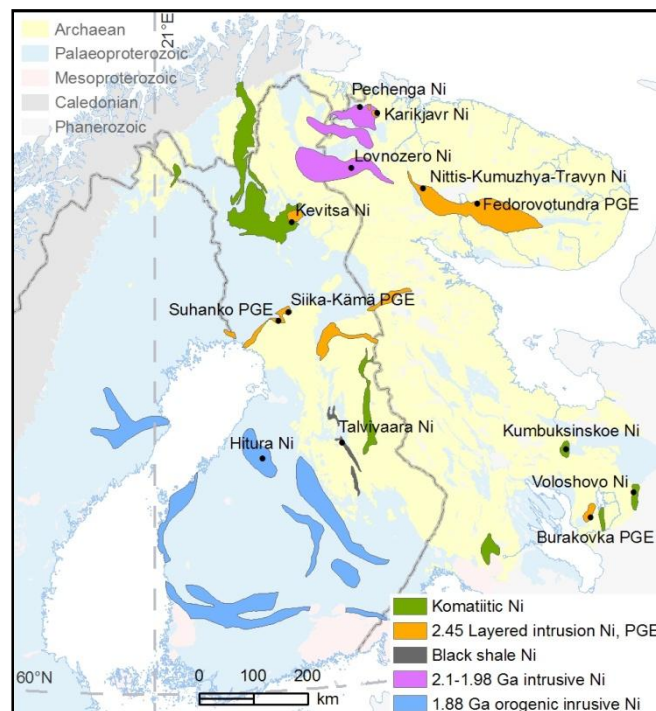


**Figure 1.** Major Ni and PGE deposits and main metallogenic belts characterised by Ni and PGE deposits in the Archaean and Palaeoproterozoic parts of the Fennoscandian shield (Eilu et al. 2009, Eilu 2012).

### 3. Assessment of undiscovered metal content of Ni and PGE potential tracts in Finland

The undiscovered Ni and PGE resources down to the depth of one kilometre in the Finnish bedrock were assessed by the Geological Survey of Finland using the three-part quantitative mineral resource assessment method (Singer 1993, Singer & Menzie 2010). This included the construction of deposit models for the relevant mineral deposit types, the delineation of areas where geology permits the existence of the deposit types (permissive tracts), the estimation of the number of undiscovered deposits within the permissive tracts, and the calculation of metal tonnages in the undiscovered deposits at various levels of probability.

Altogether, 100 permissive tracts were delineated, 19 for contact-type and 24 for reef-type PGE-Ni-Cu deposits, 27 for synorogenic intrusive Ni-Cu deposits and 30 for komatiitic Ni-Cu deposits (Fig. 2). Nearly all of these resources are in the metallogenic areas described above, and are related to the Kenorland breakup (layered intrusion-hosted PGE-Ni and

Proterozoic komatiitic Ni) and Columbia assembly (orogenic intrusion-hosted Ni). The total mean estimate of the number of undiscovered PGE-Ni-Cu and Ni-Cu deposits within these tracts is 151 deposits. At the 50 % confidence level, the undiscovered deposits are estimated to contain at least 4,960,000 t of Ni, 5,959,000 t of Cu, 33,000 t of Co, 5,530 t of Pt and 11,300 t of Pd (Table 1). These results indicate that 50% of the nickel resources and 98% of the platinum+palladium resources in the bedrock of Finland occur in undiscovered or poorly known deposits.

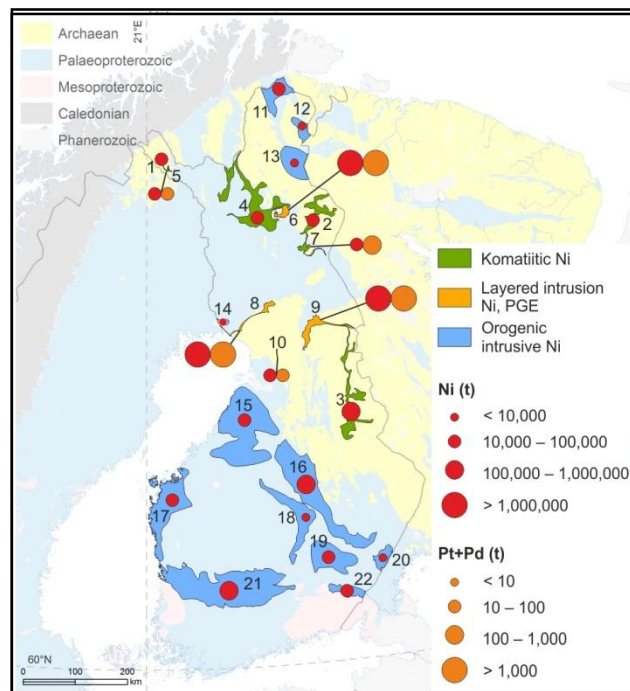


**Figure 2.** Generalized main permissive tracts (Table 1) for komatiitic Ni-Cu deposits, layered intrusion-hosted PGE deposits and synorogenic intrusive Ni-Cu deposits. The assessed undiscovered Ni and PGE endowment is shown for each tract.

## References:

- Eilu, P. (ed.) 2012. Mineral deposits and metallogeny of Fennoscandia. Geol. Surv. Finland, Spec. Paper, 53, 401 pages.
- Eilu, P., Bergman, T., Bjerkgård, T., Feoktistov, V., Hallberg, A., Ihlen, P.M., Korneliussen, A., Korsakova, M., Krasotkin, S., Muradymov, G., Nurmi, P.A., Often, M., Perdahl, J.-A., Philippov, N., Sandstad, J.S., Stromov, V. & Tontti, M. (comp.) 2009. Metallogenic Map of the Fennoscandian Shield, 1:2,000,000. Geol. Surv. Finland, Geol. Surv. Norway, Geol. Surv. Sweden, Fed. Agency Use of Min. Res., Ministry of Nat. Res. Ecol., Russian Fed.
- Groves, D.I. and Bierlein, F.P. 2007. Geodynamic settings of mineral deposits. *J. Geol. Soc. London*, 164, 19–30.
- Hallberg, A., Bergman, T., Gonzalez, J., Larsson, D., Morris, G., Perdahl, J. A., Ripa, M., Niiranen, T. and Eilu, P. 2012. Metallogenic areas in Sweden. *Geol. Surv. Finland, Spec. Paper*, 53, 140–205.
- Lahtinen, R., Gaarde, A.A. and Melezhik, V.A. 2008. Palaeoproterozoic evolution of Fennoscandia and Greenland. *Episodes*, 31, 20–28.
- Mertanen, S. and Pesonen, L.J. 2012. Paleo-Mesoproterozoic assemblages of continents: paleomagnetic evidence for near Equatorial supercontinents. In: *From the Earth's core to outer space. Lecture notes in Earth system sciences* 137. Berlin: Springer, 11–35.
- Mutanen, T. 1997. Geology and ore petrology of the Akanvaara and Koitelainen mafic layered intrusions and the Keivitsa-Satovaara layered complex, northern Finland. *Geol. Surv. Finland, Bull.* 395. 233 pages.
- Papunen, H. 1998. Geology and ultramafic rocks of the Paleoproterozoic Pulju greenstone belt, western Lapland. Technical Report 6.5. Brite-EuRam BE-1117 GeoNickel. Univ. Turku, Dept. Geology. 57 pages.

- Peltonen, P. 2005. Svecofennian mafic-ultramafic intrusions. In: Lehtinen, M., Nurmi, P. A. & Rämö, O. T. (eds.) Precambrian Geology of Finland – Key to the Evolution of the Fennoscandian Shield. Amsterdam: Elsevier, 407–442.
- Rasilainen K., Eilu P., Halkoaho T., Iljina M. & Karinen T. 2010. Quantitative mineral resource assessment of nickel, copper, platinum, palladium and gold in undiscovered PGE deposits in mafic-ultramafic layered intrusions in Finland. Geol. Surv. Finland, Rep. Invest., 180, 300 pages.
- Rasilainen, K., Eilu, P., Äikäs, O., Halkoaho, T., Heino, T., Iljina, M., Juopperi, H., Kontinen, A., Kärkkäinen, N., Makkonen, H., Manninen, T., Pietikäinen, K., Räsänen, J., Tiainen, M., Tontti, M. & Törmänen, T. 2012. Quantitative mineral resource assessment of nickel, copper and cobalt in undiscovered Ni-Cu deposits in Finland. Geol. Surv. Finland, Rep. Invest., 194, 521 pages.
- Singer, D.A. 1993. Basic concepts in three-part quantitative assessments of undiscovered mineral resources. Nonrenewable Resources 2, 69–81.
- Singer, D.A. & Menzie, W.D. 2010. Quantitative mineral resource assessments: An integrated approach. New York: Oxford University Press. 219 pages.

**Table 1.** Median estimated undiscovered metal resource, in tonnes of metal, in the main Ni and PGE tracts in Finland (based on Rasilainen et al. 2010, 2012). Numbers in the first column refer to the permissive tracts in Figure 2.

	Ni	Cu	Co	Pt	Pd
<i>Komatiitic Ni deposits</i>					
<i>Archaean</i>					
1 Ropi-Ruossakero-Sarvisoaivi	42,400	8,900	1,510		
2 East Lapland	33,400	6,860	1,165		
3 Jonkeri-Kuhmo-Suomussalmi	127,900	27,900	4,690		
<i>Palaeoproterozoic</i>					
4 Central Lapland	71,900	14,000	2,500		
<i>2.45 Ga layered intrusion PGE±Ni±Cu deposits</i>					
5 Kaamajoki	53,300	69,000		19	46
6 Koitelainen	1,100,000	1,100,000		2,700	5,300
7 Akanvaara	58,000	59,000		130	260
8 Portimo-Penikat-Kemi-Tornio	1,487,000	2,375,300		1,377	3,191
9 Koillismaa	1,404,700	1,903,300		1,239	2,754
10 Kärppäsuo	77,000	110,000		10	35
<i>1.89–1.87 Ga synorogenic intrusive Ni deposits</i>					
11 North Utsjoki	13,100	5,960	615		
12 Allarechka	1,600	720	73		
13 Lotta	9,200	4,200	440		
14 Liakka	9,300	4,000	430		
15 Hitura and surroundings	44,900	19,210	2,088		
16 Kotalahti	140,000	57,000	6,800		
17 Pohjanmaa	21,000	9,200	1,000		
18 Ilmolahti	9,500	4,100	450		
19 Juva	11,000	4,800	510		
20 Parikkala	8,800	3,800	400		
21 Vammala and surroundings	177,000	73,800	8,490		
22 Telkkälä	15,000	6,800	750		

## Petrology of an enriched gabbro in the Bothnian core complex

O. Eklund<sup>1</sup> and S. Fröjdö<sup>1</sup>

<sup>1</sup>Åbo Akademi University, geology and mineralogy  
Domkyrkotorget 1, 20500 Åbo  
E-mail: olav.eklund [at] abo.fi

Shoshonitic rock series use to be generated tectonically in the post-collisional uplift event of an orogeny. Geochemically, shoshonite rock series have  $K_2O+Na_2O>5\%$ ,  $K_2O/Na_2O>0.5$ ,  $Al_2O_3>9\%$  over a wide spectrum of  $SiO_2$ . The rock series is enriched in Ba and Sr and the LREE and show depletion in Ti, Nb and Ta. In this article we describe an enriched gabbro from the Bothnian core complex that evidence a geochemistry and mineralogy similar to a shoshonitic gabbro and discuss a potential origin to it and how it can be related to the Bothnian core complex.

**Keywords:** lithosphere, crust, upper mantle, Fennoscandia

### 1. General

The central part of the The Bothnian core complex seems to be situated around Vasa on the west coast of Finland. The radius of the complex is about 100 km. The outer part of the core complex was metamorphosed in lower amphibolites facies and the central parts in granulite facies (Hölttä pers. Com.) The gabbro in focus was sampled from Tiströnskärr in the central part of the core complex. Tiströnskärr is situated south east of Replot in the archipelago of Vasa. On the geomagnetic map, the gabbro is east-west trending with a length of about 4 km and a width of 1.5 km. Unfortunately it outcrops only on the small island Tiströnskärr.

### 2. Petrography

The rock is even-grained with micas (biotite) 1-5 mm across, amphiboles 1-3 mm across and plagioclase 1-3 mm across. Interstitially quartz occur. Abundant minor minerals are titanite and apatite.

It seems that amphibole (sometimes alkaline amphibole) and an older biotite crystallized together with apatite in an initial stage of the evolution of the rock. Later, a younger generation of biotite is growing on the cost of amphibole and the older mica. Simultaneously with the growth of the younger biotite, titanite is formed. The plagioclase is altered to micas and in places calcite. It contains euhedral apatite why it is considered that it has grown in a late stage. Euhedral apatite is common in the interstitial quartz, why the quartz is interpreted as a late phase of the rock. Opaque minerals appear together with the amphiboles and the titanite.

The rock evidences only few signs of deformation. These are kink bands in biotite and undulating quartz.

### 3. Geochemistry

The geochemical data was collected from Lehtinen et al. (2003) complemented with a new analysis from Acme Laboratory in the autumn 2012.

In the TAS-diagram, the gabbro plot in the field of gabbro and alkaline gabbro. Total alkalies vary between 3.98 and 5.36. In a diagram discriminating shoshonitic rocks from calc-alkaline and ultra-potassic rocks (Turner et al. 1996), the gabbro plot in the field of shoshonitic rocks (Fig. 1). The highest Mg# of the analyses is 65. Highest Cr and Ni contents are 528 ppm and 100 ppm respectively. Highest Ba and Sr contents are 3219 ppm and 2107

ppm respectively. In a spider diagram normalised to primitive mantle composition, the gabbro has a pattern similar to magmas generated in a destructive plate margin with negative spikes for Nb, P, Zr and Ti, Fig. 2a. In a REE- diagram normalised to chondrite composition, the gabbro is enriched in LRE elements, La = 600 x chondrite while Yb is enriched only 7 x chondrite,  $[La]_N/[Yb]_N = 77.28$ . (Fig. 2b).

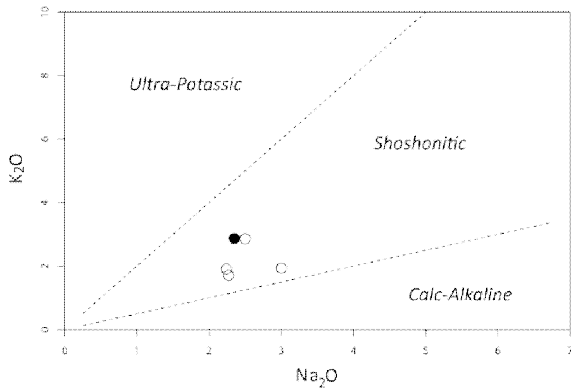


**Figure 1.** Diagram discriminating calc-alkaline, shoshonitic and ultrapotassic rocks. The gabbro on focus plot in the shoshonitic field. Open circles are from Lehtonen et al.(2003) and the solid circle from this study.

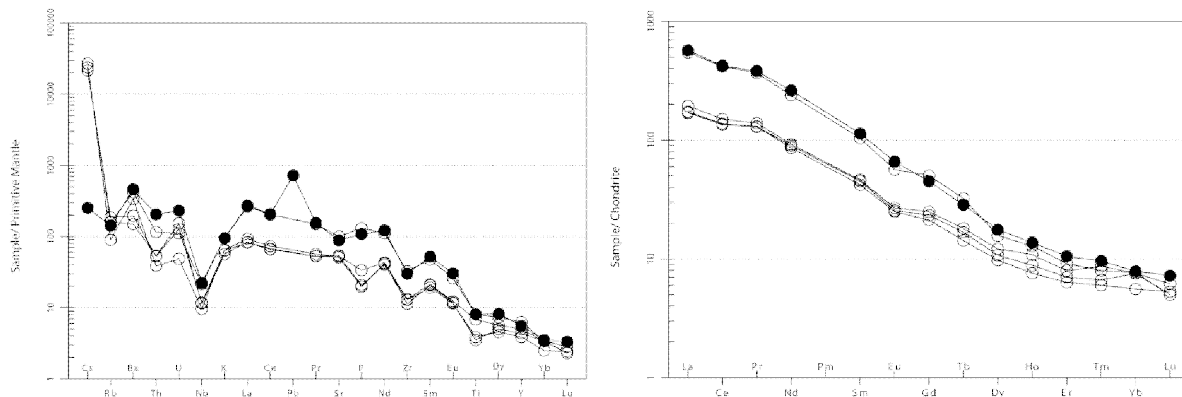


**Figure 2a and 2b.** 2a.Primitive mantle normalised (Sun & McDonough 1989) trace element pattern for the gabbro and 2b. Chondrite normalised (Nakamura 1974) RE-element pattern for the gabbro. Note the enrichment in LIL-elements and LRE-elements.

#### 4. Interpretation

The high Mg# indicate that the gabbro did not fractionate much after it was derived from the mantle, this is also supported by the high concentrations of Cr and Ni even though the rock don't contain olivines or pyroxenes. The concentrations of Ba and Sr exceed the concentration of these elements in any of analysed rocks in southern Ostrobothnia (Lehtinen et al 2003). We interpret that the high contents of Ba and Sr refer to an enriched source for the gabbro and not contamination of LIL-elements from the surrounding rocks.

In comparison with other enriched mafic magmatic rocks, the most similar are the 1869 Ma potassic mafic rocks from Putseri island in Ladoga (Konopelko and Eklund 2003)

and Neoproterozoic mafic sanukitoids in western Karelian Province, Finland (Heilimo et al. 2010).

The gabbro does not contain any relict olivines or pyroxenes, only amphiboles and two generations of biotite as mafic minerals and apatite. This paragenesis suits well to collect the particular elements the gabbro is strongly enriched in. Biotite collects Ba and Rb and apatite is a good collector for Sr and LRE elements (Prowatke and Klemme 2006).

During subduction, a mantle wedge can be enriched in fluids and sediments from the subducting slabs. It results in a metasomatized mantle that principally contains mica and amphiboles. Based on trace element distribution it is possible to trace the intensity of mantle metasomatism, the more LIL-elements and LRE-elements for analyses with the same Mg# (around 60), the more has the mantle been metasomatized.

The Tiströnskärs gabbro is situated close to the high grade central parts of The Bothnian Core complex. If the core complex was formed due to a rise in the geothermal gradient caused by mantle processes, the temperature in the enriched lithospheric mantle seems to have exceeded the solidus for the enriched mantle and the magma for the Tiströnskärs gabbro was generated.

## 5. Conclusions

The shoshonitic gabbro at Tiströnskärs was generated from a subduction enriched mantle. Tectonically, these types of melts are usually interpreted that they were generated by lithospheric delamination or slab break-off with subsequent rise of the asthenospheric mantle after a major collisional event. However without age determinations and isotope data it is difficult to do any more detailed interpretations at this stage of the survey.

This is a study within the Academy of Finland consortium Timing and P-T-conditions for the orogenic extension in the Fennoscandian shield. The isotope part of the study will be made by the consortium members of Helsinki University.

## References:

- Heilimo, E., Halla, J., Hölttä, P. 2010. Discrimination and origin of the sanukitoid series: Geochemical constraints from the Neoproterozoic western Karelian Province (Finland). *Lithos* 115, 27-39.
- Konopelko, D., Eklund, O. 2003. Timing and geochemistry of potassic magmatism in the eastern part of the Svecofennian domain. NV Ladoga Lake Region, Russian Karelia. *Precambrian Research* 120, 37-53.
- Lehtonen, M.I., Kujala, H., Kärkkäinen, N., Lehtonen, A., Mäkitie, H., Mänttari, I., Virransalo, P., Vuokko, J. 2003. Pre-Quaternary rocks of the Southern Ostrobothnian Shist Belt.
- Nakamura, N. 1974. Determination of REE, Ba, Fe, Mg, Na and K in carbonaceous and ordinary chondrites. *Geochimica et Cosmochimica Acta* 38, 757 – 773.
- Prowatke, S., Klemme, S. 2006. Trace element partitioning between apatite and silicate melts. *Geochimica et Cosmochimica Acta* 70, 4513–4527.
- Sun, S.S., McDonough, W.F. 1989. Chemical and isotopic systematics of ocean basalts: implications for mantle composition and processes. *Special Publication of the Geological Society of London* 42, 313-345.
- Turner, S., Arnaud, N., Liu, J., Rogers, N., Hawkesworth, C., Harris, N., Kelley, S., van Calsteren, P., Deng, W. 1996. Post-collision, shoshonitic volcanism on the Tibetan plateau: Implication for convective thinning of the lithosphere and source of ocean island basalts. *Journal of Petrology* 37, 45-71.



## The Polyphase ductile deformation at Olkiluoto, SW Finland

J. Engström<sup>1</sup>, A. Kärki<sup>2</sup> and S. Paulamäki<sup>1</sup>

<sup>1</sup>Geological Survey of Finland, P.O. Box 96, FIN-02151 Espoo

<sup>2</sup>Department of Geosciences, University of Oulu, P.O. Box 3000, FIN-90014 Oulun yliopisto

E-mail: jon.engstrom [at] gtk.fi

In this abstract we describe the ductile deformation at Olkiluoto which has been investigated in detail and evident crosscutting relationships between the different structures have been detected. The age span of the ductile deformation is rather extensive ranging from 1.92 - 1.79 Ga and four separate deformation phases have been defined. These different phases all have characteristic signatures representing each individual deformation phase.

**Keywords:** Ductile deformation, Fennoscandia, Olkiluoto, SW Finland

### 1. Introduction

A deep repository for spent nuclear fuel is under construction on the Olkiluoto Island in SW Finland, and detailed characterization of the bedrock within the whole Island and its near surroundings has been carried out for several years. One part of the geological characterization is the definition of the evolution of the ductile deformation within the area. We introduce a model for the late Svecofennian evolution in the Olkiluoto area, with emphasis on the polyphase ductile deformation. Olkiluoto is situated in the western end of the Svecofennian Accretionary Arc Complex of Southern Finland and the rocks have an age span between 1.82-1.90 Ga (Korsman et al. 1997). The bedrock has been described by Suominen et al. (1997). Majority of supracrustal rocks consists of migmatized meta-pelites, whereas metabasites, hornblende gneisses, amphibolites and uralite porphyrites are more scattered. The supracrustals are intruded by Paleoproterozoic felsic, granitic – tonalitic plutonic rocks and pegmatites, as well as by Mesoproterozoic rapakivi granites and olivine diabases. The Olkiluoto Island mostly consists of variably migmatized supracrustal, high-grade metamorphic rocks. On the basis of major mineral composition, texture and migmatite structure, the rocks of Olkiluoto can be divided into (1) migmatitic gneisses, (2) tonalitic-granodioritic-granitic gneisses both plutonic and supracrustal in origin, (3) mica gneisses, quartz gneisses and mafic gneisses occurring as inclusions in the migmatitic gneisses, and (4) pegmatitic granites related to the leucosome generation processes. These rocks are cut by a few probably Sub-Jotnian diabase dykes (Kärki & Paulamäki 2006).

A tectonic model for the formation the Fennoscandian Shield has been provided by Lahtinen et al. (2005). In the model they divide the Svecofennian evolution into the accretionary Fennian orogen at 1.92-1.87 Ga, followed by an extensional period prior to the subsequent Svecobaltic continent-continent collision at 1.84-1.79 Ga. The continent-continent collision includes the collision of an unknown microcontinent and the NW-SE to E-W continent-continent collision between Fennoscandia and Amazonia. Allen et al. (1996) described a second major deformation phase in Skellefte district causing N-trending open to tight folds. Late, ca. 1.80 Ga N-S compressional deformation zones are found in northern Sweden (Bergman & Weihed, 1997; Bergman et al. 2001). The close relationship between granites and migmatites indicates that for the latest stage (at ca. 1.80 Ga), the metamorphism and migmatization could possibly be related to decompression (Perttunen et al., 1996).

## 2. Structural geology in southern and south western Finland

Generally four major ductile deformation stages have been described and documented in southern and south-western Finland (e.g. Selonen & Ehlers 1998; Väisänen & Hölttä 1999). The earliest deformation phase ( $D_1$ ) is described to precede the major granitic and migmatitic phases (e.g. Ehlers et al., 1993) and the structures produced during this phase are usually obliterated by later deformation phases. Skyttä et al. (2006) described the second deformation phase ( $D_2$ ) as the major deformation phase in the Orijärvi area (southern Finland) with an age of ca. 1.88 Ga. In SW Finland,  $D_2$  deformation is characterised by recumbent or reclined  $F_2$  folds with NE-SW-trending subhorizontal to gently plunging fold axis and axial planes (Selonen & Ehlers 1998; Väisänen & Hölttä 1999). The synorogenic tonalitic to granodioritic intrusions were emplaced before or during  $D_2$ . The third deformation phase ( $D_3$ ) is defined as a overthrusting event, (coeval with the formation of the LSGM zone at 1.83-1.81 Ga) which re-deformed the older structures and produced shearing in certain zones where deformation has been partitioning already earlier during the main deformation phase ( $D_2$ ) (e.g. Ehlers et al., 1993; Skyttä et al., 2006). Evidence for the  $D_4$  deformation is sparsely documented in southern and south-western Finland and it is mostly reported as steep strike-slip type deformation zones associated with ~1.80 Ga postorogenic intrusions (e.g. Branigan 1987) or ultra-mylonitic to ultracataclastic shear zones, deforming ca. 1.81 Ga old pegmatites indicating a younger age than these pegmatites (Lindroos et al., 1996).

## 3. Field studies and results from Olkiluoto

The ductile deformation on the Olkiluoto Island can be divided into four distinct stages. Relicts of lithological layering and a weak foliation created by the first phase of deformation ( $D_1$ ) represent the oldest observed structural elements. The second deformation phase ( $D_2$ ) caused strong migmatitisation associated with intense folding and thrust related ductile shearing. The NW part of the Olkiluoto Island is characterized by  $D_2$  and signs of the later deformation phases are mostly rather sparse. These rocks have distinct migmatitic appearance with dominant veined or stromatic texture and E-W striking foliation composed of pegmatitic neosome veins and mica foliation within the paleosome. Deformation phase  $D_2$  is the most significant phase of the ductile deformation at Olkiluoto as it has pervasively and homogeneously deformed the whole region. The migmatites attained most of their present appearance in consequence of this deformation. The igneous-type tonalitic to granodioritic gneisses, dated at ca. 1860 Ma (Mänttari et al. 2006; Mänttari et al. 2007) were emplaced before or during  $D_2$ . Tuisku & Kärki (2010) concluded that the peak metamorphic conditions (660 – 700 °C and 3.7 – 4.2 kbar) were attained after  $D_2$  but before  $D_3$  deformation phase at some time between 1.86-1.82 Ga. The cooling phase took place in low pressure, as evidenced by such retrograde reaction products as andalusite, chlorite and muscovite replacing cordierite (Tuisku & Kärki 2010). Normally it is difficult to identify the relicts of primary sedimentary structures and products of the earliest deformations as well as to evaluate the exact significance of the earliest deformation events. Most commonly the foliations created by the earliest phases are coplanar with lithological layering ( $S_0$ ) and actually the visible foliation can be expressed as a composite  $S_{0/1/2}$  foliation.

The central part of the Island is dominated by the elements of the third deformation phase ( $D_3$ ), but signs of those can be seen all over the Island. During this deformation the migmatites were re-deformed and folded. Subareas dominated by  $D_3$  structural elements were formed simultaneously with pegmatite-like dykes or migrated leucosomes, which intruded mainly parallel to the  $D_3$  shear zones and  $S_3$  axial surfaces having a NE-SW orientation. Generally the dip of the  $S_3$  axial surfaces is steeper (~60°) than that of the  $S_2$  axial surfaces, which shows a more moderate dip (~40°).  $D_3$  deformation is one of the most important ductile

deformation phases in Olkiluoto and several subareas dominated by  $D_3$  structures are localized. Intensity of the  $D_3$  deformation is highest in the central part of the site where  $F_3$  fold structures are more or less asymmetrical, ranging from open to tight, and often showing a dextral sense of shear. Amplitudes and wavelengths of the folds detected on outcrops vary from a few centimetres up to several metres.  $S_3$  axial surface foliation is rarely developed even at the hinges of the tightest  $F_3$  folds, but  $S_2$  foliation has rotated into parallelism with  $F_3$  axial surfaces. Small-scale shear bands indicate the same sense of shear as the folds.  $D_3$  shear structures contain blastomylonites as characteristic fault rocks. These rocks contain intensively sheared leucosomes and porphyroclasts that commonly indicate SE side up – movement. Leucosomes from the migmatite rock have been dated with conventional U-Pb zircon dating and monazite dating indicating ages between 1870-1820 Ma (Mänttari et al., 2006; Mänttari et al., 2010). However, it is worth noting that the Olkiluoto area shows a strong overprinting caused by thermal phases, which makes the interpretation of the U-Pb zircon data even more complicated.

Subsequently, all earlier structural elements were again re-deformed in fourth deformation phase ( $D_4$ ), which caused local small-scale shear bands together with symmetric tight folding and occasionally also large-scale open folds. These folds usually show axial surfaces striking N-S mostly with a sub-vertical dip. This latest deformation phase also shows a distinct metasomatic or migmatitic type of rock with pronounced feldspar porphyroblasts in a fine-grained matrix. This rock type is located in zones of a few centimeters to several meters and usually show a distinct contact to the older deformation. It seems to be spatially, temporally and genetically related to  $D_4$  shear zones. Monazite dating of these feldspar porphyroblasts indicates that this deformation has an age of ca. 1.80 Ga (Mänttari et al., 2010), which is in accordance with the age of  $D_4$  deformation phase recognized in other areas of southern and south-western Finland (Branigan, 1987 and Lindroos et al., 1996). The  $D_4$  deformation phase transposes all older deformation phases in certain areas in a roughly N-S direction. The remarkable difference in  $D_4$  deformation at Olkiluoto in comparison to other parts in southern and south-western Finland is the more ductile nature of the deformation phase in Olkiluoto, whereas elsewhere it is described mostly as shear zones produced in the transition between ductile and brittle deformation.

#### 4. Summary and Conclusion

The ductile deformation at Olkiluoto has been investigated in detail and evident crosscutting relationships between the different structures have been detected. Consequently, four remarkable deformation phases have been defined. Even though the deformation structures of earlier phases may be transposed and overprinted by the subsequent events and the different phases occasionally show similar structural signatures, it is possible to find distinguishing elements for each individual deformation phase. The age span of the ductile deformation is rather extensive ranging from 1.92 - 1.79 Ga. The metamorphic peak at Olkiluoto was probably reached between 1.86-1.82 Ga, which is well in accordance with other studies carried out in Central and Southern Finland. This metamorphic peak is actually situated just in between the peak interpreted in Central Finland being at 1.88 Ga (e.g. Kilpeläinen 1998; Lahtinen et al. 2009) and the one occurring in Southern Finland between 1.83-1.81 Ga (e.g. Ehlers et al. 1993; Skyttä & Mänttari, 2008).

#### References:

Allen, R.L., Weihed, P. and Svensson S.-Å., 1996. Setting of Zn-Cu-Au-Ag massive sulphide deposits in the evolution and facies architecture of a 1.9 Ga marine volcanic arc, Skellefte district, Sweden. *Econ. Geol.* 91,1022-1053.

- Bergman, S. and Weihed P., 1997. Regional deformation zones in the Skellefte and Arvidsjaur areas. Final research report of SGU-project 03-862/93. 35p.
- Bergman, S., Kübler L., and Martinsson P., 2001. Description of regional geological and geophysical maps of northern Norrbotten County (east of the Caledonian orogeny). Sveriges Geologiska Undersökelse Ba 56, 1-110.
- Branigan, N. P., 1987. The role of the shearing in the Proterozoic development of the Åland archipelago, S.W. Finland. *Bulletin of the Geological Society of Finland* 59, 117-128.
- Ehlers, C., Lindroos, A. and Selonen, O., 1993. The late Svecofennian granite-migmatite zone of southern Finland; a belt of transpressive deformation and granite emplacement. *Precambrian Research* 64, nos. 1-4, pp. 295-309.
- Kilpeläinen, T., 1998. Evolution and 3D modeling of the structural and metamorphic patterns of the Paleoproterozoic crust in the Tampere-Vammala area, southern Finland. *Geological Survey of Finland, Bulletin* 397, 124 p.
- Korsman, K., Koistinen, T., Kohonen, J., Wennerström, M., Ekdahl, E., Honkamo, M., Idman, H. and Pekkala, Y., 1997. Suomen kallioperäkarta = Berggrundskarta över Finland = Bedrock map of Finland 1:1 000 000.
- Lahtinen, R., Huhma, H., Kähkönen, Y., and Mänttari, I., 2009. Paleoproterozoic sediment recycling during multiphase orogenic evolution in Fennoscandia, the Tampere and Pirkanmaa belts, Finland. *Developments in Precambrian research* 17, pp. 310-336.
- Lahtinen, R., Korja, A. and Nironen, M., 2005. Paleoproterozoic tectonic evolution. In: Lehtinen, M., Nurmi, P. A. & Rämö, O. T. (eds.) *Precambrian geology of Finland : key to the evolution of the Fennoscandian Shield*. *Developments in Precambrian geology* 14. Amsterdam: Elsevier, pp. 481-531.
- Lindroos, A., Romer, R.L., Ehlers, C. & Alviola, R., 1996: Late-orogenic Svecofennian deformation in SW Finland constrained by pegmatite emplacement ages. *Blackwell Science Ltd., Terra Nova*, 8, p. 567-574.
- Mänttari, I., Talikka, M., Paulamäki, S. & Mattila, J. 2006. U-Pb ages for tonalitic gneiss, pegmatitic granite, and diabase dyke, Olkiluoto study site, Eurajoki, SW Finland. Working Report 2006-12. Posiva Oy, Eurajoki. 18 p.
- Mänttari, I., Aaltonen, I., Lindberg, A., 2007. U-Pb-ages for two tonalitic gneisses, pegmatitic granites and K-feldspar porphyries, Olkiluoto Study Site, Eurajoki, SW Finland. Working Report 2007-70. Posiva Oy, Eurajoki..
- Mänttari, I., Pere, T., Engström, J. and Lahaye, Y., 2010. U-Pb Ages for PGR Dykes, KFP, and Adjacent Older Leucosomic PGRs from ONKALO Underground Research Facility, Olkiluoto, Eurajoki, SW Finland. Working Report 2010-31.
- Paulamäki, S., 2007. Geological mapping of the region surrounding the Olkiluoto site. Posiva Oy, Working Report 2007-30.
- Perttunen V., Hanski E., Väänänen, J., Eilu P., and Lappalainen M., 1996. Rovaniemen kartta-alueen kallioperä. Summary: Pre-Quaternary rocks of the Rovaniemi map-sheet area. *Geological map of Finland 1: 100 000*. Explanation to the maps of Pre-Quaternary rocks, Sheet 3612 Rovaniemi. *Geol. Surv. Finland, Espoo*. 1-63.
- Selonen, O. and Ehlers, C., 1998. Structural observations on the Uusikaupunki trondhjemite sheet, SW Finland. *GFF* 120 (4), pp. 379-382.
- Skyttä, P. and Mänttari, I., 2008. Structural setting of late Svecofennian granites and pegmatites in Uusimaa belt, SW Finland: Age constrains and implications for crustal evolution polyphase strain partitioning. *Precambrian Research* 164, 86-109.
- Skyttä, P., Väisänen, M., and Mänttari, I., 2006. Preservation of Paleoproterozoic early Svecofennian structures in the Orijärvi area, SW Finland: Evidence for polyphase strain partitioning. *Precambrian Research* 150, 153-172.
- Suominen, V., Fagerström, P., and Torssonen, M., 1997. Pre-Quaternary rocks of the Rauma map-sheet area (in Finnish with an English summary). *Geological Survey of Finland, Geological Map of Finland 1:100 000*, Explanation to the maps of PreQuaternary rocks, Sheet 1132, 54 p.
- Tuisku, P. and Kärki, A., 2010. *Metamorphic Petrology of Olkiluoto*. Posiva Working Report 2010-54, 76 pp.
- Väisänen, M. and Hölttä, P., 2002. Structural and metamorphic evolution of the Turku migmatite complex, southwestern Finland. *Geological Survey of Finland. Bulletin* 71, pp. 177-218.

## Juxtaposed Lithospheres of Norway and Sweden – insights from 3D integrated geophysical modelling

S. Gradmann<sup>1</sup>, J. Ebbing<sup>1</sup> and J. Fulla<sup>2</sup>

<sup>1</sup>Geological Survey of Norway (NGU), Trondheim, Norway

<sup>2</sup>Dublin Institute of Advanced Studies, Dublin, Ireland

E-mail: sofie.gradmann [at] ngu.no

### 1. Introduction

The northern, central and southern domains of the Scandinavian mountains exhibit distinctly different large-scale geophysical and geological characteristics (Ebbing and Olesen, 2006). These include, for example, topography, Moho depth and gravity lows (Figure 1). Recent studies have revealed major lateral changes in lithosphere thickness and composition underneath southern Norway and southern Sweden (Maupin et al., in review). A juxtaposition of lithosphere of different age and composition can consistently explain the isostatic compensation of the topography, the gravity signal and the seismic velocities of the uppermost mantle in southwestern Fennoscandia. These lithospheric variations roughly correlate with the near-surface boundary between the Sveconorwegian (Neoproterozoic) and Svecofennian (Palaeoproterozoic) domain (Figure 2). The northward continuation of the geological domain boundary is obscured by the overlying nappes of the Caledonian orogen. A number of geophysical data sets (topography, gravity, geoid, magnetotellurics, seismology), that can be used to better constrain the mantle boundary zone, have been collected in recent years.

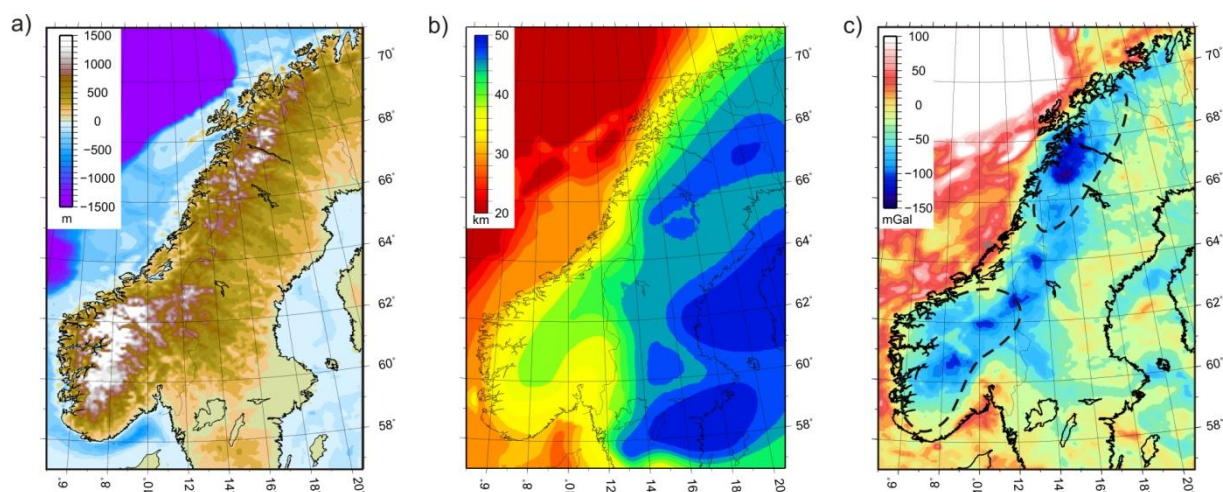


**Figure 1.** (a) Topography of western Fennoscandia. (b) Moho depth of western Fennoscandia, compiled from Kinck et al. (1993) and Stratford et al. (2009). (c) Bouguer anomaly of western Fennoscandia (EGM2008). Offshore reduction density is  $1670 \text{ kg/m}^3$ .

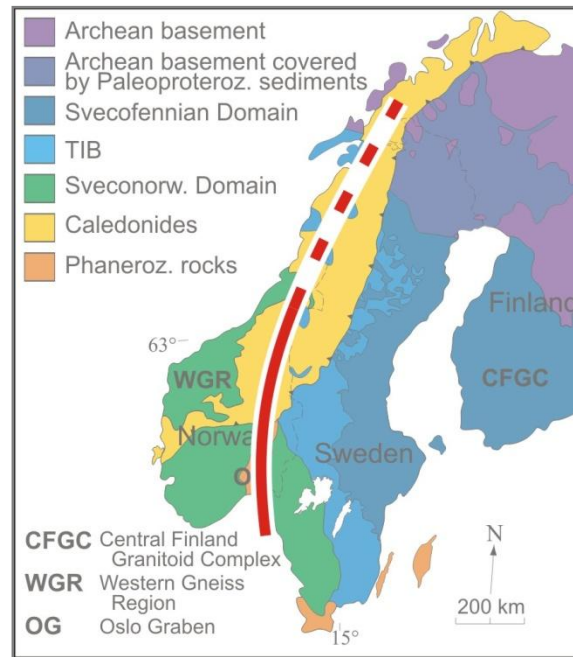


**Figure 2.** Simplified geological map of Fennoscandia (after Gorbatchev, 2004) with proposed mantle boundary zone between southern Norway and Sweden (red line).

## 2. Methods

We perform combined geophysical-petrological forward modelling of the lithosphere and sublithospheric upper mantle using the interactive modelling program LitMod3D (Afonso et al., 2008; Fullea et al., 2009). All relevant properties are functions of temperature, pressure and composition. Therefore the models are self-consistent and can be used to fit available geophysical and petrological observables simultaneously. The software has been extended to include calculations of mantle electric resistivities so that comparison to magnetotelluric data is possible (Fullea et al., 2011).

## 3. Results

We show that a juxtaposition of lithospheric mantles of different composition can locally create positive buoyancy and thereby provide isostatic support for the topography of northern Norway. We suggest a northward continuation of the mantle boundary zone along the highest topography.

Such a subsurface model is consistent with a resistivity profile through central Norway and Sweden (Korja et al., 2008; Smirnov et al., in prep). A low-resistivity anomaly in the uppermost mantle could be caused by a palaeo-suture zone, where highly conductive minerals like graphite or sulfites may still be present (Figure 3; Jones et al., 2003).

We furthermore investigate a prominent gravity and geoid low in northern Norway, which lies just south of the Lofoten peninsula extending across onshore and offshore domains. A similar, yet larger anomaly is found on the conjugate margin in northeastern Greenland. We compare two possible origins of this anomaly: a low-density upper crust, representing the northward extension of the Transscandinavian Igneous Belt and thick, depleted lithospheric mantle of possibly Archean origin.

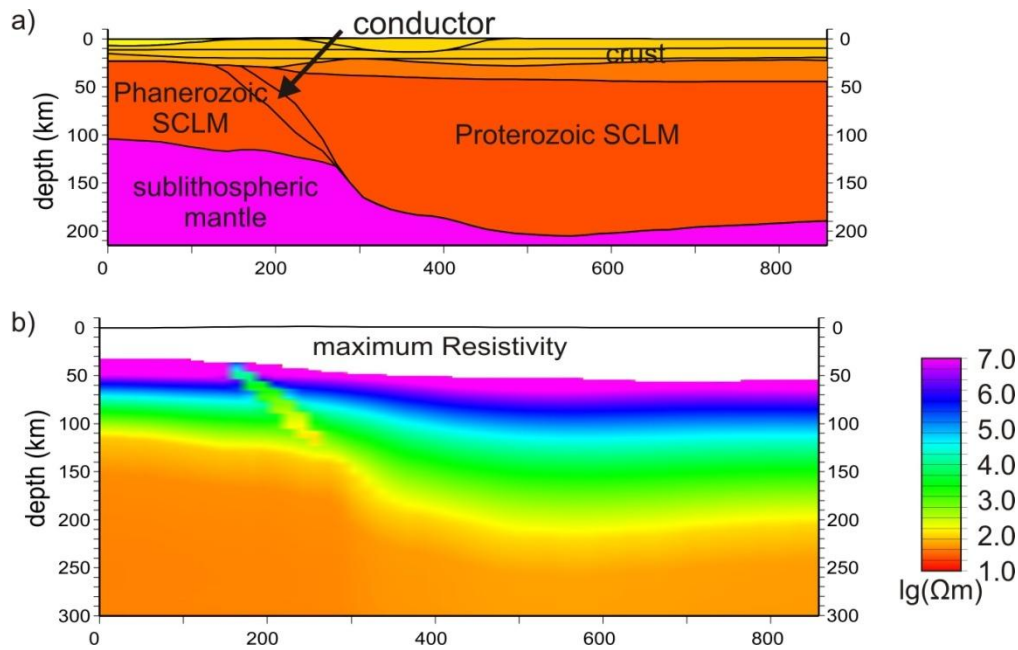


**Figure 3.** Cross section through subsurface model of SW Fennoscandia. (a) Geometry displaying lateral changes in lithosphere thickness and composition. (b) Calculated electric resistivities.

### References:

- Afonso, J. C., M. Fernandez, G. Ranalli, W. L. Griffin, and J. A. D. Connolly, 2008. Integrated geophysical-petrological modeling of the lithosphere and sublithospheric upper mantle: Methodology and applications, *Geochem. Geophys. Geosyst.*, 9 (5), doi: 10.1029/2007GC001834.
- Ebbing, J. and Olesen, O. 2006: The Northern and Southern Scandes - Structural differences revealed by an analysis of gravity anomalies, the geoid and regional isostasy. *Tectonophysics* 411, 73-87.
- Fullea, J., J. C. Afonso, J. A. D. Connolly, M. Fernandez, D. Garcia-Castellanos, and H. Zeyen, 2009. LitMod3D: An interactive 3-D software to model the thermal, compositional, density, seismological, and rheological structure of the lithosphere and sublithospheric upper mantle, *Geochem. Geophys. Geosyst.*, 10 (8), doi: 10.1029/2009GC002391.
- Fullea, J. and Muller, M.R. and Jones, A.G., 2011. Electrical conductivity of continental lithospheric mantle from integrated geophysical and petrological modeling: Application to the Kaapvaal Craton and Rehoboth Terrane, southern Africa. *JGR*, 116, B10202.
- Gorbachev, R. 2004. The Transscandinavian Igneous Belt - introduction and background, in *The Transscandinavian Igneous Belt (TIB) in Sweden: A review of its character and evolution*, Geological Survey of Finland, Special Paper, vol. 37, edited by K. Högdahl, U. Andersson, and O. Eklund, pp. 9-15, Geological Survey of Finland.
- Kinck, J., E. Husebye, and F. Larsson, 1993. The Moho depth distribution in Fennoscandia and the regional tectonic evolution from Archean to Permian times, *Precambrian Research*, 64 (1-4), 23-51, doi:10.1016/0301-9268(93)90067-C.
- Korja, T., Smirnov, M., Pedersen, L.B. and Gharibi, M., 2008. Structure of the Central Scandinavian Caledonides and the underlying Precambrian basement, new constraints from magnetotellurics *GJI*, 175, 55-69.
- Jones, A.G., Lezaeta, P., Ferguson, I.J., Chave, A.D., Evans, R.L., Garcia, X. and Spratt, J., 2003. The electrical structure of the Slave craton. *Lithos*, 71, 505-527.
- Maupin, V. and the TopoScandiaDeep working group, in review. The deep structure of the Scandes and its relation to tectonic history and present topography. *GJI*, doi: 10.1111/j.1365-246X.2011.04989.x.
- Smirnov et al., in prep.
- Stratford, W., H. Thybo, J. I. Faleide, O. Olesen, and A. Tryggvason, 2009. New Moho map for onshore southern Norway, *Geophysical Journal International*, 178 (3), 1755-1765, doi:10.1111/j.1365-246X.2009.04240.x.



# Seismic 3D modelling: case studies from Pyhäsalmi and Kevitsa, Finland

S. Heinonen<sup>1</sup>, E. Koivisto<sup>1</sup>, M. Heinonen<sup>2</sup> and P. Heikkinen<sup>1</sup>

<sup>1</sup>Institute of Seismology, Department of Geosciences and Geography, PL 68, 00014 University of Helsinki, Finland

<sup>2</sup>Helsinki institute of Information Technology, Department of Computer Science, PL 68, 00014 University of Helsinki, Finland

E-mail: suvi.heinonen [at] helsinki.fi

Seismic reflection profiles can be effectively used for 3D modelling of the subsurface geological structures and also to guide the deep exploration efforts in the mining districts. The experiences from Pyhäsalmi and Kevitsa, Finland, show how drill hole and seismic data can be efficiently integrated and used to develop the understanding of geological structures and tectonic evolution of the study regions.

**Keywords:** seismic reflection survey, 3D modelling, Pyhäsalmi, Kevitsa

## 1. Introduction

The Geological Survey of Finland (GTK) led a seismic reflection project called HIRE (high-resolution reflection seismics for ore exploration) during 2008–2010 (Kukkonen et al., 2011). In this project, 2D seismic reflection profiles were acquired at 16 different mining camps in Finland, including the Pyhäsalmi (Kukkonen et al., 2010) and Kevitsa (Kukkonen et al., 2009). Pyhäsalmi is a volcanic hosted massive sulphide (VHMS) deposit located in a Proterozoic volcanic belt in central Finland. Kevitsa is a mafic-ultramafic intrusive complex in northern Finland, hosting Ni, Cu and Platinum group elements. In Pyhäsalmi, six seismic profiles were acquired using both vibroseis (4 lines) and explosives sources (2 lines), depending of the field conditions, while all four profiles in Kevitsa employed explosive sources. Configurations of the seismic surveys are shown in Figure 1 on geological maps of the survey areas. The networks of seismic profiles enable modelling of the subsurface structures well beyond the exploration depths.

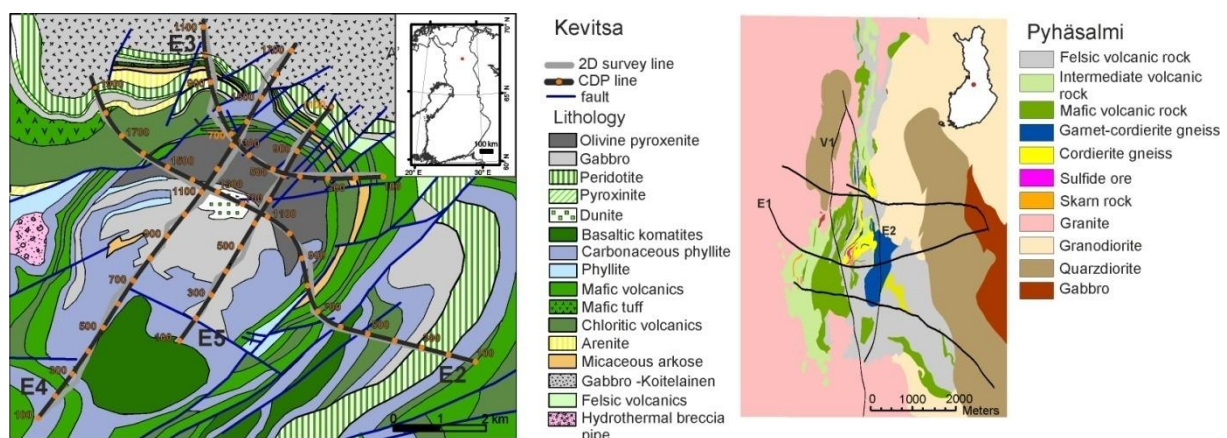


**Figure 1.** Seismic profiles of Kevitsa and Pyhäsalmi on geological maps.

## 2. Petrophysical constraints to seismic interpretation

Seismic velocities and densities derived from full waveform sonic logging and gamma-gamma density measurements provide crucial information about physical rock properties. Product of seismic P-wave velocity and density, i.e., the acoustic impedance, is used to calculate the reflection coefficients. Reflection coefficient is proportional to the difference in acoustic impedances of the rocks in contact with each other. In hardrock seismic environments, the minimum reflection coefficient to cause detectable reflection is typically estimated to be 0.06 (Salisbury et al., 2003).

The average rock properties from Pyhäsalmi show, that sulphide ore is a strong reflector in contact with any lithology (Figure 2). Also contacts between mafic volcanic rocks and other rock types are expected to be imaged, but for example granites in contact with felsic volcanic rocks have too small reflection coefficients to produce detectable reflection. In Kevitsa, rocks of the mafic-ultramafic intrusion cause strong reflections at the contact to the hosting sequence of inter-layered sedimentary and volcanic rocks. Also, compositional differences within the intrusion can give raise to reflections. It is noteworthy that average seismic velocities and densities in Kevitsa mafic rocks are substantially higher when compared to those in Pyhäsalmi.

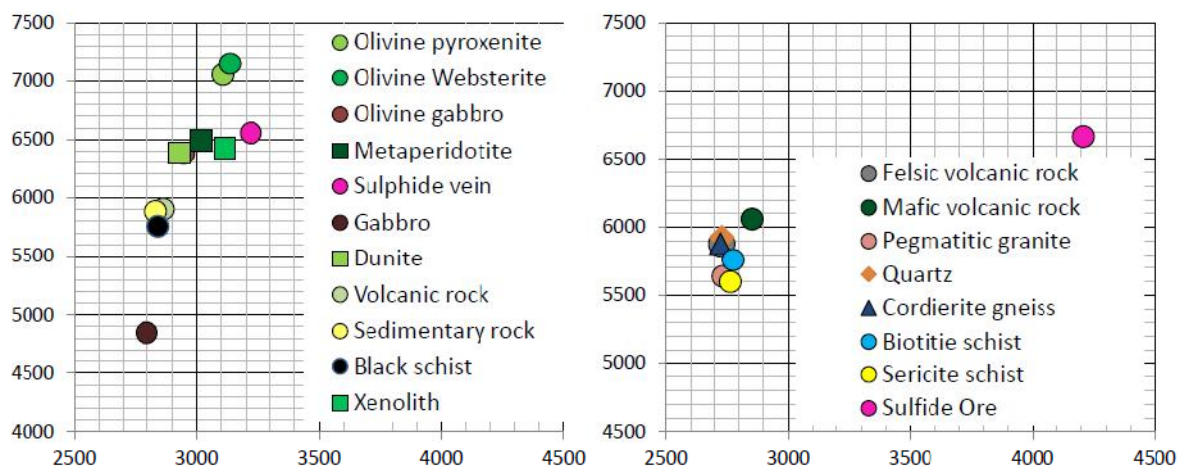


**Figure 2.** Average P-wave velocities and densities in rocks of Pyhäsalmi and Kevitsa, respectively. The mafic-ultramafic composition of Kevitsa is clearly seen as higher seismic velocities and densities when compared to those of Pyhäsalmi.

## 3. Geological interpretation of seismic profiles

In Kevitsa, seismic profiles are effectively used to define the shape and extent of the ore-bearing intrusion (Figure 3), as well as the geometry of some of the surrounding host rock units (Koivisto et al., 2012 and manuscript in preparation). Because the Kevitsa deposit is a low-grade disseminated ore, the ore deposit itself is not associated with distinct reflectivity solely attributed to increased sulphide contents.

Besides the acoustic impedance, also the size and orientation of the geological structure influence its reflectivity. In Pyhäsalmi, it was shown that subvertical structures are not imaged directly with seismic reflection data and only the subhorizontal fold hinges are visible in seismic section (Figure 3) while steep flanks need to be interpreted indirectly by recognizing change in reflectivity characteristics (Heinonen et al., 2012). Even though physical properties of massive sulphides suggest the ore to be strong reflector, no clear seismic signal was observed from the deposit. The noise caused by the active mine,

heterogeneous geological surroundings and unfavorable shape of the ore deposit are likely causes for the lack of obvious seismic signal.

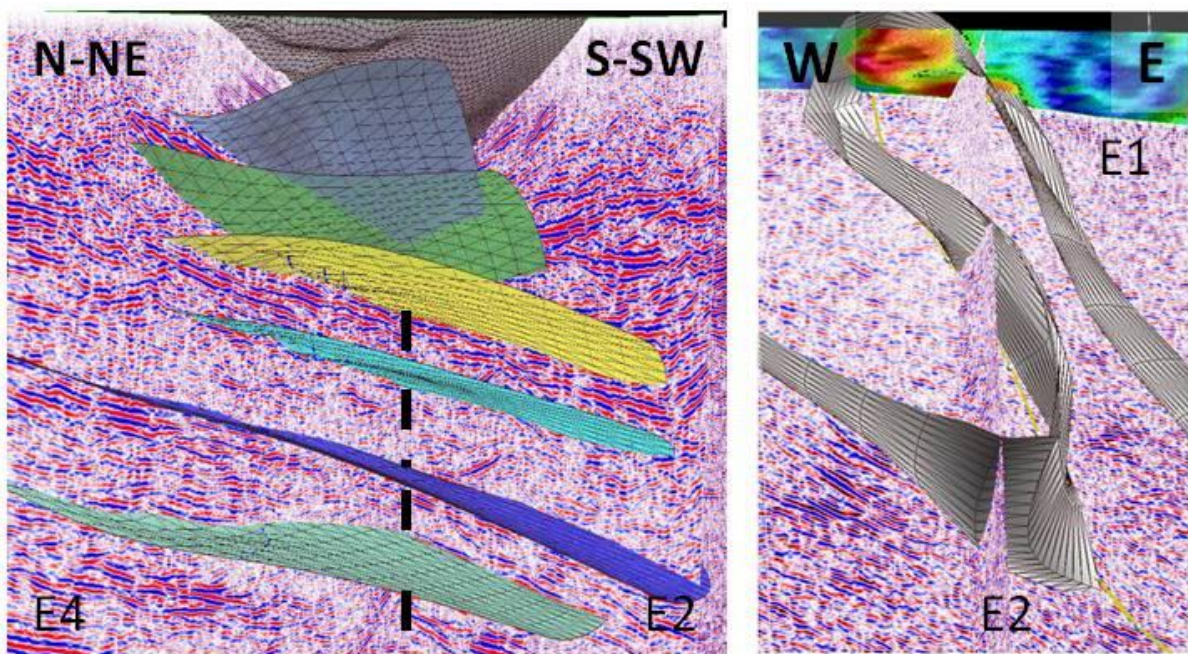


**Figure 3.** Network of the seismic profiles is used to interpolate the seismic interpretation to geological 3D model. Figure shows the modelled base of Kevitsa intrusion (in grey) and some of the host rock units (Koivisto et al., manuscript in preparation) and interpreted folding of Pyhäsalmi volcanic district.

In both study areas, the network of profiles enables interpolation of the 2D interpretations to 3D and thus creation of 3D models of the target areas. However, interpretation of seismic reflection data is far from being unambiguous. In particular, the occurrence of the out-of-plane reflections is a challenge for interpretation of the crooked-line seismic reflection data. The influence of chosen processing parameters during early stages of data handling can be dramatic, and later the velocity field chosen for migration and time-to-depth conversion drastically affect the fit between drill hole lithologies and observed reflectors.

The validity of seismic interpretation can be tested with drilling. In active exploration areas, such as Kevitsa and Pyhäsalmi, geological 3D models can be efficiently used to set exploration targets. When these targets are drilled, the model validity is simultaneously tested. However, drilling only provides a means to test specific targets, while seismic forward modelling can be used to test the validity of the whole model.

#### 4. Future work: seismic forward modelling

Seismic forward modelling can be used to test the validity of interpretations; that is to test if the simulated seismic response of the modelled geological structures would generate an observed response with given survey geometry. Propagation of seismic waves depends on seismic velocities and densities of the rocks, and these properties can be derived from drill hole logging data.

Representation of the geological model through a grid imposes several problems. A sufficiently dense grid is computationally unfeasible as the number of grid points increases exponentially to the grid density, while a sparse grid dramatically limits the model accuracy. A

grid is fundamentally a discrete model, which is unable to model shapes without approximate interpolation methods. We alleviate these problems by introducing a generative model, which represents a continuous and accurate geological 3D model with a collection of multivariate normal distributions, each associated with a specific rock formation. The complete model is a mixture of individual distributions, which is capable of representing any geological model.

Hence, the dimensionality of the model is dramatically reduced, which allows iterative model optimization to fine-tune the geological model to give a better match with the observed seismic responses through forward modelling simulations. In the optimization we employ well-known gradient descent and MCMC techniques on mixture models to search for models that generate seismic forward modelling simulation patterns that are closer to the observed seismic response. Out of the multitude of potential geological models that fit the data equally well, we choose the simplest by minimizing the number of parameters necessary to represent the model. In the optimization, the high-performance computer cluster resources are exploited.

Finally, we explore the explicit inclusion of drill hole data to the model as prior information on the geological model according to Bayesian principles (Gouveia et al., 1996), and the introduction of geological model constraints to exclude emergence of unrealistic rock formations in the model.

## 5. Conclusions

Case studies from Pyhäsalmi and Kevitsa show how seismic reflection profiling can be used for geological 3D modelling. In both areas seismic data has increased the knowledge about areal geological structures, continuation of ore-hosting lithologies in depth and also helped to better understand the tectonic evolution of the area. These studies show that 3D modelling of seismic profiles is efficient in guiding exploration efforts and in improving geological understanding of the structures controlling the ore deposits. Future seismic forward modelling will increase the reliability of the seismic interpretations.

## References:

- Gouveia, W., Scales, J., 1996. Resolution of seismic waveform inversion: Bayes versus Occam. *Inverse Problems* 13, p. 323-349.
- Heinonen, S., Imaña, M., Snyder, D.B., Kukkonen, I.T., and Heikkinen, P.J., 2012. Seismic reflection profiling of the Pyhäsalmi VHMS-deposit: A complementary approach to the deep base metal exploration in Finland. *Geophysics* 77, p. WC15-WC23.
- Koivisto, E., Malehmir, A., Heikkinen, P., Heinonen, S., and Kukkonen, I., 2012. 2D reflection seismic investigations at the Kevitsa Ni-Cu-PGE deposit, northern Finland. *Geophysics* 77, p. WC149-WC162.
- Kukkonen, I., I. Lahti, and P. Heikkinen, 2009, HIRE seismic reflection survey in the Kevitsa Ni-PGE deposit, North Finland: Geological Survey of Finland Unpublished report Q 23/2008/59.
- Kukkonen, I. T., P. J. Heikkinen, S. E. Heinonen, and J. Laitinen, 2010, HIRE seismic reflection survey in the Pyhäsalmi Zn-Cu mining area, central Finland: Geological Survey of Finland, Report Q 23/2009/43.
- Kukkonen, I. T., P. J. Heikkinen, S. E. Heinonen, and J. Laitinen, 2011, Seismic reflection in exploration for mineral deposits: Initial results from the HIRE project: Geological Survey of Finland, Special Paper 49, p. 49–58.
- Salisbury, M., C.W. Harvey, and L. Matthews, 2003, The acoustic properties of ores and host rocks in hardrock terranes, in D. Eaton, B. Milkereit, and M. Salisbury, eds., *Hardrock seismic exploration*: SEG, 9–19. [www.gpi.kit.edu/SOFI3D.php](http://www.gpi.kit.edu/SOFI3D.php) (accessed 9.11.2012)

## Crustal structure in the Kiruna district, northern Sweden: Preliminary results from a seismic reflection study

N. Juhojuntti<sup>1</sup>, S. Bergman<sup>1</sup> and S. Olsson<sup>1</sup>

<sup>1</sup>Geological Survey of Sweden, Villavägen 18, Uppsala  
E-mail: niklas.juhojuntti [at] sgu.se

Seismic reflection data have been acquired along a ~74 km long profile in the Kiruna district, northern Sweden, in order to obtain information about the crustal structure for e.g. planning of deep exploration activities and tectonic modelling. Major geological units are an Archaean metagranitoid complex overlain by supracrustal units that are dominated by metabasalt, acidic metavolcanic rocks and clastic metasedimentary rocks. These units are intruded by plutonic rocks, and to variable degrees folded, sheared and metamorphosed. Many of the lithological contacts and deformation zones are expected to be seismically reflective. The seismic data from low-resolution recording using explosive charges do indeed show numerous reflections from the upper crust, including a band of reflections near the base of the upper crust, in addition to reflections from deeper levels. The high-resolution data, recorded using an impact source, are presently being analysed. However, preliminary seismic sections show reflections in the uppermost crust, several of which are dipping.

**Keywords:** seismic, reflection, crustal structure, mineral resources, northern Sweden

### 1. Introduction

The northernmost part of Sweden is an important ore province and a major producer of copper and iron in the country. Although numerous exploration campaigns, geological and geophysical surveys and academic research efforts for more than one hundred years have resulted in a large amount of accumulated geological knowledge, the regional three-dimensional crustal structure is still poorly understood. Such information is vital for e.g. planning of deep exploration activities and tectonic modelling. As part of the national mineral strategy the Geological Survey of Sweden is committed to increasing the geoscientific knowledge of northernmost Sweden. In this context a seismic investigation was performed in order to obtain information about the crustal structure in the Kiruna district (Fig. 1). This area was chosen for study because a large portion of the regional stratigraphic succession is represented and contrasts in seismic impedances are expected. The area contains large fold structures and regional shear zones, and there are many known mineral deposits. Data processing is still in progress and we here report some preliminary results after a summary of the main geological units and structures.



**Figure 1.** Location of the seismic line in the Kiruna district in northern Sweden. The geological information is from Bergman et al. (2000).

## 2. Geological units and structure of the Kiruna district

The Archaean Råstojaure complex, dominated by metagranitoids, is unconformably overlain by metaconglomerate, quartzite and metaandesite of the Kovo Group. The overlying Kiruna greenstone group consists mainly of metabasalt, metaultramafic rock, graphite schist, iron formation and marble. Swarms of mafic dykes exist in the Råstojaure complex, and the overlying rocks contain numerous mafic sills. The unconformably overlying Svecofennian supracrustal rocks predominantly consist of metaconglomerate and metaandesite (Porphyrite group), a bimodal group of basic and acidic metavolcanic rocks (Kiirunavaara group) and clastic metasedimentary rocks. Several suites of intrusions, which were formed during the time interval c. 1.9-1.8 Ga ago, have been distinguished in the area (Bergman et al. 2000).

In the area surrounding Kiruna in the west, bedding and contacts between rock units are moderately to steeply dipping and the single cleavage is always steeper than the bedding (e.g. Vollmer et al. 1984). Major southward plunging folds in the Kiruna greenstone group, with wavelengths of several kilometres, are evident in geophysical and geological interpretations. The distribution of mapped units suggests a sheet-dip that is gently southward-dipping. A more complex structural history is indicated in the easternmost part of area where two cleavages have been observed and a dome-shaped structure suggests refolded early folds.

There are several steep, ductile shear zones with orientations between NW-SE and NE-SW. The regionally most important zones are the Kiruna-Naimakka Deformation Zone and the Karesuando-Arjeplog Deformation Zone. These are both prominent belts of steeply dipping, ductile shear zones enclosing low-strain lenses. Their widths are 8-10 km, including the intervening lenses, their lengths are hundreds of kilometres and their depths have been estimated to at least 5 kilometres. Both zones have stretching lineations generally close to the dip direction of the mylonitic foliation. Kinematic indicators show that the NW side has moved upward relative to the SE side, but locally the opposite shear sense has been noted.

Various models have been proposed to explain the structure of the Kiruna area (Vollmer et al. 1984, Forsell 1987, Wright 1988, Talbot & Koyi 1995), including processes such as thrusting, imbrication, isoclinal folding, syntectonic sedimentation and diapirism. The new seismic data gives the opportunity to evaluate such models and integrate them in a regional tectonic model.

The range in rock compositions of the geological units and the presence of major folds and deformation zones offer a wide range of potential seismic reflectors. Water-bearing fracture zones may also be detected at shallower levels.

## 3. Seismic measurements

Seismic measurements were carried out along a ~74 km long profile, extending roughly between Kiruna and Vittangi. The main fieldwork campaign lasted 5 weeks, in July and early August 2012. On average the field crew consisted of about 10 persons. We used a receiver interval of 25 m, and normally approximately 350 recording channels. The main seismic source was the Vibrist system (Park et al. 1996, Juhojuntti et al. 2012), which utilizes a hydraulic hammer to generate the seismic signal. Normally the Vibrist system was employed at every receiver position, with the exception of a few areas where the profile either passed through terrain or close to buildings. Also, large explosive charges (8-16 kg) were fired at a few locations along the profile to image deeper structures, although at much lower resolution. Wireless seismometers were also placed along the profile and in the surroundings, to achieve better velocity control and to assess possible cross-dip components in the reflections. Some of the mining blasts in Kiruna were also recorded, but these records have not yet been analysed.

#### 4. Seismic reflections

The shot records from the explosions show a fairly reflective upper crust throughout the profile. Many shot records also show a set of sub-horizontal reflections at about 3-4 s TWT (Fig. 2), corresponding to depths on the order of 10 km, the origin of which is unknown at present. Several of the explosive shot records show reflections which likely originates in the lower crust. The Vibisist shot records also display reflections from the upper crust, although less clear than in corresponding explosive shot records, due to the much weaker signal from the Vibisist source. In particular around Kiruna the Vibisist data are strongly affected by cultural noise. However, the Vibisist have a high fold (nominally around 150), thus it should be possible to enhance the reflections through the ongoing data processing. Preliminary seismic sections from the eastern part of the profile show several dipping reflections in the uppermost part of the crust, as well as sub-horizontal reflections.

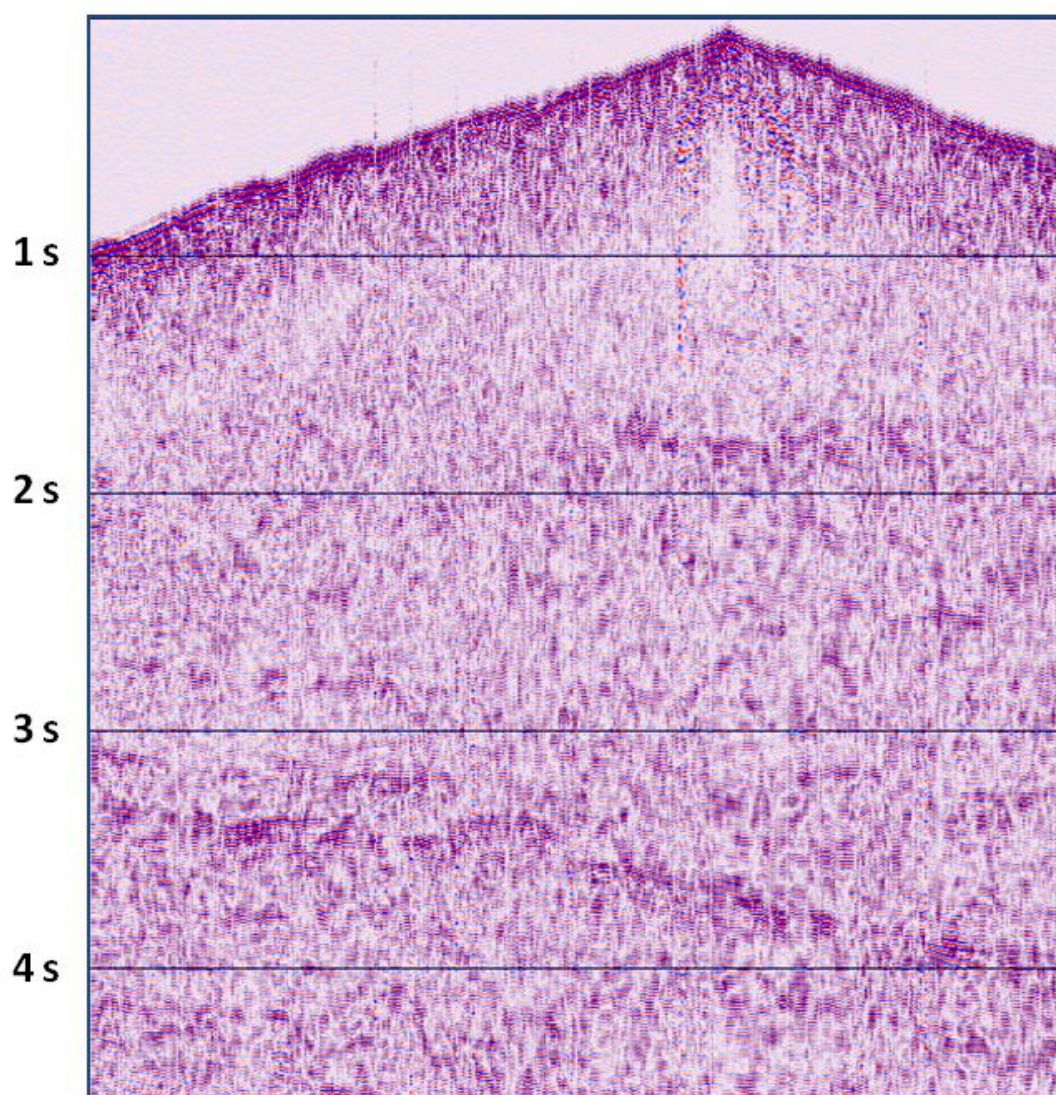


**Figure 2.** Seismic record from explosion shot along the eastern part of the profile. The geophone spread is approximately 9 km. The vertical axis shows time in seconds. Note bands of sub-horizontal reflections at approximately 1.7 s and 3.5 s (corresponding to depths of roughly 5 and 10 km). Bandpass filtering and automatic gain control has been applied.

## 5. Conclusions

The initial analysis of the seismic data shows a fairly reflective upper crust in the Kiruna district, as can be expected based on the heterogeneous bedrock lithology at the surface and the numerous deformation zones in the area. Several of the reflections in the upper crust appear to originate from dipping structures, although there are also reflections indicating sub-horizontal structures, e.g. near the base of the upper crust. The low-resolution recording using explosive charges has proved to be a valuable addition to the high-resolution data from the impact source.

## References:

- Bergman, S., Kübler, L. & Martinsson, O., 2000: Regional geological and geophysical maps of northern Norrbotten County: Bedrock map (east of the Caledonian orogen). Sveriges geologiska undersökning Ba 56:1.
- Forsell, P., 1987: The stratigraphy of the Precambrian rocks of the Kiruna district, northern Sweden. Sveriges geologiska undersökning C 812, 36 pp.
- Juhonjuntti, N., Wood, G., Juhlin, C., O'Dowd, C., Dueck, P. & Cosma, C., 2012. 3D seismic survey at the Millennium uranium deposit, Saskatchewan, Canada: Mapping depth to basement and imaging post-Athabasca structure near the orebody. *Geophysics* 77, WC245-WC258.
- Park, C. B., R. D. Miller, D. W. Steeples, and R. A. Black, 1996, Swept impact seismic technique (SIST): *Geophysics* 61, 1789-1803.
- Talbot, C.J. & Koyi, H., 1995: Palaeoproterozoic intraplate exposed by resultant gravity overturn near Kiruna, northern Sweden. *Precambrian Research* 72, 199-225.
- Vollmer, F.W., Wright, S.F. & Huddleston, P.J., 1984: Early deformation in the Svecokarelian greenstone belt of the Kiruna district, northern Sweden. *Geologiska Föreningens i Stockholm Förhandlingar* 106, 109-118.
- Wright, S.F., 1988: Early Proterozoic deformational history of the Kiruna district, northern Sweden. Unpublished Ph.D. thesis, University of Minnesota, 170 pp.

## Indications of Neo-tectonic Movements at Swan Water (Joutenvesi) of Saimaa Lake System

J.V. Korhonen<sup>1</sup>

<sup>1</sup>Geological Survey of Finland  
E-mail: juha.korhonen [at] gtk.fi

Some glaciated shore rocks at Swan Water of Saimaa Lake system indicate postglacial movements. The lateral extent, amount and temporal scale of the phenomenon is studied.

**Keywords:** crust, land uplift, Fennoscandia, Lake Saimaa

### 1. The region

On central Fennoscandian Shield, Eastern Finland extends Saimaa Lake system, which is rich of islands and islets, many having glaciated cliffs as shore lines. A sub-area of Saimaa to the south of inland-island Soisalo has been named Joutsenvesi (Swan Water) by kartographer Hällström (1799). Nowadays the Finnish name of the lake is spelled Joutenvesi, reflecting local dialectic form of the name of the same bird. Swan Water belongs to the most island rich lakes of the world. Its bedrock has been crushed by ancient tectonic movements and tops and sides of blocks polished by Weichsel glacier. Water fills this mosaic approximately half way. The southernmost part of the lake is followed by a long, continuous deeper underwater valley, trench which leads waters from Joensuu direction to Pike Water (Haukivesi). The location of this stream in a lake can be best seen on satellite images exposed in March-April. The stream is open and dark inside frozen and white lakes. The ship channel for international traffic has been marked on the stream, because of its greater water depth, normally more than 20 m.

### 2. Precambrian geological setting

The trench locates near contact of Svecofennides and Karelides. To the west expose mafic schistose rocks of Haukivesi and to the east migmatitic rocks of Kaleva. A refraction seismic profile (Baltic) crosses the trench near island Tikansaari, where geological western contact dips deep to the east, as interpreted from the magnetic anomalies caused by volcanites comprising the rocks of the island. On the Baltic profile has been made an unpublished upper crustal interpretation, where the present trench coincides with the ancient collision zone between foreland and forearc sediments of the Archaean craton and the Svecofennian province (Korhonen 1992).

### 3. Local indications of postglacial movements

The Fennoscandian land uplift map by Kakkuri (1992) displays an uplift anomaly, which follows the lake bottom trench of the southern Swan Water. Shores of some deep sounds, like between Halmesaari and Kruununluoto 4 km upstream of Tikansaari, consist of angular local boulders, hence indicating relatively young age of the process which broke the rock. In the beginning of eighties the present author observed proximally uplifted faults on a glaciated shore exposure of Tikansaari. Four steps summed up to 45 cm of vertical displacement. This was evidently of postglacial origin. An excursion was arranged to the Tikansaari and skilled scientists of geology and geodesy agreed on postglacial origin of the faults. Unfortunately nothing more related was found close by. Conclusion was that either faults were secondary, related to movements of major faults below water level or a subhorizontal fracture zone exists

and has been frozen, hence causing the faults. The rock should be drilled and study mineralogy of fractures to be found. A geodetic follow up study would be useful to establish.

#### **4. Quantitative observations**

The closest observed earthquakes since 1610 have occurred c. 50 km to the northwest. Only minor seismic energy release has taken place in the lake area (Map 29b of Mäntyniemi 1992). No observations exist on micro seismic events. The apparent lack of seismic activity gives reason to think that movements took place either soon after glacier retreated or are rare or non seismic in nature.

The area is mainly owned by Metsähallitus and belongs to the Natura protection programme. It is possible to have permission to establish a geodetic follow up network there. Geodetic studies have not been started, however, because of lack of means to do the work systematically in the forthcoming years.

The land uplift map suggests that decimeter class differential movement may have taken place within a 20 km range since 1899, in which year water rose to an anomalously high level, leaving a definite flood mark to the shore rock faces, called Valarikon viiva (line of the broken oath). This line and some later but lower flood marks are still to some extent visible on semi vertical rock surfaces of shores. This is why the present author has started to measure existing flood marks by traditional, easily accessible tools. Provided that indications of differential movements would be discovered in this way, these marks may be optically sharpened for more accurate measurements by false color and hyper spectral images.

#### **5. Conclusions**

Recently, it showed out in New Zealand that non seismic geotectonic events takes place close to a present plate boundary, although invisible in observations ten years ago (Gledhill 2012). Hence, to plan major building activities of the society, it would be useful to know whether in our relatively solid bedrock exist essential movements which cannot be detected by present geodetic or seismic networks.

#### **References:**

- Gledhill, K., 2012. The Geophysical Data Explosion: Improving Our Understanding of Planet Earth. <http://igc.conferenceshare.com.au/>
- Hällström, C.P., 1799. Suomen karttakirja. Uusintapainos, Karttakeskus 2012.
- Kakkuri, J., 1992. Fennoskandian maankohoaminen. Suomen kartasto, vihko 123-126, ss. 35-36
- Korhonen, J.V., 1992. Magneettisten karttojen geologisesta hyödyntämisestä. Unpublished Licentiate thesis. Helsinki University of Technology.
- Mäntyniemi, P., 1992. Suomen maanjäristyksistä. Suomen kartasto, vihko 123-126, ss. 34-35

# North European Transect (NET) – Growth of Northern Europe in Supercontinent Cycles

A. Korja<sup>1</sup>, P. Heikkinen<sup>1</sup>, Y. Roslov<sup>2</sup> and S. Mertanen<sup>3</sup>

<sup>1</sup> Department of Geosciences and Geography, University of Helsinki, Finland

<sup>2</sup> Sevmorgeo, St. Petersburg, Russia

<sup>3</sup> Geological Survey of Finland, Finland

E-mail: annakaisa.korja [at] helsinki.fi

North European Transect (*NET*) – a compilation of three deep seismic reflection datasets *BABEL* (1600 km), *FIRE 4-4A* (580 km) and *I-AR* (1440 km) – transects the Baltic and Bothnian Seas, Northern Finland and Kola Peninsula, Barents Sea and ends at Franz Joseph Land. The profile covers the transition from Phanerozoic Central Europe to Precambrian Northern Europe and back to the Phanerozoic Barents Sea shelf. The profile images the growth of Northern Europe around Baltica in three supercontinental formation and break up cycles: Nuna, Rodinia and Pangaea. With the help of seismic sections and paleomagnetic reconstructions we show, how Northern Europe has attained its present continental architecture

**Keywords:** seismic reflection, paleomagnetic reconstructions, transect, crust, supercontinent, Baltica, Northern Europe

## 1. Introduction

Continents grow around stable nuclei in supercontinent cycles. The nuclei grow outward during collisional and accretional orogenies associated with the supercontinent formation. But also during the break up minor amounts of material is added to the rifted margins of the dispersed pieces of the supercontinent.

North European Transect (*NET*) – a compilation of three deep seismic reflection datasets *BABEL* (1600 km), *FIRE 4-4A* (580 km) and *I-AR* (1440 km) – transects the Baltic and Bothnian Seas, Northern Finland and Kola Peninsula, Barents Sea and ends at Franz Joseph Land (Figure 1; Abramovitz et al., 1997; Dvorniko 2000; Korja and Heikkinen, 2005; Ivanova et al., 2006; Pattison et al., 2006). The profile covers the transition from Phanerozoic Central Europe to Precambrian Northern Europe and back to the Phanerozoic Barents Sea shelf. The profile images the growth of Northern Europe around Baltica in three supercontinental formation and break up cycles: Nuna, Rodinia and Pangaea. With the help of seismic sections and paleomagnetic reconstructions we will show how Northern Europe grew to its present continental geometry.

## 2. Growth and dispersal of Nuna

The early stages of Nuna formation was characterized by the oblique convergence of Baltica and Laurentia (Figure 2; Mertanen and Pesonen, 2012) in the present northern part of Baltica, resulting in series of short lived orogenies or collisional phases (Lapland-Savo, Lapland-Kola, Svecofennian; Korja et al., 2006) at 1.9-1.85 Ga (*BABEL1 and 4&3and FIRE4*; Korja and Heikkinen, 2005). The seismic data image, how the core of Baltica was formed by sequential accretion of continental and arc terranes in the vicinity of an old continental margin (*BABEL1 and 4&3and FIRE4*). The accreted, thickened crust was thinned via lateral spreading (*BABEL 4&3, FIRE4*).

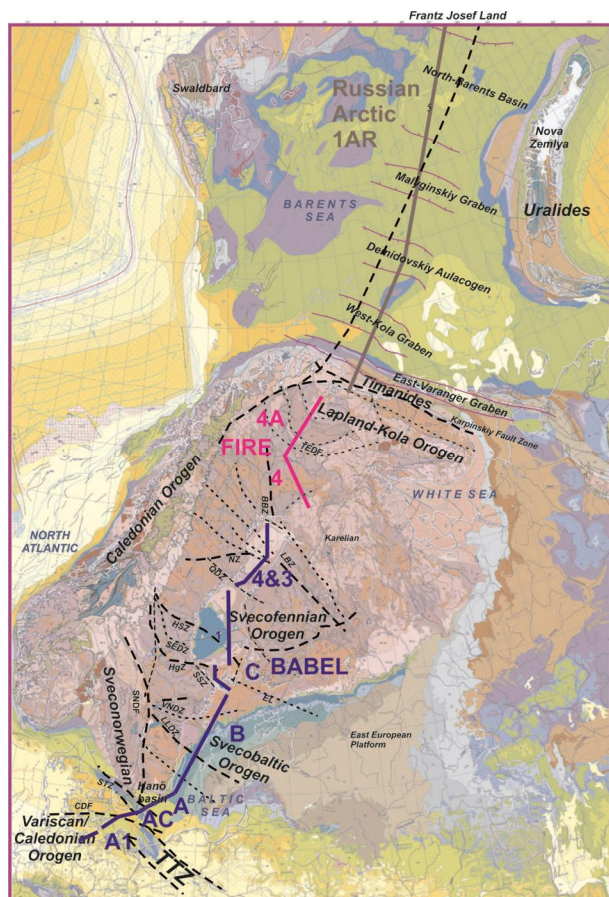


**Figure 1.** Orogenic belts, the main tectonic boundaries and the North European Transect (NET) on the International Geological Map of Europe and Adjacent Areas (Asch, 2005).

Simultaneous convergence of another continent in the South initiated arc formation south/southwest of Baltica. Based on paleomagnetic data this continent may have been North China, along with Amazonia that was in close connection with the growing Nuna supercontinent. The convergence and final collision of North China and Baltica around 1.85 Ga resulted in Svecobaltic orogen (**BABEL B**). After North China craton drifted apart from Baltica, a long lived, subduction margin (1.78 - TIB) was established at the western and southern margin of the Baltica-Laurentia (**BABEL B**). The long term (1.63-1.53 Ga) convergence of Amazonia and Baltica was finalized by docking of the continents in Danopolonian orogeny (**BABEL A**). This finalized the compilation of Nuna supercontinent. The dispersal of Nuna initiated a failed rift stage that completed the thinning of the crust and produced voluminous rapakivi provinces and associated sandstone basins (BABEL 1).

Although the dispersal of Nuna had begun earlier in intracratonic areas, a rifted margin was formed in the Southern Baltica only after 1.2 Ga. The margin evolved into transtensional Songfreid-Törnqvist Zone (STZ) characterized by subvertical shear zones (**BABEL A**). In the north, the departure of Laurentia from Baltica took place at about 1.12 Ga (Salminen et al., 2009). After this event the continents were separated.

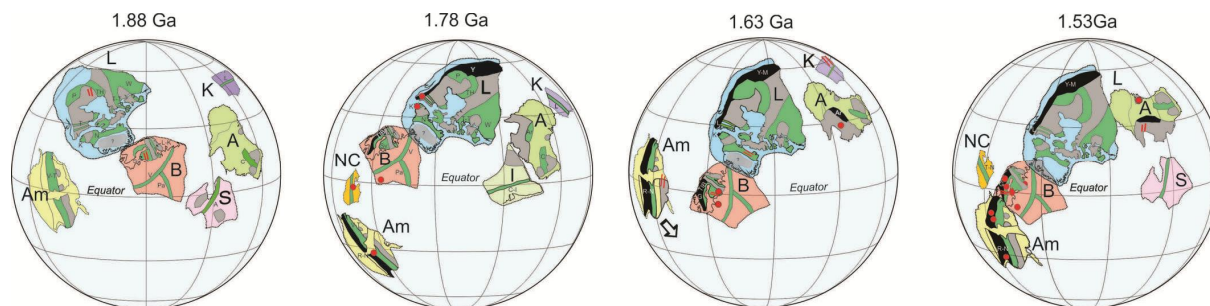


**Figure 2.** A paleomagnetic scenario for the growth of Baltica during the formation of Nuna supercontinent. The reconstructions of cratons and orogenic belts at 1.88, 1.78, 1.63, 1.530, 1.260, 1.04 Ga are after Mertanen and Pesonen (2012). Only those continents are shown where reliable paleomagnetic data are available. Paleolatitudes and orientations of the continents can be determined, but the relative paleolongitudes are based on geological continuities. Successive orogenic belts formed in different stages are shown in green (ca. 1.90-1.84 Ga), black (ca. 1.80-1.70 Ga) and red (ca. 1.1-0.9 Ga). The Achaean cratons are shown in gray. Abbreviations: Australia (A), Amazonia (Am), Baltica (B), Congo/SãoFrancisco (C-Sf), Kalahari (K), Laurentia (L), North China (NC), and Siberia (S).

### 3. Growth and dispersal of Rodinia and Pangaea

During the compilation of the next supercontinent Rodinia, Baltica converged with Amazonia along STZ and grew outward with Sveconorwegian (1.0-0.9 Ga) terranes (**BABEL A**). The dispersal of Rodinia after ca. 600 Ma led to the opening of Tornquist Sea in the South and concurrently the Iapetus Ocean was opened in the West. The Tornquist Sea and Iapetus Ocean were closed at ca. 490-390 Ma when Avalonia and Laurentia collided obliquely with Baltica, resulting to the Variscan and Caledonian orogenic belts, respectively. The subvertical Trans-European Suture Zone (**BABEL A**) was formed in these early stages of Pangaea assembly.

As part of Rodinia supercontinent formation, Baltica collided with Barentsia resulting in Timanide orogeny, in the northeast (**IAR**). The suture zone is transposed by subvertical fault zone indicating transtensional or transpressional tectonic setting at the plate margin. During the break-up of Rodinia an aborted rift was formed within the Barentsia. Later peripheral tectonic events modified the interior parts of Barentsia that proved to be a very successful basin. It acted first as a back arc basin and later as a foreland basin to the Uralian and Caledonian orogens during the formation of the Pangaea supercontinent. Some of the basins were inverted during the break-up of the Pangaea.

#### References:

- Abramovitz, T., Berthelsen, A. and Thybo, H., 1997. Proterozoic sutures and terranes in the southeastern Baltic Shield interpreted from BABEL seismic data: *Tectonophysics*, 270, 259-277.
- Asch, K. 2005. The 1 : 5 Million International Geological Map of Europe and Adjacent Areas. BGR (Hannover), 1 map.
- Bogdanova, S.V., Bingen, B., Gorbatshev, R., Kheraskova, T.N., Kozlov, V.I., Puchkov, V.N., Volozh, Yu.A., 2008. The East European Craton (Baltica) before and during the assembly of Rodinia. *Precambrian Research* 160, 23-45.
- Dvornikov, L.G. 2000. The results of deep seismic investigations on geotraverses in the Barents Sea from Kola Peninsula to Franz-Joseph Land. *Tectonophysics*, vol. 329, pp. 319-331.
- Ivanova, N.M., Sakoulina, T.S., Roslov, Yu.V., 2006. Deep seismic investigation across the Barents-Kara region and Novozemelskiy Fold Belt (Arctic Shelf). *Tectonophysics*, vol. 420, issues 1-2, pp. 123-140.
- Korja, A. & Heikkinen, P., 2005. The Accretionary Svecofennian Orogen - Insight from the BABEL profiles. *Precambrian Research*, 136, 241-268.

- 
- Korja, A., Lahtinen, R. and Nironen, M., 2006. The Svecofennian Orogen: a collage of microcontinents and island arcs. In: D. Gee, R. Stephenson (eds) *European Lithosphere Dynamics*, Geological Society, London, *Memoirs*, 32, 561-578.
- Mertanen, S. and Pesonen, L.J., 2012. Paleo-Mesoproterozoic Assemblages of Continents: Paleomagnetic Evidence for Near Equatorial Supercontinents. In: I. Haapala (Ed.), *From the Earth's Core to Outer Space. Lecture Notes in Earth System Sciences 137*, Springer-Verlag Berlin Heidelberg 2012, 11-35.
- Nikishin, A.M. et al., 1996. Late Precambrian to triassic history of the East European Craton: dynamics of sedimentary basin evolution. *Tectonophysics* 268, 23-63.
- Patison, N.L., Korja, A., Lahtinen, R., Ojala, V.J. and the FIRE Working. 2006. FIRE seismic reflection profiles 4, 4A and 4B: Insights into the Crustal Structure of Northern Finland from Ranua to Näättämö., Geological Survey of Finland, Special Paper 43, 161-222.
- Sakulina, T.S., Roslov, Yu.V., Ivanova, N.M., 2003. Deep Seismic Investigations in the Barents and Kara Seas. *Izvestiya, Physics of the Solid Earth*, vol. 39, No. 6, pp. 438-452. (Translated from *Fizika Zemli*, No. 6, 2003, pp. 5-20).
- Salminen, J., Pesonen, L. J., Mertanen, S., Vuollo, J. and Airo, M.-L., 2009. Palaeomagnetism of the Salla Diabase Dyke, northeastern Finland, and its implication for the Baltica-Laurentia entity during the Mesoproterozoic. In: *Palaeoproterozoic supercontinents and global evolution. Geological Society Special Publication 323*. London: Geological Society, 199-217.

## Evolution of the middle crust in Central Fennoscandia – MIDCRUST

A. Korja<sup>1</sup>, O.T. Rämö<sup>1</sup>, O. Eklund<sup>2</sup>, T. Korja<sup>3</sup>, A. Kärki<sup>3</sup> and P. Hölttä<sup>4</sup>

<sup>1</sup> University of Helsinki

<sup>2</sup> University of Åbo Akademi

<sup>3</sup> University of Oulu

<sup>4</sup> Geological Survey of Finland

E-mail: Annakaisa.Korja [at] helsinki.fi

MIDCRUST is a research initiative of a new Finnish Geoscience consortium "Evolution of the 3D structure of the Svecofennian bedrock". The main objective is to study the mechanisms of crustal spreading and subsequent freezing and exhumation and what is the role of shear zones. The second objective is to determine at what levels, when and for how long the middle crust was flowing and which lithologies and rheologies were involved in the process and how do the shear zones and flow structures interact. These parameters maybe later used in numerical modelling. The third objective is outline how the middle crust effects the upper crust and the upper and middle crust are juxtaposed at surface. The fourth objective is to compile the geophysical and geological data sets a three dimensional crustal model, and to create a conceptual of that can be tested with dynamical analogue and numerical models.

**Keywords:** middle crust, lateral spreading, collapse, Svecofennian, Fennoscandia

### 1. Introduction

For the past decades, the Himalayas have been in the focus of geosciences. The Himalayas are the largest natural laboratories of continental collision and post-collisional stabilization of the crust. Recently numerical modelling experiments based on indirect geophysical evidence and upper crustal surface observations (e.g. Beaumont et al., 2001; Rey et al. 2001; Culshaw et al. 2006) have shown that large part of the stabilization process takes place at middle and lower crust, from where there are only a few direct samples and observations. To better constrain the processes additional observational data is needed from deeper orogenic crustal sections exposed in ancient orogens, such as the Precambrian Svecofennian Orogen in the Fennoscandian Shield. The shields also offer observations on the how and why the process became extinct and what are the end products. These observations will help us to understand the ongoing processes and to better constrain the orogenic models.

The orogenic evolution has three distinct phases, (1) construction of a crustal accretionary wedge, (2) development of a continental plateau, and (3) gravitational collapse - each of which will leave different tectonic and magmatic markers (Beaumont et al., 2004; Vanderhaeghe and Teyssier, 2001a, b). The wedge to plateau transition is caused by the thermal maturation of the thickened crust and the associated genesis of a partially molten, magma bearing, low-viscosity layer within the thickened crust (Vanderhaeghe et al., 2001). The development of a continental plateau is associated with lateral gravity-driven flow of the thermally matured low-viscosity mid- to lower crust composed of migmatites and granulites. Escaping magmas are emplaced as "new granite" and volcanic suites in the plateau. The crust begins to thin only after a plate tectonic setting changes from convergent to extension – driving the thickened orogenic system in to the collapse phase. Although both the lateral spreading and collapse results in thinning and uplifting of the crust, the magmatic families, metamorphic paths, deformation patterns differ considerably.

## 2. Geological and geophysical background

The Svecofennian bedrock is a typical granite gneiss terrane that represents 15-20 km deep section through an evolved orogen. It is part of a larger orogenic system associated with the compilation of the Nuna supercontinent. Similarly to Alpine systems the Svecofennian consists of accreted arc terranes at an older continental margin and it has been evolved in many stages including subduction, oblique collision and post-collisional extension (Lahtinen et al, 2005; Korja A. et al., 2006). Svecofennian is located in the core of a larger orogen and thus it can serve a proxy for the evolution of the modern orogenic cores like the Tibetan plateau or Tauern window in the Alps.

The present exposure level of the Svecofennian orogenic crust (15-25 km), is very close to the upper-middle crust transition (20 km) and thus it should expose lower parts of upper crust, upper-middle crust detachment zones and upper parts of middle crust. Therefore, offers an excellent opportunity to directly study the crustal processes related to the formation of the layering, structures and lithologies formed during this process and during its subsequent exhumation. It also offers excellent opportunities to study midcrustal flow and core complexes – exposed middle crust bordered by blocks and/or fragments from higher crustal levels and/or lower metamorphic grade.

The orogenic core area is covered by world-class observations on granites and migmatites as well as top class crustal scale reflection, tomography and electrical conductivity data sets and models as well as regional scale geological and geophysical maps (Eklund and Shebanov, 2005; Hyvönen et al., 2007; Kärki and Laajoki, 1995; Korja et al., 2009; Korja et al., 2002; Korsman et al., 1999; Kurhila et al., 2010; Rämö et al., 2001; Väisänen et al., 2000). Combining these data sets into a 3D model enables us to work on complex, large scale problems, such as lateral spreading, in space and time.

## 3. Research group

The consortium members are: The Universities of Helsinki, Turku, Oulu and Åbo Akademi, the Geological Survey of Finland, the Finnish Geodetic Institute and Posiva Oy.

The consortium is financed by the Finnish Academy (MIDCRUST 2011-2014) and K.H. Renlund Foundation (2008-). The MIDCRUST project has five subprojects: 3D structure and evolution (A. Korja), Magmatic evolution of the middle crust (O.T. Rämö), Bothnian belt metamorphic core complex (P. Hölttä), Extension, exhumation and mantle process (O. Eklund), Middle and upper crustal shear zones, RLZ (A. Kärki), Geophysical anomalies of the Bothnian belt core complex (T. Korja).

The consortium holds two workshops every February and September and at least one field excursion to the study areas. Workshops and excursions rotate around the study areas. The meetings are open to research partners and collaborators having common research areas or focusing on the same research problems.

## 4. Study areas

For a good three dimensional view of the spreading process, we have chosen four test areas: Central Finland, Bothnian Belt, Southern Finland migmatite zone and Raahe-Ladoga deformation zone. **Central Finland granitoid complex** is situated on the former upper plate (Keitele mc) and it displays the deformation patterns of the lower part of the upper crust and hosts exposures of upper-middle crust (U-M or S-I) detachment zone. Geophysical and magmatic patterns are similar to Tibetan plateau and the area is a test site for plateau building phase. It is potential site also to test late stage magmatic underplating models.

**Bothnian belt** is a potential middle crustal metamorphic core-complex at the western edge of the Keitele mc where the crustal thickness begins to decrease. It displays a migmatitic

core surrounded by lithologies with decreasing metamorphic degree, pervasive low angle lineations. It is hypothesized to represent an uprise of the westward flowing middle crust. This is a test site for middle crustal flow conditions and core complex formation.

**Raahe-Ladoga deformation zone** is a major strike-slip shear zone situated at the eastern margin of Keitele mc. It has been active at several stages and records deformation and associated magmatism at different depths. It is an example on deep level process at major strike slip faults and/or continental transform boundaries or transfer shear zones. The zone records the 3D effects of sideways spreading and interactions between midcrustal flow and deep level shear zones. Mantle involvement will be tested with petrogenetic studies of subalkaline intrusions and lamprophyres and bimodal basaltic - microtonalitic dykes localized at the plate boundary.

**Southern Finland migmatite zone** is located within the Bergslagen microcontinent. Although its plate tectonic position just prior to the collision is debated, it is assumed that the plate boundary was free to move, and that it has been active for a prolonged period of time. Migmatites, which are partially molten rocks of the middle crust, are well exposed in this area, so they can be studied for midcrustal flow mechanisms, directions and depths. Deformation mechanisms below the hypothesized migmatite channel may be exposed in a core complex structure within this zone (West Uusimaa Complex).

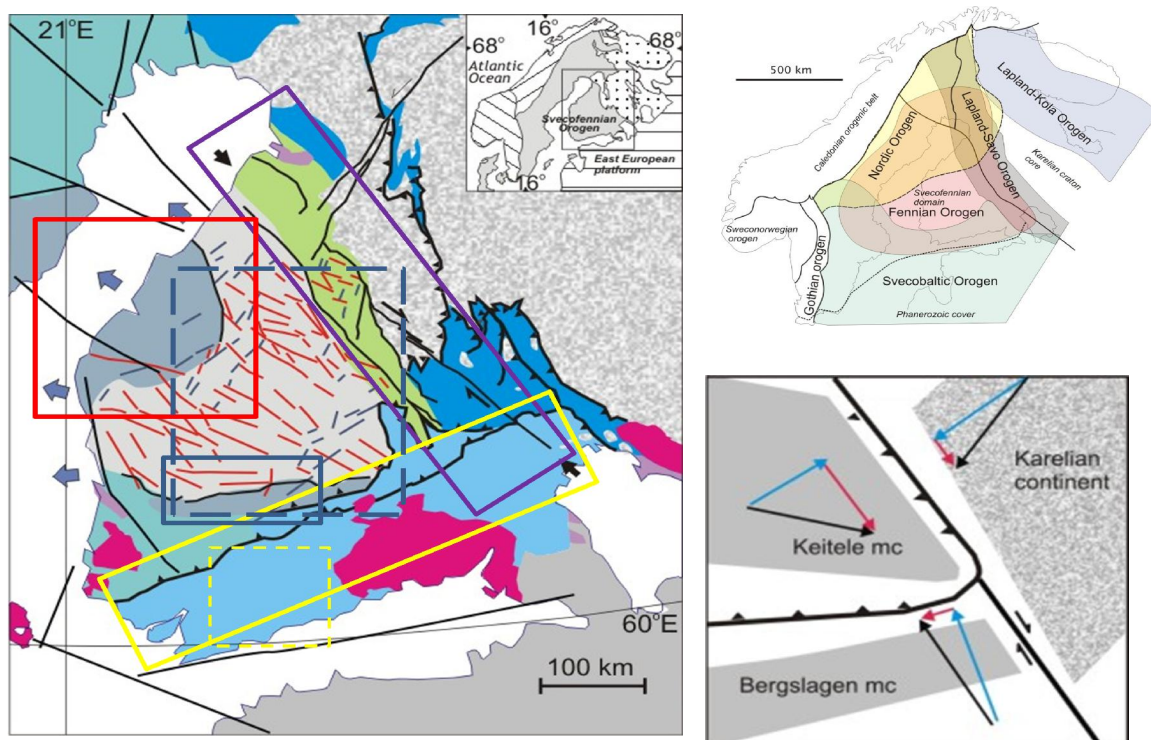


**Figure 1.** Study areas of the MIDCRUST project are shown with rectangular. Bothnian belt - red; Central Finland granitoid complex - dashed blue; Raahe-Ladoga deformation zone – lila, Southern Finland migmatite zone – solid yellow. The maps are after Korja et al., 2009 and lahtinen et al., 2009.

## 5. Conclusions

MIDCRUST project work is in midphase. Data has been acquired from several subregions, interdisciplinary studies have been initiated and new researcher methods are being tested. The preliminary results of the project will be reported by individual researchers during

Lithosphere 2012 - symposium. For more details see: Chopin et al., 2012; Eklund and Fröjdö, 2012; Kurhila et al., 2012; Kärki et al., 2012; Nikkilä et al., 2012; Rämö et al., 2012; Vaittinen et al., 2012 in this volume. Researchers interested in the project are encouraged to contact the authors of this paper.

### References:

- Andersen, T., Rämö, O.T. (Guest Editors), 2007. Granites and Crustal Anatexis, Special Issue. *Lithos* 93 (3-4), 215-339.
- Beaumont, C., Jamieson R.A., Nguyen, M.H. & Medvedev, S. 2004. Crustal channel flows: 1. Numerical models with applications to the tectonics of the Himalayan-Tibetan orogen. *Journal of Geophysical Research - Solid Earth*, 109, doi:10.1029/2003JB002809.
- Culshaw, N. G., Beaumont, C. & Jamieson, R. A. 2006. The orogenic superstructure-infrastructure concept; revisited, quantified, and revived. *Geology*, 34, 733-736.
- Eklund, O., Shebanov, A. (2005) The prolonged Svecofennian post-collisional shoshonitic magmatism in the southern part of the Svecofennian domain – a case study of the Åva granite – lamprophyre ring complex *Lithos* 80: 229-247.
- Hyvönen, T., Tiira, T., Korja, A., Heikkinen, P., Rautioaho, E. and SVEKALAPKO Seismic Tomography Work, 2007. A tomographic crustal velocity model of the central Fennoscandian Shield. *Geophys J. Int.* 168, 1210-1226.
- Kärki, A. & Laajoki, K. 1995. An interlinked system of folds and ductile shear zones - late stage Svecokarelian deformation in the central Fennoscandian Shield. *J. Struct. Geol.* 17:1233-1247.
- Korja, A., Kosunen, P. and Heikkinen, P.J. 2009. A Case Study of Lateral Spreading the Precambrian Svecofennian Orogen In: Ring, U. and Wernicke, B. *Extending a Continent: Architecture, Rheology and Heat Budget*. Geological Society of London, Special Paper 321, 225–251. DOI: 10.1144/SP321.11
- Korja, A., Lahtinen, R. and Nironen, M., 2006. The Svecofennian Orogen: a collage of microcontinents and island arcs. In: D. Gee, R. Stephenson (eds) *European Lithosphere Dynamics*, Geological Society, London, *Memoirs*, 32, 561-578.
- Korja T., Engels M., Zhamaletdinov A.A., Kovtun A.A., Palshin N.A., Smirnov M.Yu., Tokarev A., Asming V.E., Vanyan L.L., Vardaniants I.L., and the BEAR Working Group, 2002. Crustal conductivity in Fennoscandia - a compilation of a database on crustal conductance in the Fennoscandian Shield. *Earth Planets Space*, 54, 535-558.
- Korsman, K., Korja, T., Pajunen, M., Virransalo, P. and the GGT/SVEKA Working Group, 1999. The GGT/SVEKA Transect: Structure and Evolution of the Continental Crust in the Palaeoproterozoic Svecofennian Orogen in Finland. *International Geology Review*, 41,4, 287-333.
- Kurhila, M., Andersen, T., Rämö, O.T., 2010. Diverse sources of crustal granitic magma: Lu-Hf isotope data on zircon in three Paleoproterozoic leucogranites of southern Finland. *Lithos*, in press.
- Lahtinen, R., Korja, A. and Nironen, M., 2005. Paleoproterozoic tectonic evolution. In: Lehtinen, M., Nurmi, P. and Rämö, O.T. (Eds.): *Precambrian Geology of Finland - Key to the Evolution of the Fennoscandian Shield*. Elsevier B.V., Amsterdam, pp. 481-532.
- Lahtinen, R., Korja, A., Nironen, M. & Heikkinen, P., 2009. Palaeoproterozoic accretionary processes in the Fennoscandia. p. 237-256. In: P. Cawood, and A. Kroener (eds.) *Earth Accretionary Orogens in Space and Time*, Special Pub. Geol. Soc. London, v. 318; p. 237-256. doi:10.1144/SP318.
- Rämö, O.T., Vaasjoki, M., Mänttari, I., Elliott, B.A., Nironen, M., 2001. Petrogenesis of the post-kinematic magmatism of the Central Finland Granitoid Complex I; radiogenic isotope constraints and implications for crustal evolution. *Journal of Petrology* 42 (11), 1971-1993.
- Rey, P., Vanderhaeghe, O. & Teyssier, C. 2001. Gravitational collapse of the continental crust; definition, regimes and modes. *Tectonophysics*, 342, 435-449.
- Rey PF, Teyssier, C., Whitney DL, 2009. Extension rates, crustal melting, and core complex dynamics. *Geology* 37, 5, 391-394.
- Väisänen, M., Mänttari, I., Kriegsman, L.M., Hölttä, P., 2000. Tectonic setting of post-collisional magmatism in the Palaeoproterozoic Svecofennian Orogen, SW Finland. *Lithos* 54 (1–2), 63–81.
- Vanderhaeghe, O. & Teyssier, C. 2001a. Crustal-scale rheological transitions during late-orogenic collapse: *Tectonophysics*, 335, 211-228.
- Vanderhaeghe, O. and Teyssier, C. 2001b. Partial melting and flow of orogens: *Tectonophysics*, 342, 451-472.

# Structure of the upper mantle in the northern Fennoscandian Shield obtained by joint inversion of POLENET/LAPNET P- and S- receiver functions

E. Kozlovskaya<sup>1</sup>, L. Vinnik<sup>2</sup>, G. Kosarev<sup>2</sup>, S. Oreshin<sup>2</sup> and POLENET/LAPNET Working Group

<sup>1</sup>Sodankyla Geophysical Observatory/Oulu Unit, University of Oulu  
POB 3000 FIN-90014 University of Oulu, FINLAND

<sup>2</sup>Schmidt Institute of Physics of the Earth, RAS, Moscow, Russia  
E-mail: elena.kozlovskaya [at] oulu.fi

We present results of joint inversion of P- and S- receiver functions estimated from data of the POLENET/LAPNET temporary array in northern Fennoscandian Shield.

**Keywords:** joint inversion, P-receiver functions, S-receiver functions, lithosphere, asthenosphere

## 1. Introduction

In order to understand structure of the crust and sub-continental lithospheric mantle (SCLM) beneath the northern Fennoscandian Shield, we used joint inversion of P- and S- receiver functions (PRF and SRF, respectively) estimated from data of the POLENET/LAPNET seismic array experiment in northern Fennoscandia during the International Polar Year (IPY) 2007-2009. The array consisted of 37 temporary stations deployed in northern Finland, Norway and Russia and of 21 permanent broadband stations operated by several research institutions in northern Fennoscandia. Most of the stations of the array were equipped by the broadband instruments. The array registered teleseismic, regional and local events during May 2007 – September 2009.

## 2. Method

The P- and S-receiver functions were estimated at broadband stations of the array using recordings of teleseismic events. The filtered PRF and SRF from individual events were then stacked and resulting waveforms were inverted using the global optimization procedure based on the Simulated Annealing (SA) algorithm (Kiselev, 2008). The obtained models were also constrained by the travel time residuals of Ps conversions from 410 km and 660 km discontinuities. In inversion we assumed that the structure of the Earth in the vicinity of the station is laterally homogeneous and isotropic. Results of previous wide-angle reflection and refraction profiles in the area were used to define the range of variations of P- and S-wave velocities in the crust. At first, the inversion procedure was verified with the data from stations located along the POLAR wide-angle reflection and refraction profile and FIRE4 near-vertical reflection transect, for which the structure of the crust is known. After that the technique was used with the data of other stations of the array.

## 3. Results and conclusions

- 1) The Moho depth estimated by joint inversion of PRF and SRF is in good agreement with the Moho obtained by controlled-source experiments in the areas with the flat Moho. However, the joint inversion of PRS and SRF is not very reliable and should be applied with caution in the areas with large variations of the Moho depth.
- 2) The deepest Moho (about 60 km) was found in the southeastern part of our study area.

- 3) Joint interpretation of PRF and SRF revealed heterogeneous structure of the upper mantle beneath the eastern part of the POLENET/LAPNET array down to 200-250km;
- 4) S-wave velocities beneath 200-230 km are close to the S-wave velocities in the IASP91 model;
- 5) Mantle with  $V_s > V_s(\text{iasp91})$  from the Moho down to 200-230 km has been revealed in the southern part of the study area corresponding to the non-reworked part of the Karelian Craton;
- 6) Mantle with heterogeneous layer from the Moho down to 90-120 km has been revealed in the northern part of the array (Kola Craton and Belomorian Belt and reworked part of the Karelian craton);
- 7) No low S-wave velocity layer corresponding to the asthenosphere has been revealed;
- 8) A boundary with positive contrast of P-wave velocities at 200-230 km has been found beneath the whole study area; P-wave velocities beneath this boundary are higher than the velocities in the IASP91 model.

The future work will be comparison of our results with the results of surface wave studies and teleseismic body wave tomography.

### **Acknowledgments:**

*POLENET/LAPNET Working Group:* Elena Kozlovskaya, Helle Pedersen, Jaroslava Plomerova, Ulrich Achauer, Eduard H Kissling, Irina Sanina, Teppo Jämsen, Hanna Silvennoinen, Catherine Pequegnat, Riitta Hurskainen, Helmut Hausmann, Petr Jedlicka, Igor Aleshine, Ekaterina Bourova, Reynir Bodvarsson, Ewald P Brueckl, Tuna Eken, Pekka J Heikkinen, Gregory A Houseman, Helge Johnsen, Kari Komminaho, Helena Munzarova, Roland Roberts, Bohuslav Ruzek, Zaher Hosein Shomali, Johannes Schweitzer, Artem Shaumyan, Ludek Vecsey, Sergei Volosov

*Institutions participating in the POLENET/LAPNET experiment:*

Sodankylä Geophysical Observatory of the University of Oulu (FINLAND)

Institute of Seismology of the University of Helsinki (FINLAND)

University of Grenoble (FRANCE)

University of Strasbourg (FRANCE)

Institute of Geodesy and Geophysics, Vienna University of Technology (AUSTRIA)

Geophysical Institute of the Czech Academy of Sciences, Prague (CZECH REPUBLIC)

Institute of Geophysics ETH Zürich (SWITZERLAND)

Institute of Geospheres Dynamics of the Russian Academy of Sciences, Moscow (RUSSIA)

Geophysical Centre of the Russian Academy of Sciences, Schmidt Institute of Physics of the Earth of the Russian Academy of Sciences (RUSSIA)

Swedish National Seismological Network, University of Uppsala (SWEDEN)

Institute of Solid Earth Physics, University of Bergen (NORWAY)

NORSAR (NORWAY)

University of Leeds (UK)

---

## **Delineating ophiolite-derived host rocks of massive sulfide Cu-Co-Zn deposits with 2D high resolution seismic reflection data in Outokumpu, Finland**

I.T. Kukkonen<sup>1</sup>, S. Heinonen<sup>2</sup>, P. Heikkinen<sup>2</sup> and P. Sorjonen-Ward<sup>3</sup>

<sup>1</sup>Geological Survey of Finland, Southern Finland Office, P.O.Box 96, FI-01251 Espoo, Finland,

<sup>2</sup>Institute of Seismology, Department of Geosciences and Geography, P.O. Box 68,  
00014 University of Helsinki, Finland

<sup>3</sup>Geological Survey of Finland, Eastern Finland Office, P.O.Box 1237,  
FI-70211 Kuopio, Finland

E-mail: ilmo.kukkonen [at] gtk.fi

Seismic reflection method is a very effective tool in structural studies of mine camps and exploration areas. We present a case history from the Outokumpu ore belt, eastern Finland. The seismic survey has shed new light on the much discussed deep structures of this classical ore belt and has provided new ideas for further exploration in the area.

**Keywords:** seismic reflection, massive sulphides, upper crust, Outokumpu, Fennoscandian Shield

### **Summary**

Seismic reflection data was applied to study the upper crustal structures in the Outokumpu mining and exploration area, eastern Finland. The Cu-Co-Zn sulfide ore deposits of the Outokumpu area are hosted by Palaeoproterozoic ophiolite-derived altered ultrabasic rocks (serpentinite, skarn rock and quartz rock) and black schist within turbiditic mica schist. Mining in the Outokumpu area has produced a total of 36 Mt of ore from three historical and one active mine. Seismic data comprises 2D Vibroseis data surveyed along a network of local roads. The seismic sections provide a comprehensive 3D view of the reflective structures. Acoustic rock properties from down-hole logging and synthetic seismograms indicate that the strongly reflective packages shown in the seismic data can be identified as the host rock environments of the deposits. Reflectors show excellent continuity along the structural grain of the ore belt which allows correlating reflectors with surface geology, magnetic map and drilling sections into a broad 3D model of the ore belt. Massive ores have acoustic properties which make them directly detectable with seismic reflection methods assuming the deposit size is sufficient for applied seismic wave lengths. The seismic data revealed numerous interesting high-amplitude reflectors within the interpreted host rock suites potentially coinciding with sulfides.

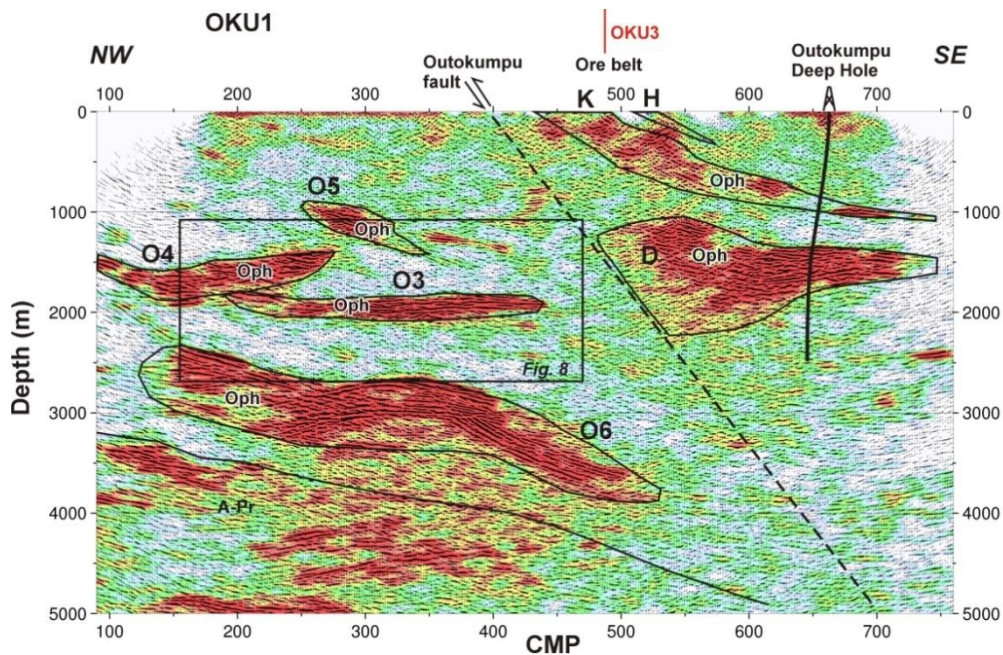


**Figure 1.** Migrated NMO section of one of the the Outokumpu reflection seismic survey lines (OKU1) crossing the ore belt in NW-SE direction and showing the interpreted reflectors and the Outokumpu fault. Oph: Known and interpreted reflectors from ophiolite-derived altered ultrabasic rocks (the host rocks of the Outokumpu-type massive sulphide deposits) (adopted from Kukkonen et al., 2012).

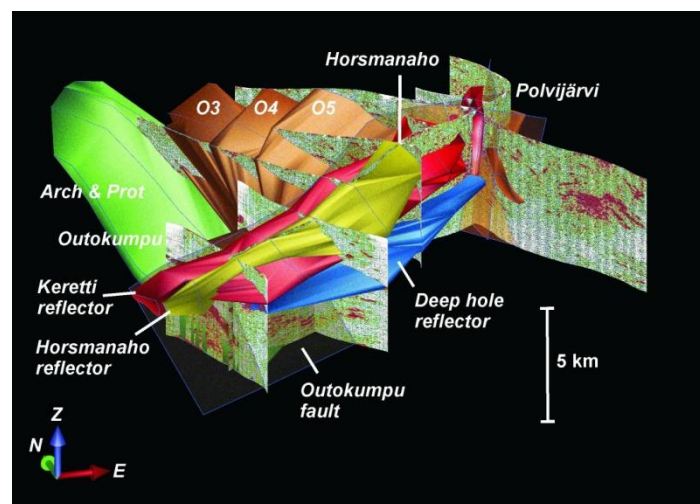


**Figure 2.** Perspective view from south of the seismic profiles in the Outokumpu area together with 3D modeling results of reflector bodies.

#### Reference:

Kukkonen, I.T., , Heinonen, S., Heikkinen, P. and Sorjonen-Ward, P., 2012. Delineating ophiolite-derived host rocks of massive sulfide Cu-Co-Zn deposits with 2D high-resolution seismic reflection data in Outokumpu, Finland. *Geophysics*, 77, No. 5, p. WC213–WC222.

## Geochronology and isotopic characterization of the Vaasa complex in western Finland

M. Kurhila<sup>1</sup>, E. Suikkanen<sup>2</sup> and A. Kotilainen<sup>2</sup>

<sup>1</sup>Institute of Seismology, Department of Geosciences and Geography, FIN-00014 University of Helsinki

<sup>2</sup>Division of Geology, Department of Geosciences and Geography, FIN-00014 University of Helsinki

E-mail: matti.kurhila [at] helsinki.fi

We present new U-Pb ages and Hf isotopic data on zircon as well as whole-rock Nd isotopic data from granitoid and migmatite rocks from the Paleoproterozoic Vaasa complex in western Finland. For comparison, a mica schist from the adjacent Evijärvi schist belt and an A-type granite south of the Vaasa complex were also included in the set of samples. The results imply emplacement ages of ~1.88 to 1.85 Ga for the granitoid rocks. Inherited zircon is abundant. Initial  $\epsilon_{\text{Hf}}$  values are mostly negative, except for the northernmost granitoid which has more juvenile zircon. Nd isotope results comply with these, displaying mostly slightly negative initial  $\epsilon_{\text{Nd}}$  values and depleted mantle model ages between 2.3 Ga and 2.6 Ga. Our results support the idea of the surrounding schists as the sources of the granitoid rocks within the complex.

**Keywords:** Granitoid, migmatite, U-Pb, Lu-Hf, Sm-Nd, zircon, Fennoscandia

### 1. Introduction

The Svecofennian domain of the Fennoscandian shield was accreted onto the Archean Karelian craton ~2.0 – 1.9 Ga ago with several magmatic events (e.g., Nironen, 1997; Korsman et al., 1999), collectively known as the Svecofennian orogeny. The Bothnian belt in western Finland is thought to represent a metamorphic core complex structure, formed after the initial collision in an extensional environment. The complex has a migmatitic core, surrounded by gneisses and schists. The metamorphic grade decreases concentrically outwards from the core. The Vaasa complex is clearly visible on an aeromagnetic map (Fig. 1). Most of our samples are from within the migmatite zone, and represent granitoid or diatexitic migmatite rocks. For comparison a garnet-cordierite-mica schist (A2182) from the Evijärvi belt and an A-type granite (n4279) from Kurikka south of the complex were also included.

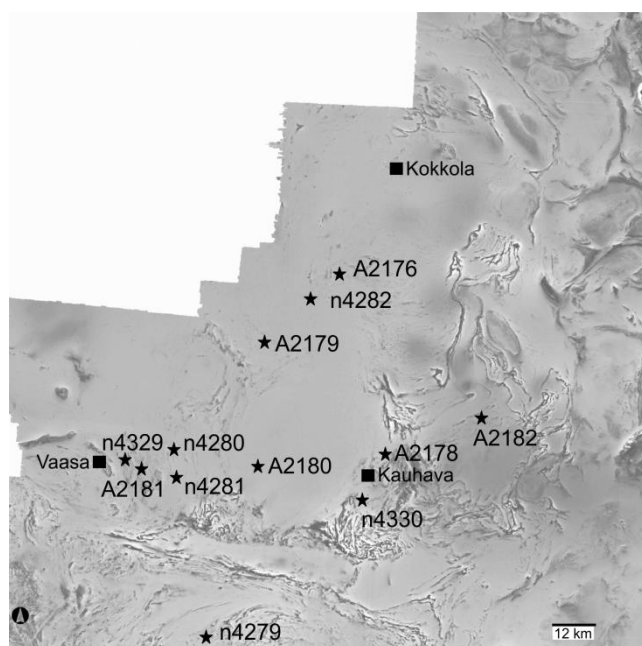


**Figure 1.** Aeromagnetic map of the Vaasa complex with sampling sites indicated. The complex is clearly distinguishable from the surrounding schist belts by its lack of magnetic anomalies

## 2. U-Pb results

The U-Pb isotopic analyses were performed by secondary ion mass spectrometry (SIMS) in Stockholm and by laser-ablation ICP-mass spectrometry (LAMS) at the SIGL laboratory in Espoo. The age results are shown in Tables 1 and 2 below.

**Table 1.** U-Pb ages of the samples dated with SIMS. Locations marked in Fig. 1

Sample	n4279	n4280	n4281	n4282	n4329	n4330
Age (Ma)	1868	1874	1878	1869	1873	1876
Error (Ma)	6	4	3	3	6	3
Inherited age groups (Ga)	2.0	2.0, 2.6, 2.9	2.5	2.0	-	2.0, 2.9

**Table 2.** U-Pb ages of the samples dated with LAMS. Locations marked in Fig. 1

Sample	A2176	A2178	A2179	A2180	A2181	A2182
Age (Ma)	1870	1849	1932	1853	1858	1985
Error (Ma)	8	10	33	13	10	12
Inherited age groups (Ga)	-	-	2.7	2.2, 2.6, 2.7	2.0, 2.5, 2.7	2.5-2.9

Most of the age results coincide with the main stage of the Svecofennian orogeny, i.e., 1.88-1.87 Ga. These ages are also in accordance with the (sparse) previously published results from the area (Sipilä et al., 2008, Lehtonen et al., 2005, Alviola et al., 2001). Inherited zircons are abundant in most samples, the most common inherited ages are either ~2.0 Ga or Archean. Even the A-type granite outside of the Vaasa complex yielded inherited ages.

The Evijärvi schist has more inherited zircon than the granitoids and migmatites, but their age ranges are roughly the same, suggesting that the schist could be the protolith of the granitoid rocks. This is corroborated by the fact that the main zircon population in the schist has an approximate age of ~2.0 Ga, the same as a major inherited population in many granitoids and migmatites.

## 3. Hf and Nd isotopic results

Hf isotopic composition of zircon was determined by LAMS, and the whole-rock Nd isotopes were analysed by thermal ionization mass spectrometry at the laboratory of isotope geology in GTK, Espoo. Both of these were only done for the A-coded samples. The Hf results are depicted in Figure 2.

The northernmost sample A2176 has the most juvenile zircon, with mostly positive initial  $\epsilon_{\text{Hf}}$  values. We also did not encounter any inherited zircon in this sample. Towards the south, the Hf isotope composition becomes less radiogenic, indicating longer crustal residence

ages. Overall, there are quite large differences within any single sample, which suggests that the source rocks had mixed, detrital zircon populations.

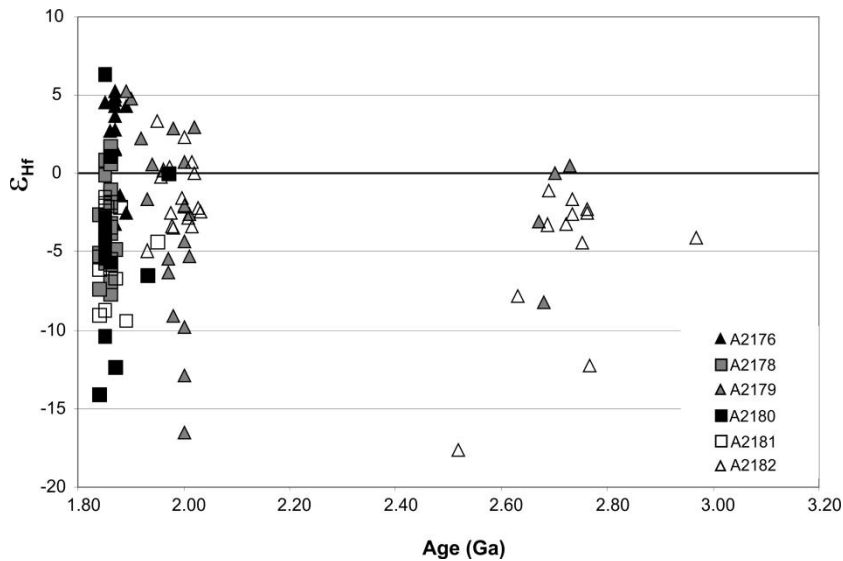


**Figure 2.** Initial epsilon-Hf values of selected zircon grains from the Vaasa complex (A2176-2181) and from the Evijärvi schist belt (A2182)

Remarkably, many inherited Archean zircon grains also have very unradiogenic initial Hf isotope composition, implying that the source contained already a significantly older recycled component at that time. In general, the Hf isotopic compositions of the granitoid rocks and the schist are similar, which supports their common origin.

Whole-rock Nd isotopes do not show that much variation. All analysed samples have moderately unradiogenic Nd isotope composition, with initial  $\epsilon_{Nd}$  values between -2 and -4, and depleted mantle model ages (dePaolo, 1981) from ~2.3 Ga to ~2.6 Ga. The samples do, however, show considerable variation in their REE concentrations, which might derive from different degrees of melting.

#### 4. Conclusions

Combined U-Pb, Lu-Hf and Sm-Nd isotopic evidence points to the origin of the Vaasa complex at the culmination of the Svecofennian orogeny at ~1.88-1.87 Ga. The source rocks for the granitoids in the core of the complex were most likely the schists surrounding the complex, which in turn contain a significant detrital zircon component. An ancient crustal recycling is reflected in the unradiogenic Archean inherited zircons. Whole-rock Nd isotopes reflect late Archean to early Proterozoic depleted mantle model ages, in concordance with the Hf and U-Pb results.

#### References:

- Alviola, R., Mänttari, I., Mäkitie, H. and Vaasjoki, M., 2001. Svecofennian rare-element granitic pegmatites of the Ostrobothnia region, western Finland : their metamorphic environment and time of intrusion. In: Mäkitie, H. (ed.) Svecofennian granitic pegmatites (1.86-1.79 Ga) and quartz monzonite (1.87 Ga), and their metamorphic environment in the Seinäjoki region, western Finland. Geological Survey of Finland. Special Paper 30, 9-29.
- DePaolo, D.J., 1981. Neodymium isotopes in the Colorado Front Range and crust-mantle evolution in the Proterozoic. *Nature* 291, 193-196.
- Korsman, K., Korja, T., Pajunen, M., Virransalo, P. and GGT/SVEKA Working Group, 1999. The GGT/SVEKA Transect: Structure and evolution of the continental crust in the Paleoproterozoic Svecofennian orogen in Finland. *International Geology Review* 41, 287-333.
- Lahtinen, R. and Huhma, H., 1997. Isotopic and geochemical constraints on the evolution of the 1.93-1.79 Ga Svecofennian crust and mantle in Finland. *Precambrian Research* 82, 13-34

- 
- Lehtonen, M., Kujala, H., Kärkkäinen, N., Lehtonen, A., Mäkitie, H., Mänttari, I., Virransalo, P. and Vuokko, J., 2005. Etelä-Pohjanmaan liuskealueen kallioperä. Summary: Pre-Quaternary rocks of the South Ostrobothnian Schist Belt. Geologian tutkimuskeskus. Tutkimusraportti 158. Espoo: Geologian tutkimuskeskus. 155 pages.
- Nironen, M., 1997. The Svecofennian orogen: a tectonic model. *Precambrian Research* 86, 21-44.
- Sipilä, P., Kujala, H. and Torssonen, M., 2008. Pre-Quaternary rocks of the Oravainen–Lapua–Alahärmä area. Geological Survey of Finland, Report of Investigation 170, 40 pages.

# Revised U-Pb zircon ages of supracrustal rocks of the Palaeoproterozoic Tampere Schist Belt, southern Finland

Yrjö Kähkönen<sup>1</sup> and Hannu Huhma<sup>2</sup>

<sup>1</sup>Division of Geology, P.O. Box 64, FI-00014 University of Helsinki, Finland

<sup>2</sup>Geological Survey of Finland, P.O. Box 96, FI-02151 Espoo, Finland

E-mail: yrjo.kahkonen [at] helsinki.fi

Revised U-Pb zircon datings by CA-TIMS and LA-MC-ICP-MS indicate that subduction-related volcanism in the Central Tampere Schist Belt (CTSB) commenced at 1895-1900 Ma, i.e. five to ten Ma later than earlier studies have suggested. The results also provide signs of ca. 1.88 Ga volcanism and deposition, i.e. five to ten Ma after the formation of the youngest volcanic rocks identified so far in the CTSB. Some implications of these results are briefly discussed in the text.

**Keywords:** U-Pb, zircon, CA-TIMS, LA-MC-ICP-MS, volcanic, Palaeoproterozoic, Svecofennian, Tampere

## 1. Introduction

The ca. 1.9 Ga Central Tampere Schist Belt (CTSB; Figure 1) shows evolution from EMORB/WPB-type Haveri pillow basalts to deposition of the voluminous turbidites of the Myllyniemi Formation at ca. 1.92-1.90 Ga, and further to subduction-related volcanism and related sedimentation at ca. 1.90-1.89 Ga (e.g. Kähkönen, 2005; Lahtinen et al., 2009). Taken largely, the CTSB composes an E-W trending syncline but its southern parts consist of 1.90-1.89 Ga arc-type volcanic and related sedimentary rocks coeval with those relatively high in the stratigraphic column of the major syncline (Kähkönen et al., 2004).

We present and discuss here results of multigrain CA-TIMS (chemical abrasion thermal ionization mass spectrometry) analyses on four CTSB samples as well as results of LA-MC-ICP-MS (laser ablation multi-collector inductively coupled plasma mass spectrometry) analyses on two of these. Most of the samples have formerly been dated by multigrain TIMS. In addition, we briefly discuss some implications of the results for the evolution of the CTSB.

## 2. Volcanic rocks A384 & A385 Koskuenjärvi and A386 Sammatinjärvi

Based on discordant TIMS data, Kähkönen et al. (1989) dated two volcanic rocks near *Lake Koskuenjärvi* (Figure 1) at an age of  $1904 \pm 4$  Ma. This age has since then been considered to represent oldest subduction-related volcanic events in the CTSB.

The new CA-TIMS data from the *Koskuenjärvi* samples (dacite A384, rhyolite A385) yields concordant results at  $1895 \pm 3$  Ma. The age is consistent with the  $1896 \pm 3$  Ma age of the nearby Pukala porphyry (A1675; Talikka and Mänttari, 2005).

The *Sammatinjärvi* dacite (A386; Figure 1) has a published age of  $1898 \pm 4$  Ma (Kähkönen et al., 1989). The new CA-TIMS analysis on A386 yields nearly concordant data and together with the old data gives an age of  $1897 \pm 3$  Ma. In all, reference to ages exceeding 1.9 Ga should no more be made for these rocks.

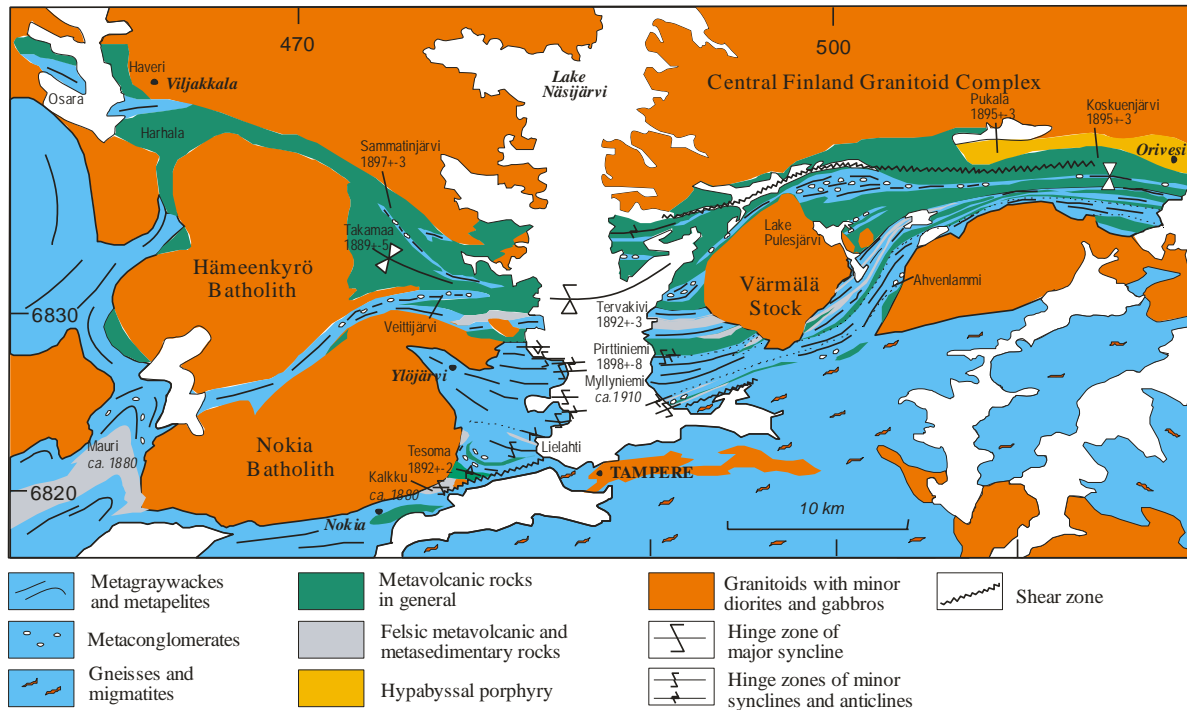


**Figure 1.** Lithological map of the CTSB with major and minor synclines and anticlines as well as U-Pb zircon ages. The dotted lines give postulated boundaries of the Myllyniemi Formation to the younger volcanic and related sedimentary rocks in the north and in the south. The numbers below locality names give U-Pb zircon ages in Ma; *those in italics are maximum ages of deposition in Ma*. Modified from Kähkönen (2005). Data from (Kähkönen et al., 1989, 2004) and this study.

### 3. Kalkku arenite A7

The Kalkku arenite was classified as acid porphyry by Matisto (1961) but later Matisto (1977) mentions it as an eastern equivalent of the Mauri arkose (see below). It is characterized by cross-bedded sandstones but in places cross-bedding is poorly visible (Kähkönen, 1999). Both types are dominated by clasts of felsic volcanic material. In addition, a few rounded to angular, dark-coloured volcanic clasts, intermediate to mafic in composition, do occur. The Kalkku arenite is situated in the southernmost CTSB and composes a minor syncline bordered to the south by a shear zone (Figure 1). Sample A7 comes from the southernmost cliffs of the syncline, where no cross-bedding has been observed.

The Kalkku arenite was dated by Kähkönen et al. (1989) at  $1889 \pm 19$  Ma. The CA-TIMS analysis from the Kalkku A7 zircon gave a  $^{207}\text{Pb}/^{206}\text{Pb}$  age of 1951 Ma, which is much older than expected from the old results.

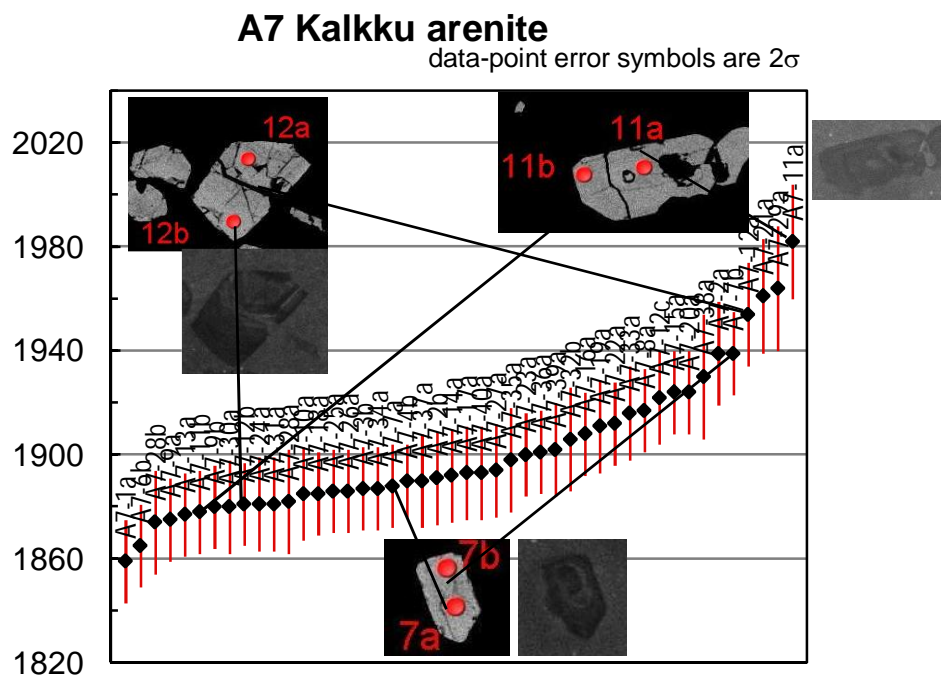


**Figure 2.** Zircon  $^{207}\text{Pb}/^{206}\text{Pb}$  ages for concordant U-Pb LA-MC-ICP-MS data from A7 Kalkku.

Most of the 47 LA-MC-ICPMS analyses on 40 zircon grains of A7 Kalkku give concordant results, but yield a range of ages from ca. 1.86 Ga to 1.98 Ga with abundant ca. 1.88 Ga grains (Figure 2). Some grains have older cores and large ca. 1.88 Ga mantle domains. The proportion of inherited zircon was significant and the data do not allow pointing out a single source age.

A major magmatic crystallization probably took place ca. 1.88 Ga ago. Thus the Kalkku arenite was deposited only after ca. 1.88 Ga, i.e. some 5 to 10 Ma after the latest volcanic events (see Kähkönen et al., 1989; Lahtinen et al., 2009) identified so far in the CTSB. In addition, there seems to be a ca. 10 Ma gap between the Kalkku arenite and the  $1892 \pm 3$  Ma dacite (Kähkönen et al., 2004) exposed in the minor Tesoma anticline immediately north of Kalkku.

#### 4. Mauri arenite A1398

Matisto (1968, 1977) considered the up to 2 km thick, predominantly cross-bedded Mauri sandstone (Figure 1) as arkose while Kähkönen (1999) interpreted these rocks as largely lithic volcanoclastic arenites. Zircon in the Mauri arenite has been dated at ca. 1.9 Ga (Matisto, 1968) and the results of three unpublished U-Pb TIMS analyses, made on this unit since then at the Geological Survey of Finland, are consistent with this age.

The zircon population from the Mauri arenite sample A1398 looks heterogeneous. Many grains are euhedral, prismatic, short and only slightly rounded on crystal edges. A lot of strongly reddish grains occur but some zircons are pale.

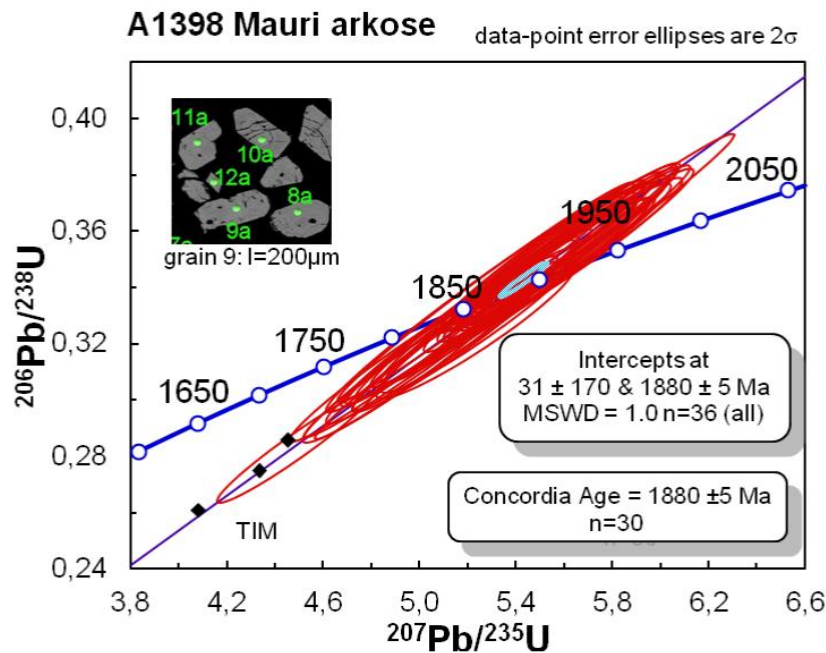


**Figure 4.** Concordia diagram showing TIMS (black dots) and LA-MC-ICP-MS (red error ellipses) U-Pb isotopic data on zircon from A1398 Mauri.

Most of the current 37 LA-MC-ICP-MS analyses on zircon from A1398 yield concordant data and give an age of  $1880 \pm 5$  Ma. A short period for formation of the source(s) of zircon is evident for this sandstone. The Mauri arenite, like the Kalkku arenite, indicates relatively late magmatism and deposition in the CTSB.

#### References:

- Claesson, S., Huhma, H., Kinny, P.D., Williams, I.S., 1993. Svecofennian detrital zircon ages - implications for the Precambrian evolution of the Baltic Shield. *Precambrian Research* 64, 109-130.
- Huhma, H., Claesson, S., Kinny, P.D., Williams, I.S., 1991. The growth of Early Proterozoic crust: new evidence from Svecofennian zircons. *Terra Nova* 3, 175-179.
- Kähkönen, Y., 1999. Stratigraphy of the central parts of the Palaeoproterozoic Tampere Schist Belt, southern Finland; review and revision. *Bulletin of the Geological Society of Finland* 71, 13-29.
- Kähkönen, Y., Huhma, H., Aro, K., 1989. U/Pb zircon ages and Rb/Sr whole-rock isotope studies of early Proterozoic volcanic and plutonic rocks near Tampere, southern Finland. *Precambrian Research* 45, 27-43.
- Kähkönen, Y., Huhma, H., Mänttari, I., 2004. TIMS and SIMS U-Pb zircon ages on metavolcanic rocks from central parts of the Paleoproterozoic Tampere belt, Finland. In: *The 26th Nordic Geological Winter Meeting, January 6th - 9th 2004, Uppsala, Sweden: abstract volume. GFF* 126, 25.
- Lahtinen, R., Huhma, H., Kähkönen, Y., Mänttari, I., 2009. Paleoproterozoic sediment recycling during multiphase orogenic evolution in Fennoscandia, the Tampere and Pirkanmaa belts, Finland. *Precambrian Research* 174, 310-336.
- Matisto, A., 1961. Geological map of Finland, Pre-Quaternary rocks, 1 : 100 000, sheet 2123 Tampere. Geological Survey.
- Matisto, A., 1968. Die Meta-Arkose von Mauri bei Tampere. *Bulletin de la Commission géologique de Finlande* 235, 1-21.
- Matisto, A., 1977. Tampereen kartta-alueen kallioperä. Summary: Precambrian rocks of the Tampere map-sheet area. Geological map of Finland 1 : 100 000. Explanation to the map of rocks, sheet 2123 Tampere. Geological Survey of Finland, Espoo, 1-50.
- Talikka, M., Mänttari, I., 2005. Pukala intrusion, its age and connection to hydrothermal alteration in Orivesi, southwestern Finland. *Bulletin of the Geological Society of Finland* 71, 165-180.

## Structure of the Raahe –Ladoga Shear Complex

A. Kärki<sup>1</sup>, T. Korja<sup>2</sup>, M. Mahmoud<sup>2</sup>, M. Pirttijärvi<sup>2</sup>, J. Tirroniemi<sup>1</sup>, P. Tuisku<sup>1</sup>  
and J. Woodard<sup>1</sup>

<sup>1</sup>Department of Geosciences, Univ. of Oulu, PL 3000, 90014 University of Oulu, Finland

<sup>2</sup>Department of Physics, Univ. of Oulu, PL 3000, 90014 University of Oulu, Finland

E-mail: Aulis.Karki [at] oulu.fi

In this article general structural features of the Raahe – Ladoga Shear Complex (RLSC) are presented. General classification scheme for shear related structures is given. Consequently the RLSC is divided to smaller units, as shear zones. Savonranta and Pielavesi Shear Zones are discussed as examples. Shear related rocks vary lithologically from high-grade migmatites and blastomylonites to cohesive and un-cohesive cataclastites. The evolution of the RLSC was initiated in N-S convergence, after accretion of juvenile Svecofennian arc complex.

**Keywords:** ductile, shear structure, shear complex, shear zone, Fennoscandian Shield, Svecofennian.

### 1. Introduction

The Fennoscandian Shield is sheared by several stages of ductile – brittle deformations since Palaeoproterozoic era. Individual structures and groups of structures created by those events may be named and classified as:

- 1) *Shear complex*: several sets of structures, shear bands, faults etc. in which individual members have a different, unknown or unspecified age (Fig. 1.F). The Raahe – Ladoga Shear Complex (RLSC), discussed in this paper, is an example of these.
- 2) *Shear system*: sets of shear structures in which individual members have the same age (Fig. 1.E). According to field evidence the RLSC includes a number of shear systems but their absolute ages are not yet verified.
- 3) *Shear zone*: spatially limited, sub-linear set of shear structures with unspecified relative age (Fig. 1.D). Among others, the RLSC is composed of Keitele, Pielavesi and Suvasvesi Shear Zones (KSZ, PSZ, SSZ).
- 4) *Shear set*: sub-parallel set of shear structures with the same age (Fig. 1.C). Several, structurally different shear sets have been recognized in the PSZ and SSZ.
- 5) *Shear stack*: geometrically limited set of adjacent shear bands. (Fig. 1.B). The banding is produced by metamorphic differentiation in certain strain and PT condition.
- 6) *Shear band*: individual, homogeneous “layer” of rock formed by a specified deformation process (Fig. 1.A). The composition of the band may differ from protolith composition. Different shear stacks and bands represent the visible, outcrop scale structural elements and they yield the basis for structural and kinematic interpretation.

### 2. Shear strain dominated structures

The Raahe Ladoga Shear Complex (RLSC) present a ca. 100 km wide, NW – SE striking set of strongly sheared rocks and intervening crustal blocks in which antecedent structures are preserved. Keitele, Pielavesi and Savonranta shear zones are the most important shear dominated units of the RLSC (Fig. 2). These were formed by long-term and multi-phase Svecofennian convergent tectonic evolution and consist of supracrustal para-gneisses and intrusive rocks. The latter are mostly pre- or syn-kinematic granitoids but distinctly postkinematic granite veins occur in all areas.

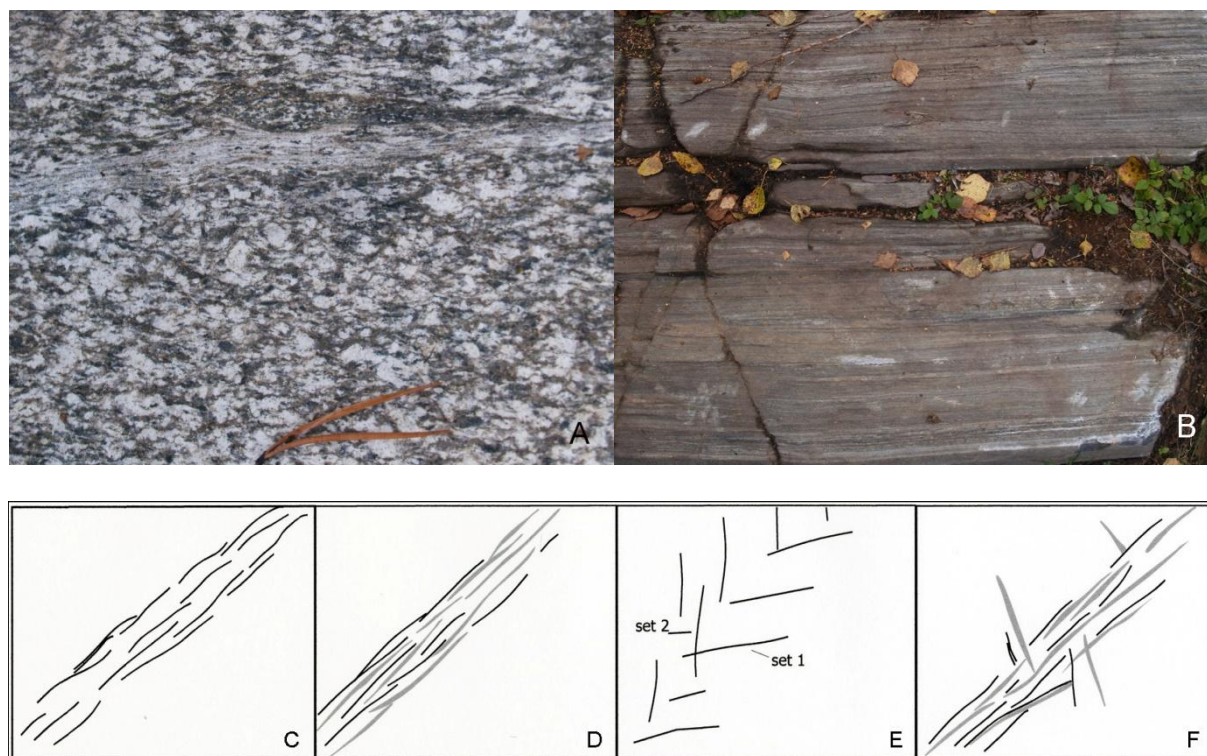


**Figure 1.** Schematic model for classification and grouping of shear structures. A) Shear band, B) Shear stack, C) Shear set, D) Shear zone, E) Shear system and F) Shear complex. For explanation see the text. Black and grey curves denote to structures of different age. Partly modified after Nystuen (1989).

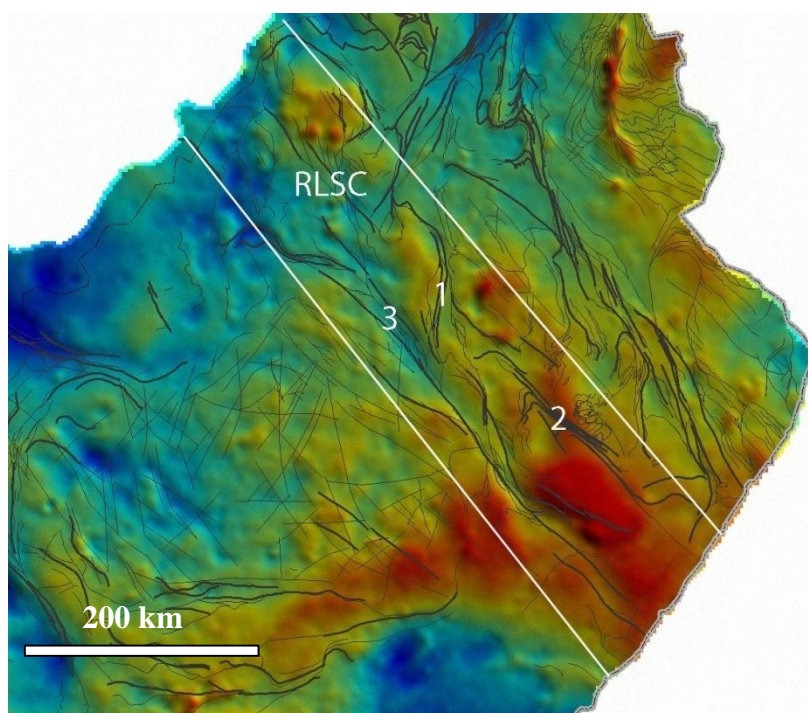


**Figure 2.** Location of Raaheladoga Shear Complex (RLSC) and Pielavesi (1), Savonranta (2) and Keitele (3) shear zones on gravimetric base map (Geol. Surv. Finland). Black curves indicate major shear related structures in Central Finland.

The Savonranta shear zone (SSZ) is located between Archean basement and the Outokumpu allochthon in the NE and Svecofennian domain in the SW. The earliest, polyphase fold interferences and migmatite structures are rotated and transposed sub-parallel to the strike of the SSZ indicating dextral, high shear strain in the ca. 5 km wide central part of the shear zone in Karvio area. Shear deformation was initiated in ductile, high temperature regime but the latest deformation phases took place in brittle environment, and produced large scale linear fractures, visible in topography and electromagnetic maps (Fig. 3).

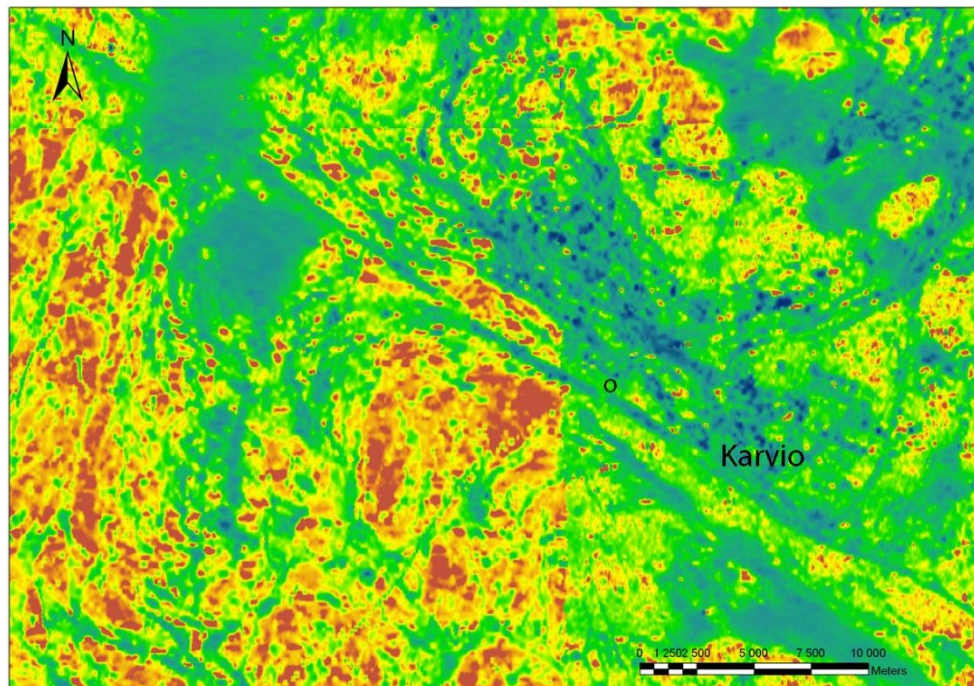


**Figure 3.** Electromagnetic map of Karvio area and location of Korkeakangas quarry (o).

Migmatitic metapelites make up the majority of the high-grade paragneisses in the SSZ and PSZ. Leucosomes in those rocks often build up asymmetric, fish or sigma structure like bodies. Felsic intrusions in the shear zones are elongated parallel to shear structures.

Most of the intrusive rocks are orientated and some are strongly sheared in later stages. Blastomylonites are useful in kinematic analysis and they can indicate both dextral and sinistral shearing. Mylonite bands range from centimetres to several metres in width and they generally indicate dextral shearing both in the SSZ and PSZ. Abundant cataclastites ranging from cohesive fault rocks to in-cohesive gouge materials and pseudotachylitic rocks indicate that tectonic movements continued to the latest stages of retrograde metamorphism. Ductile and most of the brittle planar elements are vertical or sub-vertical, excluding minor brittle, low angle reverse faults and sub-horizontal granite veins.

Palaeoproterozoic tectonic evolution of the Fennoscandian Shield has been discussed for decades and different models have been proposed (Gaál & Gorbachev, 1987; Gaál, 1990; Lahtinen et al., 2005; Lahtinen et al., 2008, Tuisku et al., in press). Late stages of Svecofennian tectonic evolution were characterized by north south convergence causing E-W striking fold and thrust structures in southern Finland (Ehlers et al., 1993). In middle Finland a conjugate shear complex with NW-SE and NE-SW striking structures as the Suvasvesi Shear Zone (Halden, 1982) and Oulujärvi Shear Zone (Kärki, 1995) was formed.

### 3. Conclusions

The Svecofennian orogen represents an accreted-arc complex according to widely accepted views (e.g. Gaál & Gorbachev, 1987; Lahtinen et al., 2005; Lahtinen et al., 2008, Tuisku et al., in press). The Raahe Ladoga Shear Complex was produced by N-S convergence during late stage Svecofennian tectonic evolution. The complex is characterized by generally dextral strike-slip tectonics. Metamorphic grade and structural style vary remarkably during evolution of different members of the complex. At early stages blastomylonites and migmatites were produced in high-grade conditions while retrograde stage was characterized by development of semi-brittle and brittle structures. Pre- and syn-kinematic intrusions had remarkable role in the evolution of the shear complex. At many places the latest granitic veins cross cut the most significant structures which will allow absolute dating of the tectonic events.

### References:

- Ehlers, C., Lindroos, A. & Selonen, O., 1993. The late Svecofennian granite-migmatite zone of southern Finland; a belt of transpressive deformation and granite emplacement. *Precambrian Research* 64, nos. 1-4, pp. 295-309.
- Halden, N. 1982. Structural and metamorphic and igneous history of migmatites in deep levels of a wrench fault regime, Savonranta, eastern Finland. *Trans. R. Soc. Edinburgh, Earth Sci.* 73:17-30.
- Gaál, G. and Gorbachev, R. 1987. An outline of the Precambrian evolution of the Baltic Shield. *Prec. Res.* 35:15-58.
- Gaál, G. 1990. Tectonic styles of Early Proterozoic ore deposition in the Fennoscandian Shield. *Prec. Res.* 46:83-114.
- Kärki, A. 1995. Papaeoproterozoic shear tectonics in the central Fennoscandian Shield, Finland. *Res Terrae, Ser. A*, No. 10, 37 pp and app.
- Lahtinen, R., Korja and A. Nironen, M. 2005. Paleoproterozoic tectonic evolution. In *Precambrian Geology of Finland – Key to the Evolution of the Fennoscandian Shield* (eds.) M. Lehtinen, P.A. Nurmi and O.T. Rämö. Elsevier. Pp. 481 – 532.
- Lahtinen, R., Garde, A., and Mellezhik, V. 2008. Paleoproterozoic evolution of Fennoscandia and Greenland. *Episodes*, 31:20–28.
- Nystuen, J.P., (ed.) 1989. Rules and recommendations for naming geological units in Norway by the Norwegian Committee on Stratigraphy. *Norsk Geologisk Tidsskrift* 69, Suppl. 2, 111 p.
- Tuisku, P., Huhma, H. and Whitehouse, M.J., (in press) Geochronology and geochemistry of the enderbite series in the Lapland Granulite Belt: generation, tectonic setting, and correlation of the belt. *Can. J. Earth. Sci.*

## Coda waves of local earthquakes: A case history from northern Finland

E. Lanne

E-mail: erkki.lanne [at] pp.inet.fi

The attenuation and random properties of the Fennoscandian lithosphere are fairly unknown. The aim of this paper is to test whether the coda waves of local earthquakes are suitable for the determination of the attenuation properties of the lithosphere. According to the test event from northern Finland the total  $Q$ -values vary from 3400 to 5700 within the frequency interval 10-40 Hz and the power law dependence on the frequency is  $Q \sim f^{0.55}$ . Though the infrequency of earthquakes may restrict some studies, data from of DSS soundings and blasts are available, which could be used for coda studies, as well.

**Keywords:** local earthquake, coda wave, attenuation, Fennoscandian shield, lithosphere, northern Finland

### 1. Introduction

In the registration of local earthquakes one can identify waves which are associated with definite layered structures of the lithosphere. Additionally, after the S-waves there is a long transient train of random wavelets which are called S-coda waves (Fig 1a). Certainly these waves represent various types of scattered waves, but their origins are still controversial. Nevertheless, coda waves have proved useful in the studies of the random nature and the attenuation properties of the lithosphere. The latest comprehensive monograph is by Sato et al. (2012). Globally, most studies have focused on seismically active areas, which offer massive amounts of data and where earthquakes are a real risk to the society, too. Earthquakes are rare on Precambrian shield areas, but any information of the properties of the lithosphere could increase both scientific knowledge and practical applications. Grad et al. (1998) have studied the uppermost crust of Finland, but the random properties of the whole lithosphere are insufficiently established. This paper aims to find out whether data from Finnish earthquakes could be applied to the estimation of attenuation properties of the lithosphere.

### 2. Observations

The test event is an earthquake recorded in northern Finland in 26.07.2011 at 1:45:46.8. Its  $M_L$ -magnitude, 1.1, is fairly small. Its exact location was N67.116, E25.767. Near to the epicenter there is a strong fault zone in the direction SE-NW. Distances to the nearest stations are 57 km to RNF (Rovaniemi), 198 km to MSF (Maaselkä) and 227 km to OUL (Oulu). Observations were made by wide-band STS-2 seismographs. The data recorded is in the standard MSEED format. The useful frequency band is between 10-25Hz, because the low-frequency part is strongly affected by the micro-seismic noise (Figure 1a). Only the z-component of RNF was studied in detail.

### 3. Theoretical background

The energy of the earthquake fades out with the time (and the distance) from the origin. Besides the geometric decay, seismic waves are attenuated by two major processes. Intrinsic absorption could be caused by micro-cracks and variations in the elastic properties between rock grains. The second process, the scattering, is caused by larger heterogeneous units like rock masses and fractured rocks in fault zones. The used parameters are the quality factor  $Q$  and its inverse  $Q^{-1}$ . The total attenuation  $Q_T^{-1}$  is expressed as a sum of the intrinsic absorption

and the scattering attenuation.  $Q_T^{-1} = Q_i^{-1} + Q_{sc}^{-1}$ . In this study, the analyzing method is based on the frequency dependent multiple scattering model of Aki and Chouet (1975).

$$A(\omega, t) = C(\omega) t^{-b} \exp(\omega t / 2Q(\omega))$$

$\omega$  is the angular frequency,  $t$  is lapse time (= time from the origin),  $A(\omega, t)$  is amplitude of the coda envelope,  $C$  is source factor and  $Q(\omega)$  is total quality factor. For body waves, the parameter  $b$  is one. The relationship is easily linearized in the log-log-scale. There are several other parameters concerning the statistical properties of the lithosphere, but for the sake of convenience, they are not included.

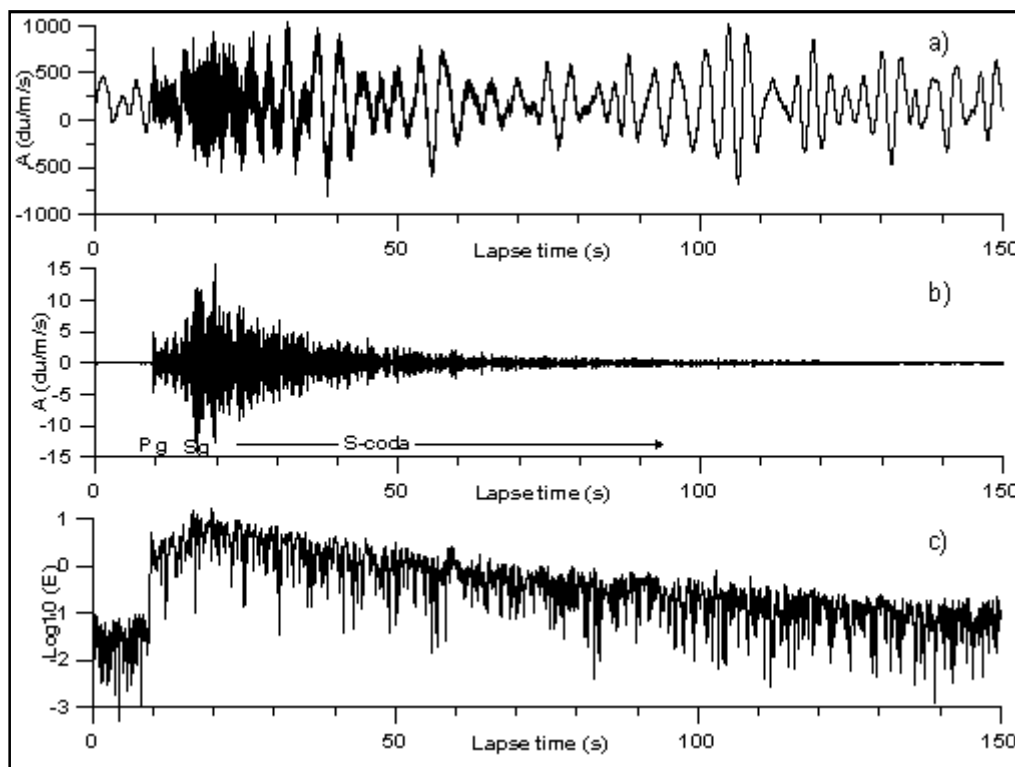


**Figure 1.** An example of the calculation of the coda. a) original data, b) filtered data (centre frequency 20Hz, band-width 5 Hz), c) envelope.

#### 4. Analysis of data and results

The method is simple, in principle. However, the randomness of the wave train and background noise need attention. For the purpose of this study, the envelope of the coda at a certain frequency was calculated as follows. Firstly, the selected data train was filtered by a narrow-banded (band-width 5 Hz) frequency filter, (Fig. 1b), and the envelope was calculated by the Hilbert transform, (Fig. 1c). These operations were performed by the Fourier transform. Next, using the linearized formula of Aki and Chouet (1975), the linear fit was applied at different time windows and lapse times. The operation was repeated at frequencies 10, 15, ..., 40 Hz.

The reading of the seismograph is proportional to the particle velocity of the ground. The magnification of the seismograph and the velocity-motion reductions are not a problem, because individual data series are narrow-banded and the processing is independent on the absolute energies or on the frequency.

For investigating the dependence on the lapse time and time windows  $Q$ -values were calculated at different lapse time windows. Figure 2 represents examples which were calculated at frequencies 20 and 30 Hz. The time window is 40 seconds. It became evident that  $Q$ -values are increasing with the lapse time, which is often typical globally. One explanation is that the sources of later wavelets originate from the deeper and more compact parts of the lithosphere. At the highest frequencies, the tendency is merely reversible, however. Because the values vary strongly, the time windows for getting stable  $Q$ -values should be longer. According to Aki and Chouet (1975), the beginning of the time window should be twice the travel time of S-waves.  $Q$ -values, which cover the entire coda, were averaged from coda values which are calculated within the time interval from 40 to 150 seconds. Time windows varied from 80 to 110 seconds. The  $Q$ -values vary from 3400 to 5700, which are to be expected for Precambrian (Figure 3). The usually represented power-law relationship  $Q \sim f^{0.55}$  from 15 to 40 Hz is within normal limits, although the fit in this single case is not very good.

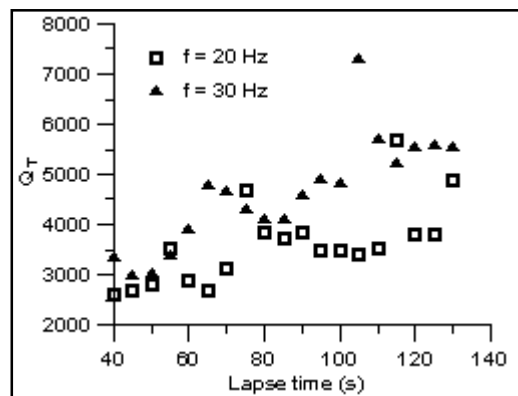


**Figure 2.**  $Q$ -values at different lapse times. Time window is 40 seconds.

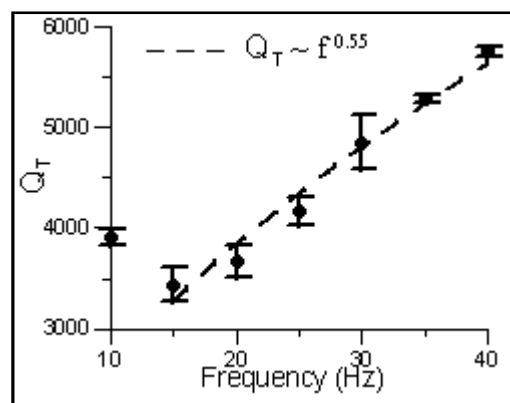


**Figure 3.**  $Q$ -values at frequencies 10,...,40 Hz and the frequency-dependent power-law relationship..

## 5. Conclusions

According to this experiment, the codas of local earthquakes of the Fennoscandian shield offer potential for future studies of the lithosphere. In this example, the estimated total  $Q$ -values and their dependence on the frequency are well in line with the ones obtained globally.

---

They are large, but generally the larger values are associated with old and tectonically tranquil areas as opposed to young and active ones. If the duration is e.g. 150 seconds, it means that the seismic energy has zigzagged more than 500 kilometers. It is difficult to imagine, that the seismic energy could be trapped in the crust alone. Large Q-values mean that codas are long and the envelopes attenuate gently. Q-values are sensitive to the random variations and the background noise. The Finnish permanent station network is fairly dense which facilitates the identification of attenuation properties between main geological units. Although earthquakes are rare in Finland, there are daily man-made events (= blasts) which offer more data for coda studies. Moreover, detailed and potential data offer several DSS data sets.

**Acknowledgements:**

Elena Kozlovskaja kindly delivered the data of Sodankylä Geophysical Observatory for my experiment.

**References:**

- Aki, K. and Chouet, B., 1975. Origin of coda waves: source, attenuation and scattering effects, *J.Geophys. Res.*, vol 80, No. 23, 3322-3342.
- Grad, M., Czuba W., Luosto U. and Zuchniak, M., 1998.  $Q_R$ -Factors in the Crystalline Uppermost Crust in Finland from Rayleigh Surface Waves, *Geophysica*, vol 34, No. 3, 115-129.
- Sato, H., Fehler, M. and Maeda, T. 2012. *Seismic Wave Propagation and Scattering in the Heterogeneous Earth* 2nd ed., Springer-Verlag, 494p.

## Constraining the age and evolution of Archean greenstone belts in the Kuhmo and Suomussalmi areas, Finland

E. Lehtonen<sup>1</sup>, T. Halkoaho<sup>3</sup>, P. Hölttä<sup>2</sup>,  
H. Huhma<sup>2</sup>, E. Luukkonen<sup>3</sup>, E. Heilimo<sup>3</sup> and A. Käpyaho<sup>2</sup>

<sup>1</sup>Finnish Museum of Natural History (Geological Museum),

P.O. Box 17 (Arkadiankatu 7), FI-00014 University of Helsinki

<sup>2</sup>Geological Survey of Finland, P.O. Box 96 (Betonimiehenkuja 4), FI-02151 Espoo

<sup>3</sup>Geological Survey of Finland, P.O. Box 1237 (Neulaniementie 5), FI-70211 Kuopio

E-mail: elina.lehtonen [at] helsinki.fi

This abstract is an introduction to a recently started four-year Ph. D. project about constraining the age and evolution of Archean greenstone belts in Finland. The study is funded by The Finnish Doctoral Program in Geology and is carried in co-operation with Finnish Museum of Natural History, Geological Survey of Finland (Espoo and Kuopio offices) and Department of Geosciences and Geography, University of Helsinki.

**Keywords:** Archean greenstone belts, Suomussalmi, Kuhmo, geochronostratigraphy

### 1. Introduction

The Archean greenstone belts of Finland were formed ca. 3.0-2.7 Ga ago. At the present erosion level these units are narrow and elongated complexes surrounded by granitoid-migmatite areas. This abstract presents the outline of research in the Kuhmo and Suomussalmi greenstone belts in Eastern Finland (Figure 1). The Archean greenstone belts represent oldest volcanic rocks preserved in Finland. They were metamorphosed in the Neoproterozoic, and have some areas with well-preserved volcanic structures (Figure 2).

The Kuhmo and Suomussalmi greenstone belts (e.g. Vaasjoki et al. 1999, Luukkonen 2002, Papunen et al. 2009) and the granitoid-migmatite areas next to the greenstone belts (e.g. Käpyaho 2007, Heilimo 2011, Mikkola 2011) have been studied using geochronological and geochemical methods. Some detailed unpublished master theses have also been made from these areas (Nieminen 1998, Tulenheimo 1999, Rautio 2000). Huhma et al. (2010, in press) have done several age determinations from the greenstone belts. The aim of this study is to provide systematical new information on the chronostratigraphy of selected areas.

### 2. Geological background

In general the Suomussalmi greenstone belt has been divided into two different volcanic that have a tectonic contact (Pirainen 1988, Luukkonen et al. 2002, Sorjonen-Ward and Luukkonen, 2005). The Luoma group has been considered as the older part, consisting mainly of basic, intermediate and acid volcanogenic lava and pyroclastic rocks. The rocks were deposited both in shallow water and on dry land. The Saarikylä group has been considered as the younger part, consisting mainly of komatiitic cumulates, and komatiitic and basaltic lava flows. The Saarikylä group might represent remnants of a deeply eroded shield volcano. According to Huhma et al. (in press) the Suomussalmi greenstone belt comprises three volcanic sections than can be divided into three different age groups: 2.82, 2.87, and 2.94 Ga.

The Kuhmo greenstone belt is situated to the south of the Suomussalmi greenstone belt. The Kuhmo greenstone belt is predominated by mafic volcanic rocks, but also felsic volcanic rocks are occasionally present (Sorjonen-Ward and Luukkonen 2005). For example following theories have been presented for the formation of the Kuhmo greenstone belt: 1) collision and subduction processes (Pirainen 1988) and 2) intracratonic, extensional rift environment (Luukkonen 1992). 3D-model for Kuhmo greenstone belt demonstrates that the Kuhmo

greenstone belt is a surface structure with depth of <7 km and has no deep “root” in the middle or lower crust (Silvennoinen and Kozlovskaya 2007). This suggests that the belt is formed by plate tectonic like processes, such as subduction, rather than mantle plume activity.

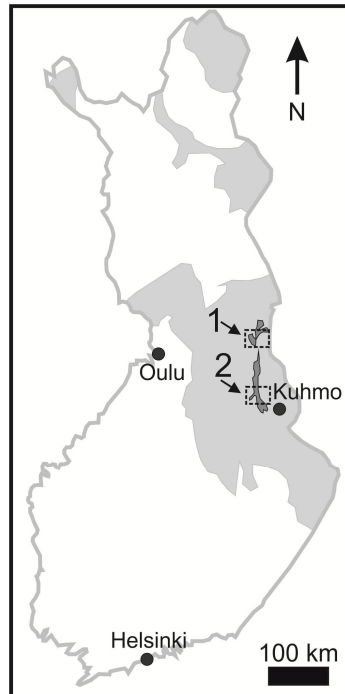


**Figure 1.** The map of Finland showing locations of the Suomussalmi (1) and Kuhmo (2) greenstone belts (= dark grey colored areas). The Archean bedrock is otherwise marked with light grey color. Black dashed squares represent the current study areas from both greenstone belts. Map modified from Korsman and Koistinen (1998) and Lehtonen et al. (2012).

### 3. Methods

The exposed parts of the greenstone belts in the Suomussalmi and Kuhmo areas have been minutely mapped in the previous studies (e.g. Luukkonen 1992, Tulenheimo, 1999). Drilling projects made by the Geological Survey of Finland and Outokumpu Co. in 1990s-2000s revealed many new rock units that are not exposed (e.g. many felsic and intermediate rock units). Our study comprises samples from both exposed rocks and drill cores.

Polished thin sections and whole rock analyses will be done from all new age determination samples, and U-Pb dating will be made from samples that contain enough zircon grains. The preparation (sawing, crushing and mineral separation) of samples will be made in autumn 2012 at the Geological Survey of Finland. After this, the zircon grains for the U-Pb dating will be hand-picked and their internal structures will be documented from mounted sections by using scanning electron microscope. The aim is to perform the U-Pb dating on zircons in 2013 by using the secondary ion mass spectrometer (SIMS) in the Nordsim-laboratory in Stockholm.

#### 4. Summary

This study aims to define more detailed chronostratigraphy for the Suomussalmi and Kuhmo greenstone belts. It also sheds light on the timescales of greenstone belt formation and tries to constrain the volcanic and tectonic processes involved. In addition, this study tries to provide new information on whether there was one long-lived tectonic process that was responsible for the genesis of the Suomussalmi and Kuhmo greenstone belts or whether multiple independent tectonic units were welded together.



**Figure 2.** Tholeiitic metabasaltic pillow lava from Kiannanniemi, Archean Suomussalmi greenstone belt. Note that remnants of gas vesicles are still visible.

#### References:

- Heilimo, E. 2011. Neoproterozoic sanukitoid series in the Karelian Province, Finland. Academic Dissertation, Department of Geosciences and Geography, Faculty of Science, University of Helsinki, 23 p.
- Huhma, H., Mänttari, I., Peltonen, P., Halkoaho, T., Hölttä, P., Juopperi, H., Konnunaho, J., Kontinen, A., Lahaye, Y., Luukkonen, E., Pietikäinen, K., and Sorjonen-Ward, P. 2010. Age and Sm-Nd isotopes on the Archean greenstone belts in Finland. In: *Lithosphere 2010: Sixth Symposium on the Structure, Composition and Evolution of the Lithosphere in Finland*, Helsinki, October 27-28, 2010: programme and extended abstracts. Institute of Seismology. University of Helsinki. Report S-55. Helsinki: Institute of Seismology, 13-16.
- Huhma, H., Mänttari, I., Peltonen, P., Kontinen, A., Halkoaho, T., Hanski, E., Hokkanen, T., Hölttä, P., Juopperi, H., Konnunaho, J., Lahaye, Y., Luukkonen, E., Pietikäinen, K., Pulkkinen, A., Sorjonen-Ward, P., Vaasjoki, M. and Whitehouse, M. The age of the Archean greenstone belts in Finland (in press, *GTK Special Paper*).
- Korsman, K. and Koistinen, T. 1998. Suomen kallioperän yleispiirteet. In: Lehtinen M., Nurmi., and Rämö, T. (Eds.), *Suomen kallioperä – 3000 vuosimiljoonaa*. Suomen geologinen seura, 96.

- Käpyaho, A. 2007. Archean crustal evolution in eastern Finland: New geochronological and geochemical constraints from the Kuhmo terrain and the Nurmes belt. Academic Dissertation, Department of Geology, Faculty of Science, University of Helsinki, 20 p.
- Lehtonen, E., Hölttä, P. and Halla J. 2012. Muinaisia tulivuoria tutkimassa. *Geologi*, 64:3, 85-87.
- Luukkonen E.J. 1992. Late Archean and early Proterozoic structural evolution in the Kuhmo-Suomussalmi terrain, eastern Finland. Academic Dissertation, University of Turku, 37 p.
- Luukkonen, E.J., Halkoaho, T.A., Hartikainen, A.A., Heino, T.O., Niskanen, M.J., Pietikäinen, K.J., and Tenhola, M.K. 2002. Itä-Suomen arkeaiset alueet – hankeen (12201 ja 210 5000) toiminta vuosina 1992-2001 Suomussalmen, Hyrynsalmen, Kuhmon, Nurmeksen, Rautavaaran, Valtimon, Lieksan, Ilomantsin, Kiihtelysvaaran, Enon, Kontionlahden, Tohmajärven, ja Tuupovaaran alueella. Geological Survey of Finland, Final Report, 265 p.
- Mikkola, P. 2011. The prehistory of Suomussalmi, eastern Finland; the first billion years as revealed by isotopes and the composition of granitoid suites. Academic Dissertation, Department of Geosciences and Geography, Faculty of Science, University of Helsinki, 24 p.
- Nieminen, J. 1998. Kuhmon Kellojärven polymiittinen vulkaaninen konglomeraatti. Master thesis, Department of Geology, University of Turku, 106 p.
- Papunen, H., Halkoaho, T. and Luukkonen E. J. 2009. Archean evolution of the Tipasjärvi-Kuhmo-Suomussalmi Greenstone Complex, Finland. Bulletin 403, Geological Survey of Finland, 68 p.
- Piirainen, T. 1988. The geology of the Archean greenstone-granitoid terrain in Kuhmo, eastern Finland. In Marttila, E. (Ed.): Archean geology of the Fennoscandian Shield. Geological Survey of Finland, Special Paper 4, 39-51.
- Rautio, J. 2000. Arkeinen Huutoniemen serpentiiniitti Suomussalmella. Master thesis, Department of Geology, University of Turku, 87 p.
- Silvennoinen, H. and Kozlovskaya, E., 2007. 3-D structure and physical properties of the Kuhmo Greenstone Belt (eastern Finland): constraints from gravity modelling and petrophysical data. *Journal of Geodynamics*, 43:3, 358-373.
- Sorjonen-Ward, P. and Luukkonen, E.J. 2005. Archean rocks. In: Lehtinen, M., Nurmi, P.A., Rämö, O.T. (Eds.), Precambrian geology of Finland – Key to the Evolution of the Fennoscandian Shield. Elsevier B.V., Amsterdam, 19-99.
- Tulenheimo, T. 1999. Kuhmon Kellojärven kerroksellinen ultramafinen muodostuma. Master thesis, Department of Geology, University of Turku, 199 p.
- Vaasjoki, M., Taipale, K. and Tuokko, I. 1999. Radiometric ages and other isotopic data bearing on the evolution of Archean crust and ores in the Kuhmo-Suomussalmi area, eastern Finland. In: Kähkönen, Y. and Lindqvist, K. (Eds.), Studies Related to the Global Geoscience Transects / SVEKA project in Finland. Special Issue, *Bulletin of Geological Society, Finland*, 71:1, 155-176.

# Effective elastic thickness of the lithosphere in the seismic POLAR profile, Northern Finland

K. Moisio<sup>1</sup> and P. Kaikkonen<sup>1</sup>

<sup>1</sup>Geophysics, Department of Physics, University of Oulu, P.O. Box 3000,  
FI-90014 University of Oulu, Finland  
E-mail: kari.moisio [at] oulu.fi

We evaluate the effective elastic thickness from the rheological profiles calculated for the seismic POLAR profile in northern Fennoscandia. We review the  $T_e$  values from earlier studies and compare them with our results.

**Keywords:** lithosphere, Fennoscandia, effective elastic thickness, rheology

## 1. Introduction

The effective elastic thickness ( $T_e$ ) of the lithosphere describes how lithospheric plate responds to applied surface and/or subsurface long-term ( $>10000$  a) geological loads at different depths. The  $T_e$  quantifies the flexure of the lithospheric plate, i.e., flexural rigidity (or resistance to flexure) and it is also a measure of the integrated lithospheric strength. Therefore it also indicates mechanisms of isostatic compensations beneath the lithosphere.

Flexural equation of a thin elastic plate gives the relationship between the flexural rigidity  $D$  and the elastic thickness  $T_e$  (e.g. Turcotte and Schubert, 2002)

$$D = \frac{ET_e^3}{12(1-\nu^2)}, \quad (1)$$

where  $E$  and  $\nu$  are elastic parameters. A large value of the elastic thickness is equivalent to rheologically strong lithosphere where elastic behaviour is dominant and respectively small value indicates that elasticity in the lithosphere is relatively smaller.

The  $T_e$  or the flexural rigidity can be evaluated with several different methods and approaches based on the analysis of the observations and modelling (forward and inverse) that reflect the lithospheric large scale movements (flexure) in time. Postglacial rebound and uplift data, sea-level changes, gravity data, rheological models and direct observations of the flexure have been widely used to estimate values for the  $T_e$  (e.g., Burov and Diament, 1995; McKenzie and Fairhead, 1997; Pérez-Gussinyé and Watts, 2005; Watts et al, 2006; Tesauro et al., 2010).

The continental lithosphere, in contrast with the oceanic lithosphere has more inhomogeneous structure. Its elastic thickness is controlled by many factors unlike in the oceanic lithosphere, where thermal age is the primary controlling factor. The continental lithosphere usually has a complex multilayered rheology and together with thermal structure, crustal thickness and its composition they create an integrated effect to the elastic thickness. This complex nature of the continental lithosphere has resulted in a large scatter in the  $T_e$  estimates.

## 3. Earlier estimates of the $T_e$ in the Fennoscandian Shield

Several methods have been applied to derive an estimate for the flexural rigidity in the Fennoscandian Shield. Wolf (1987) suggested a flexural rigidity less than  $5 \times 10^{24}$  Nm corresponding to a value of  $T_e = 80$  km from the observations of the sea-level change.

Lambeck et al (1990) gave estimate for the  $T_e$  between 100 and 150 km from inversion of the sea-level data. Mörner (1990) gave estimates of the flexural rigidity along the

FENNOLORA profile (e.g. Guggisberg et al. 1991) based on the shoreline data. Estimates were between  $7 \times 10^{24}$  Nm in the southwest and  $9 \times 10^{25}$  Nm in the northwest. Mitrovica and Peltier (1993) estimated from the inversion of the uplift data the  $T_e$  to range from 70 to 145 km.

Fjeldskaar (1997) gave values of the  $T_e$  for several locations in the Fennoscandia using the uplift rate and tilts of the paleoshorelines. In the central Fennoscandia  $T_e$  value of 50 km was obtained with the most probable glacier model and an upper bound for the  $T_e$  was set to 110 km. In the Norwegian coast in the north elastic thickness was estimated to be approximately 20 km.

Poudjom Djomani et al. (1999) used the coherence method of Forsyth (1985) where the relationship of the present-day topography and gravity data (Bouguer) as a function of wavelength was used for estimating the elastic thickness. Several analysis windows were used to calculate the distribution of the  $T_e$  in Fennoscandia. Highest values of 60 to 70 km were estimated for the eastern part of the Fennoscandia, in geologically oldest areas. Lowest values of 10-20 km were found in the Caledonides and Swedish Svecofennian areas. Milne et al. (2001) compared Global positioning system (GPS) observations with the numerical predictions and estimated the elastic thickness between 90 and 170 km.

Pérez-Gussinyé et al. (2004) and Pérez-Gussinyé and Watts (2005) used both the free-air admittance and Bouguer coherence methods. The free-air admittance method uses a linear transfer function that relates topography and free-air gravity. Estimates for the  $T_e$  with both methods for the central Finland, Svecofennian and Karelian areas were between 70 and 100 km and in the Kola peninsula between 40-60 km. Tesauro et al. (2010) estimated  $T_e$  values for the European lithosphere following the approach described by Burov and Diament (1995). Unfortunately their data set is limited to latitudes below 60 °N and thus providing estimates only partly for the Fennoscandia.

#### 4. Method

We calculated two-dimensional rheological strength profiles for the seismic POLAR profile adopting a rheological classification for the crust and mantle based on the seismic velocities and compositional analysis done for the POLAR profile (Janik et al., 2009). Several thermal models with the varying crustal heat production and lithosphere thickness were used in the rheological models. One example of the rheological strength along the POLAR profile is shown in Fig. 1. (Moisio and Kaikkonen, 2012).

The effective elastic thickness ( $T_e$ ) is defined e.g., in Burov and Diament (1995). According to them the  $T_e$  of the plate consisting of  $n$  detached (decoupled) layers is

$$T_e^{(n)} = \left( \sum_{i=1}^n \Delta h_i^3 \right)^{\frac{1}{3}}, \quad (2)$$

where  $\Delta h_i$  is the  $T_e$  of the  $i$ th layer. For a coupled rheology, the crust and mantle are mechanically welded together and the  $T_e$  is simply a sum of all layers

$$T_e^{(n)} = \left( \sum_{i=1}^n \Delta h_i \right). \quad (3)$$

We determined the thickness  $\Delta h_i$  of each layer as a depth at which the yield strength is less than 10 MPa/km.

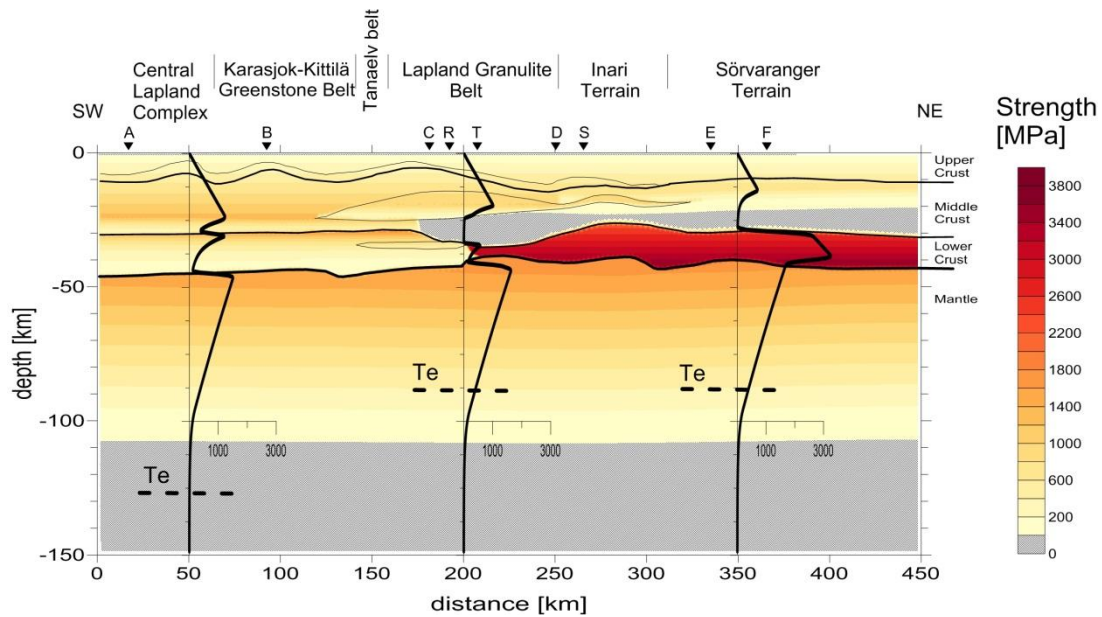


**Figure 1.** The rheological strength [in MPa] and the  $T_e$  shown with dashed line for the POLAR profile. Thermal LAB was at a depth of 250 km. Major geological terrains are shown on the top and the letters refer to shotpoint locations. Main model boundaries are shown with solid lines. Strength profiles in [MPa] are shown for the locations of 50, 200 and 350 km (Moisio and Kaikkonen, 2012).

## 5. Results

Table 1 compiles the values of the  $T_e$  evaluated from the calculated strength profiles along the POLAR profile. Used lithology together with different thermal models cause large differences in our  $T_e$  estimates. For specific conditions lithospheric layers are coupled and  $T_e$  estimates are above 100 km. These values approximately correspond with the isotherm of 750°C associated to the depth of the mechanical lithosphere as suggested by Burov and Diament (1995). In decoupled conditions  $T_e$  estimates are well below 100 km. Coupling refers to a situation where different lithospheric layers show no distinct reduction in the rheological strength.

**Table 1.** Values of the effective elastic thickness evaluated from the strength profiles. Locations refer to horizontal distances along the POLAR profile. Letter c denotes coupled rheology. LAB denotes lithosphere-asthenosphere boundary depth and M1-M3 model of the different crustal heat production (M1<M3).  $T_e$  values with bold letters are shown in Fig.1.

Location [km]	Effective elastic thickness [km]					
	LAB 250 M1	LAB 250 M2	<b>LAB 250 M3</b>	LAB 200 M1	LAB 200 M2	LAB 200 M3
50	c 132	c 129	<b>c 126</b>	c 107	c 105	c 102
200	93	90	<b>87</b>	69	66	64
350	c 130	c 128	<b>87</b>	67	65	63

Earlier estimates of the  $T_e$  values show large scatter. However, many of them are more or less general for a large area, often the whole Fennoscandia. More specific values for certain

locations are presented by Poudjom Djomani et al. (1999), Pérez-Gussinyé et al. (2004) and Pérez-Gussinyé and Watts (2005). Comparison with their estimates shows that our  $T_e$  values are generally about 20-30 km larger than their values, and even larger if coupled conditions prevail. As our estimated  $T_e$  values exceed the average crustal thickness of 45 km (Luosto et al., 1989; Janik et al., 2009) are they specifically indicative of high rheological strength in the mantle. From the values of the strength we can deduce that both the lower crust and mantle are mainly responsible for high strength values. As these values exceed the crustal thickness they also exceed seismogenic layer thickness which is approximately 20 km in the vicinity of the POLAR profile (Moisio and Kaikkonen, 2012). This is consistent with the differences between these two parameters, mainly the time-scale of the strength and strain.

### References:

- Burov, E. B. and Diament, M., 1995. The effective elastic thickness ( $T_e$ ) of continental lithosphere: What does it really mean? *J. Geophys. Res.*, 100, 3905-3927.
- Fjeldskaar, W., 1997. Flexural rigidity of Fennoscandia inferred from postglacial uplift. *Tectonics*, 16:596-608.
- Forsyth, D.W., 1985. Subsurface loading estimates of the flexural rigidity of the continental lithosphere. *J. Geophys. Res.*, 90, 12623-12632.
- Guggisberg, B., Kaminski, W. and Prodehl, C., 1991. Crustal structure of the Fennoscandian Shield: A traveltimes interpretation of the long-range FENNOLORA seismic refraction profile. *Tectonophysics*, 195: 105-137.
- Janik, T., Kozlovskaya, E., Heikkinen, P., Yliniemi, J. and Silvennoinen H., 2009. Evidence for preservation of crustal root beneath the Proterozoic Lapland-Kola orogen (northern Fennoscandian shield) derived from P and S wave velocity models of POLAR and HUKKA wide-angle reflection and refraction profiles and FIRE4 reflection transect. *J. Geophys. Res.*, 114, B06308, doi:10.1029/2008JB005689.
- Lambeck, K., Johnson, M. and Nakada, M., 1990. Holocene glacial rebound and sea level change in NW Europe. *Geophys. J. Int.*, 103, 451-468.
- Luosto, U., Flueh, E., Lund, C.-E. and Working Group, 1989. The crustal structure along the Polar profile from seismic refraction. In: R. Freeman, M von Knorring, H. Korhonen, C. Lund and St. Mueller (Eds.), *The European Geotraverse, Part 5: Polar Profile*. *Tectonophysics*, 162: 51-85.
- McKenzie, D. and Fairhead, D., 1997. Estimates of the effective elastic thickness of the continental lithosphere from Bouguer and free-air anomalies. *J. Geophys. Res.*, 102, 27523-27552.
- Mitrovica, J. and Peltier, W.R., 1993. The inference of mantle viscosity from an inversion of Fennoscandian relaxation spectrum. *Geophys. J. Int.*, 114, 45-62
- Milne, G.A., Davis, J.L., Mitrovica, J.X., Scherneck, H.G., Johnsson, J.M., Vermeer, M. and Koivula, H., 2001. Space-geodetic constraints on Glacial isostatic adjustment in Fennoscandia. *Science*, 291, 2381-2385.
- Moisio, K. and Kaikkonen, P., 2012. Thermal and rheological structures along the seismic POLAR profile in the northern Fennoscandian Shield. *Terra Nova*, in press.
- Mörner, N.-A., 1990. Glacial isostasy and long-term crustal movements in Fennoscandia with respect to lithospheric and asthenospheric processes and properties. *Tectonophysics*. 176, 13-24.
- Pérez-Gussinyé, M., Lowry, A.R., Watts, A.B. and Velicogna, I. 2004. On the recovery of effective elastic thickness using spectral methods: Examples from synthetic data from the Fennoscandian Shield. *J. Geophys. Res.*, 109, doi:10.1029/2003JB002788.
- Pérez-Gussinyé, M. and Watts, A.B., 2005. The long-term strength of Europe and its implications for plate-forming processes. *Nature*, 436, doi:10.1038/nature03854.
- Poudjom Djomani, Y.H., Fairhead, J.D. and Griffin, W.L., 1999. The flexural rigidity of Fennoscandia: reflection of the tectonothermal age of the lithospheric mantle. *Earth Planet. Sci. Lett.*, 174,139-154.
- Tesauro, M., Kaban, M.K. and Cloetingh, S.A.P.L., 2010. Thermal and rheological model of the European lithosphere. In: Cloetingh, S. and Negendank, J. (Eds.), *New frontiers in integrated solid earth sciences*, p. 71-101.
- Turcotte, D.L. and Schubert, G., 1982. *Geodynamics, Applications of continuum physics to geological problems*. John Wiley and Sons, New York, 450 pp.
- Watts, A.B., Sandwell, D.T., Smith, W.H.F. and Wessel, P., 2006. Global gravity, bathymetry, and the distribution of submarine volcanism through space and time. *J. Geophys. Res.*, 111. doi:10.1029/2005JB004083.
- Wolf, T., 1987. An upper bound of lithosphere thickness from glacio-isostatic adjustment. *J. Geophys. Res.*, 61, 141-149.

## Shearing in the northern part of the Central Finland granitoid complex

K. Nikkilä<sup>1</sup> and A. Korja<sup>1</sup>

<sup>1</sup>University of Helsinki, Institute of Seismology  
E-mail: kaisa.nikkila [at] helsinki.fi

The Paleoproterozoic Svecofennian orogenic domain of the Fennoscandian Shield hosts extensive Central Finland granitoid complex (CFGC) that has been emplaced during syn- to post-collisional orogenic events between 1.890 Ga and 1.870 Ga. The complex consists of plutonic rocks and minor amounts of supracrustal rocks. Shearing has dominantly been in SE-NW direction. In northern parts, however, also N-S shearing is evident. Shear zones in SE-NW direction are discrete narrow shear bands, whereas in N-S directions they are broader shear zones with mylonitic to Augen-gneissic fabric. The N-S trending shear structures are older than SE-NW trending ones. A comparison of models, field data and FIRE3 sections suggest that the N-S trending mylonites and augen gneisses have formed along older stacking structures, which have been reactivated during lateral spreading.

**Keywords:** Central Finland granitoid complex, Svecofennian, shear zones, FIRE, analogue modeling

### 1. Introduction

The thick Svecofennian crust (50-65 km) was formed during continental accretion of Archean and Paleoproterozoic terranes (Korja *et al.* 1993), probably at a high convergence rate. The metamorphic culmination of the Svecofennian orogen occurred at about 1.890 Ga and the extensive Central Finland granitoid complex (CFGC) was emplaced during syn- and post-collisional orogenic events between 1.890 Ga and 1.870 Ga (Fig. 1; Nironen *et al.* 2000). The complex consists of plutonic rocks and minor amount of supracrustal rocks. SE-NW shearing has been dominant and, all over the CFGC, there is a lineation in that direction. The granitoid rocks of the CFGC have intruded into the uppermost, brittle part of the crust in an extensional tectonic setting (Nironen *et al.* 2000). Korja *et al.* (2009) suggested the central part of the orogeny, characterized by Central Finland granitoid complex and associated shear systems, to have formed during lateral spreading. Kukkonen *et al.* (2008) has showed that at least 19 km of Svecofennian crust has been exhumed since the emplacement of the synkinematic rocks. They have assumed the synkinematic granitoids to be the melt product of metasedimentary and metavolcanic rock association.

### 2. Melting and magma emplacement

Crustal thickening and partial melting is a prerequisite to lateral flow of orogens (Jamieson *et al.* 2004). The thickened crust must be thick enough (50-70 km) before widespread crustal melting begins. However, if the convergence rate is high, the crust may reach over 70 km in thickness, before melting. Thick continental crust remains hot and partially molten for at least 20 My after collision has ceased. The result of large scale melting is observed as large granitic intrusions or migmatites in granitoid belts (Jamieson *et al.*, 2011).

Partial melting takes place at 25 km depth and magma rises up to depths of 12 to 15 km where it is emplaced as flat-lying granites. Shearing helps to segregate magma and to guide it toward the surface. Stress field creates zones of local extension for the magma to infiltrate. The magma bodies collect in flat, thin sheets (3-7 km thick) with flat floors

(Vigneresse, 1995). This implies that the shearing is not the origin of the plutons, but rather controls the emplacement of magma bodies.

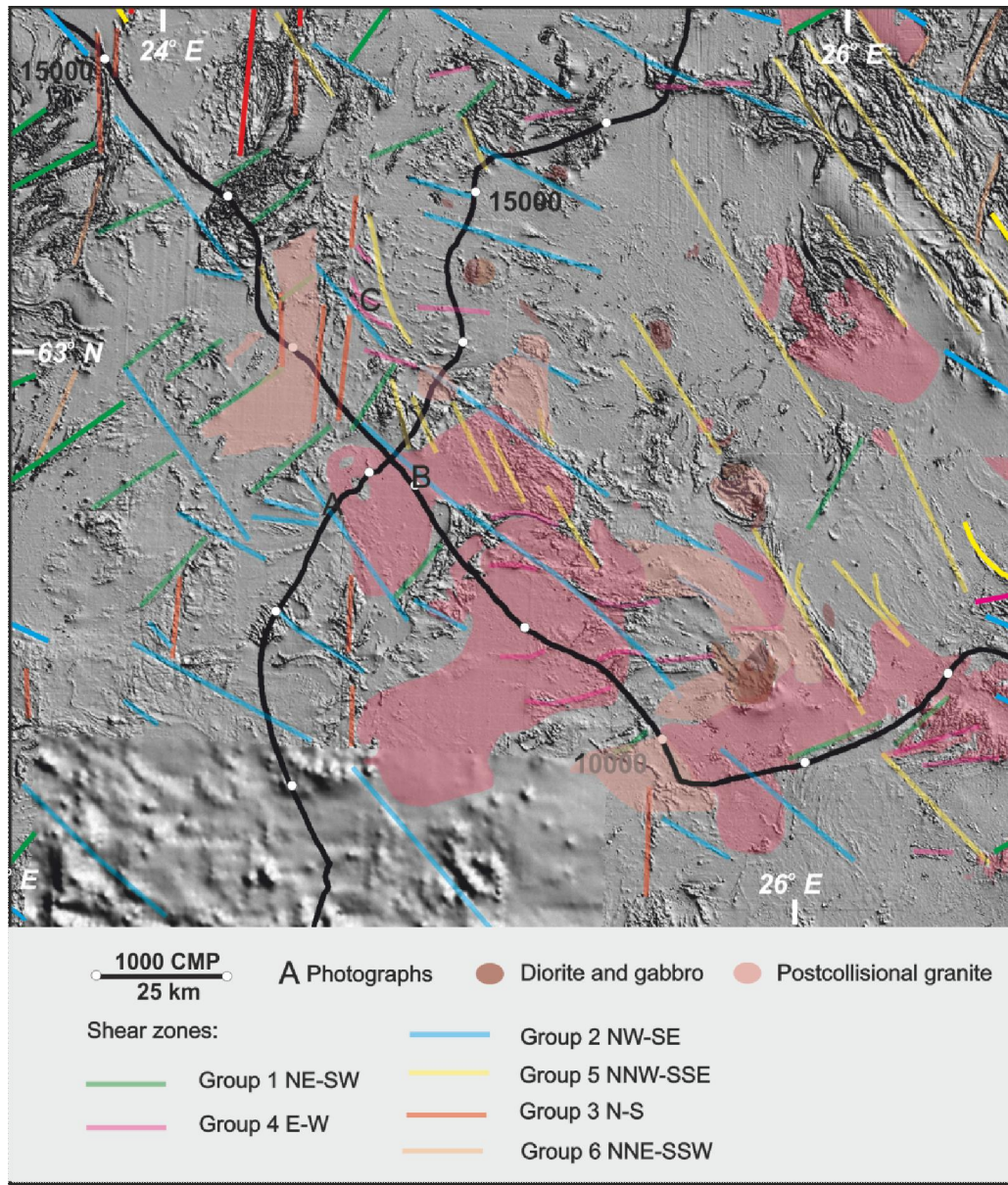


**Figure 1.** An aeromagnetic map of the Central Finland modifies after Korja *et al.* 2009. Deep seismic reflection profiles FIRE1 and FIRE3 intersect in Karstula. Magnetic anomalies interpreted as shear and fault zones are marked with lines. The lines are divided into Groups 1–6 according to Korja *et al.* 2009. The letters indicate the places of the photographs in figure 2.

### 3. Karstula-Saarijärvi area within the CFGC

In our study we focus on the Karstula-Saarijärvi district, located in the northern part of the CFGC (Fig. 1). This part of the CFGC has previously been studied only on regional scale. The new crustal scale data from the Finnish Reflection Experiment (FIRE3a, 1) has yielded a new perspective on the structure of the area. The bedrock of the CFGC is mainly composed of granitoids. In the study area, these can be roughly divided into two groups: the typically massive, coarse-porphyrific granites (postkinematic granites, 1.885-1.875 Ga; Nironen 2003)

and the typically foliated, even-grained or porphyritic granites and granodiorites (synkinematic granitoid rocks, 1.89-1.88 Ga, Nironen 2003). On an aeromagnetic map (Fig. 1), several sharp, linear, SE-NW and S-N-trending regional scale minima transect the CFGC.

#### 4. Results

Our study indicates that the even-grained or porphyritic granites and granodiorites show more pervasive shearing deformation than the coarse-porphyritic granites (Figure 2A&B). The granodiorites have been deformed and sheared at least once and they have been rheologically weak during the deformation. These deformed granodiorites form the background into which the coarse-porphyritic plutons are intruded in. There is a mylonitic zone (Figure 2C) in the western parts of the study area. The protoliths are mainly granites, which have been deformed into augen-gneisses, but there are also a mylonitic diorites and metasedimentary successions. Neither the origin of the augen-gneisses nor the age of shearing is clear. Nevertheless, the augen-gneisses locate on a dextral N-S trending magnetic lineament cut by SE-NW trending lineaments (Fig. 1), suggesting that N-S lineaments are older than SE-NW ones.



**Figure 2.** Sheared granitoid rocks from CFGC. **A.** A pervasively deformed granodiorite, S1 150/17. Picture from a boulder. **B.** Coarse-grained granite with an ultramylonitic shear zone, S1 020/90. View to W. **C.** Mylonitic granite or augen-gneiss, S1 240/88. A vertical cross section, top to N.

We can not only trace large scale shearing systems on an aeromagnetic map (Fig.1), but we can also observed them in the field as mylonitic shear zones. Two prominent shearing systems are identified in the field. SE-NW trending shears are narrow zones, with only 10 cm wide discrete mylonitic to ultramylonitic shear bands whereas the N-S trending mylonite belts or shear zones are kilometers wide areas hosting pervasively deformed mylonites to augen-gneisses.

This suggests that either the coarse-porphyritic granites are younger (an interpretation favored in earlier studies, e.g Nironen *et al.* 2000, Nironen 2003) and the shearing has happened in the upper rigid parts of the crust, or that the augen-gneisses represent a deeper section of the same granitoid series.

#### 5. Comparison with Analogue Models

We have used analogue centrifuge modeling to simulate lateral flow at the boundary zone of Archean and Palaeoproterozoic terranes in late stages of Svecofennian orogeny. The experiments were made at Hans Ramberg Tectonic Laboratory in Uppsala University (see Nikkilä *et al.* in this volume). Large scale structures that were formed in the centrifuge analogue models are geometrically similar to those found in deep seismic reflection profiles (FIRE3a), aeromagnetic maps (Fig. 1) and field observations described previously. A

comparison of models, field data and FIRE3 sections suggest that the N-S trending shear zones are old stacking structures, which have been reactivated during lateral spreading.

## 6. Conclusions

In CFGC uppermost part of the crust has been exhumed and the lower parts of the upper crust are exposed. Our study indicates that after the metamorphic peak at 1.890 Ga, SE-NW shearing prevailed and was active for a long period of time. All the examined plutonic rocks have some evidence of SE-NW movement. This shearing has controlled the magmatic activity in late stages. The coarse-grained porphyritic granites have been more rigid during shearing, because the granites have only narrow shear zones.

The large N-S trending shear zone is an old deformation structure and it has been dominant during accretion and it may have been reactivated during lateral spreading. The augen-gneisses exposed in this zone represent a deep section of a magmatic body, which has been emplaced during N-S shearing.

A comparison of models, field data and FIRE3 sections suggest that the N-S trending shear zones are old stacking structures, which have been reactivated during lateral spreading.

## References:

- Jamieson, R. A., C. Beaumont, S. Medvedev, and M. H. Nguyen (2004), Crustal channel flows: 2. Numerical models with implications for metamorphism in the Himalayan-Tibetan orogen, *J. Geophys. Res.*, 109, B06407, doi:10.1029/2003JB002811.
- Jamieson, R. A., Unsworth, M. J., Harris, N. B. W., Rosenberg, C. L., & Schulmann, K. (August 2011). Crustal melting and the flow of mountains. *Elements*, 7(4), 253-260. doi:10.2113/gselements.7.4.253
- Korja, A., Kosunen, P., & Heikkinen, P. (2009). A case study of lateral spreading: The Precambrian svecofennian orogen. Geological Society, London, Special Publications, 321(1), 225-251. doi:10.1144/SP321.11
- Korja, A., Korja, T., Luosto, U., & Heikkinen, P. (1993). Seismic and geoelectric evidence for collisional and extensional events in the fennoscandian shield implications for precambrian crustal evolution. *Tectonophysics*, 219(1-3), 129-152. doi:10.1016/0040-1951(93)90292-R
- Kukkonen, I. T., Kuusisto, M., Lehtonen, M., & Peltonen, P. (2008). Delamination of eclogitized lower crust: Control on the crust-mantle boundary in the central fennoscandian shield. *Tectonophysics*, 457(3-4), 111-127. doi:10.1016/j.tecto.2008.04.029
- Nironen, M., 2003. Keski-Suomen Granitoidikompleksi, Karttaselitys. Summary: Central Finland Granitoid Complex - Explanation to a map. Geological Survey of Finland, Report of Investigation 157, 45
- Nironen, M., Elliott, B.A. and Rämö, O.T., 2000. 1.88–1.87 Ga postkinematic intrusions of the Central Finland Granitoid Complex: a shift from C-type to A-type magmatism during lithospheric convergence. *Lithos* 53, 37–58
- Vigneresse, J. L. (1995). Crustal regime of deformation and ascent of granitic magma. *Tectonophysics*, 249(3-4), 187-202. doi:10.1016/0040-1951(95)00005-8

## Lateral flow in the middle crust– Experiments from the Svecofennian orogeny

K. Nikkilä<sup>1</sup>, H. Koyi<sup>2</sup>, A. Korja<sup>1</sup> and O. Eklund<sup>3</sup>

<sup>1</sup>University of Helsinki, Institute of Seismology

<sup>2</sup>Uppsala University, Department of Earth Sciences

<sup>3</sup>Åbo Akademi University

E-mail: kaisa.nikkila [at] helsinki.fi

In this study, we have used analogue centrifuge modeling to simulate extensional lateral flow at the boundary zone of Archean and Paleoproterozoic terranes in late stages of Svecofennian orogeny. The analogue models image evolution of the mechanical boundary between the two rheologically different blocks. The results show that during extension 1) the weak Paleoproterozoic middle crust spreads laterally resulting in vertical rotation of the boundary between the Archean and Proterozoic blocks. 2) Low viscosity middle layer starts to flow upward to fill the gaps between the upper layer blocks. The exhumation of the middle layer forms large scale folds – synforms and antiforms - during extension. The gap filling antiforms expose middle crust at the surface, where it forms a core complex structure. The experiments indicate that the exposed crustal pieces are not in their postcollisional locations. Especially the upper and middle crustal terranes, but also the lower crustal parts, have rotated during lateral flow.

**Keywords:** Fennoscandia, CFGC, Lateral flow, Analogue modeling

### 1. Lateral flow in the Svecofennian orogen

The exposed Svecofennian crust (50-65 km) has been suggested to have thickened during continental accretion between Archean and Paleoproterozoic terranes (Korja *et al.* 1993), probably at a high convergence rate. It is likely that this thickened orogen experienced lateral spreading in its final stages (Korja *et al.* 2009). The boundary zone between the two colliding terranes has had an effect on the geometry of the spreading process. Korja *et al.* (2009) suggested that the central part of the orogeny, characterized by Central Finland Granitoid Complex (CFGC) and associated shear system, has deformed during lateral spreading. Because the middle crust was ductile, the crust had to move away from the thick parts of the collision zone.

### 2. Modeling the boundary zone

In this study, we have used analogue centrifuge modeling to simulate lateral flow at the boundary zone of Archean and Paleoproterozoic terranes in late stages of Svecofennian orogeny. The analogue models image evolution of the mechanical boundary between the two rheologically different blocks (Figure 1).

A total of five experiments were made using a large centrifuge in the Hans Ramberg Tectonic Laboratory in Uppsala University (Harris & Koyi, 2003). The materials in the experiment were based on the plastilina modelling putty, which was mixed with acid oil, silicone, sweetener and/or barium sulphate to get the appropriate composition for each layer. The model thickness of 3 cm represents 60 km thick crust. In centrifuge modeling, materials are relative constant under normal conditions, but they start to deform in high-G-force conditions. The models have been extended laterally in steps and experiments consisted of 14-23 runs, each 3 to 14 minutes. After every run, the model was examined for, how the extension had developed, usually measured and photographed, and sometimes sliced. The progression of the extension affected time in the centrifuge, rpm (revolutions per minute) and bottom materials. The slices were cut always parallel to the extension.

In models upper layer is brittle, middle layer is ductile, and the lower layer is more viscous. The layers represent upper, middle and lower crust, respectively. The Proterozoic layers have lower viscosity values than the Archean layers at similar depths. Both the Archean and the Paleoproterozoic blocks have a low-viscous middle crust.

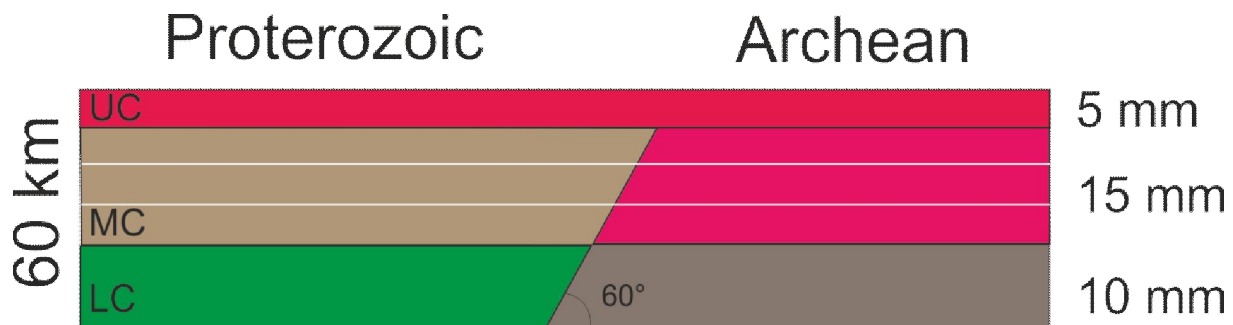


**Figure 1.** A vertical cross-section of a model before an experiment. The dimensions of the model are always the same, but the dip, the dip direction, and the stretching direction changes between the experiments. In this model the boundary zone dips  $60^\circ$  towards Proterozoic side.

### 3. Rotation increases with extension

Model results show that during extension 1) the weak Paleoproterozoic middle crust spreads laterally resulting in vertical rotation of the boundary between the Archean and Proterozoic blocks. 2) Low viscosity middle layer starts to flow upward to fill the gaps between the upper layer blocks.

The amount of rotation is dependent on the dip-direction of the boundary and the stretching direction. Rotation increases in proportion to stretching. If the stretching direction is opposite to the dip direction, the boundary becomes gentler (less steep) and often listric during the experiment. But also, when the dip direction of the boundary is parallel to the stretching direction, the boundary became gentler, not the other way around. In the latter one, the amount of rotation is less than in other experiments. Within the boundary zone, the Proterozoic middle layer formed frontal thrusts during the experiment. These structures are related to the different velocities of the mid-crustal materials on opposing sides.

Middle layer rises upward filling the gaps at surface, when upper layer is extended by faulting. Because the middle layer is less viscous on the Proterozoic side than on Archean side, the middle layer rises earlier and to high levels on the Proterozoic side. The gap filling process forms antiforms and synforms in the model. The antiforms have small amplitudes and broad shape creating open folds. The synforms are even gentler and the amplitude is smaller.

### 4. Conclusions

The experiments show geometrically similar crustal-scale structures to those observed in other seismic and geological surveys (Korja *et al.* 2009). Thus it is possible that lateral flow has taken place in the core of the Svecofennian orogen. The experiments indicate that the crustal pieces are not in their postcollisional locations. Especially the upper and middle crustal terranes, but also the lower crustal parts, have rotated during lateral flow.

The exhumation of the middle layer indicates that large scale folds – synforms and antiforms - may form during extension. The gap filling antiforms expose middle crust at the surface, where it forms a core complex structure.

---

**References:**

- Jamieson, R. A., Unsworth, M. J., Harris, N. B. W., Rosenberg, C. L., & Schulmann, K. (August 2011). Crustal melting and the flow of mountains. *Elements*, 7(4), 253-260. doi:10.2113/gselements.7.4.253
- Harris, L. & Koyi, H. (2003). Centrifuge modelling of folding in high-grade rocks during rifting. *Journal of Structural Geology*, Volume 25, issue 2, 291-305
- Korja, A., Kosunen, P., & Heikkinen, P. (2009). A case study of lateral spreading: The Precambrian svecofennian orogen. Geological Society, London, Special Publications, 321(1), 225-251. doi:10.1144/SP321.11
- Korja, A., Korja, T., Luosto, U., & Heikkinen, P. (1993). Seismic and geoelectric evidence for collisional and extensional events in the fennoscandian shield implications for precambrian crustal evolution. *Tectonophysics*, 219(1-3), 129-152. doi:10.1016/0040-1951(93)90292-R



## From the Gneiss Age to the Ice Age: Lithosphere, landscape, and the shaping of Fennoscandia

T. F. Redfield<sup>1</sup>, P.T. Osmundsen<sup>1,2</sup> and B.W.H. Hendriks<sup>3</sup>

<sup>1</sup> Norwegian Geological Survey, Leiv Eriksons vei 39, Trondheim, Norway

<sup>2</sup> Department of Arctic Geology, University Centre in Svalbard, N-9171, Longyearbyen, Norway

<sup>3</sup> Statoil ASA, Sandsliveien 90, Bergen, Norway

E-mail: tim.redfield [at] ngu.no

Despite wide variation in many of the properties of Baltica's lithosphere, the shape of the continent is remarkably predictable. Very low relief central Baltica undergoes a sharp, mappable transition to the upwarped hinterland, which in turn becomes a pronounced, seaward-facing escarpment at the extended margin. Although the stretching and final breakup of Scandinavia's northwestern margin occurred in the distant geological past, new models describing how continents break apart are becoming very relevant for how onshore topography evolves for tens to millions of years following stretching and separation. The landscapes of Baltica reflect both the properties of the lithosphere that underlies them and the tectonic template that shaped the extended margin.

**Keywords:** lithosphere, extended margin, topography, landscape, Finland

233 closely spaced transects through Baltica, oriented parallel to the direction of margin extension and final breakup, show a pronounced topographic asymmetry. A prominent and eminently mappable Hinterland Break in Slope (HBSL) separates low elevation, low relief landscapes of central/southern Finland from the low relief but gently inclined landscapes of eastern Sweden. The HBSL is to a first order geographically coincident with a sharp gradient in the flexural rigidity computed for Baltica by Pérez-Gussinyé and Watts (2005). It is also geographically coincident with a pronounced belt of seismicity (Redfield and Osmundsen, in press). These observations hint that the Gulf of Bothnia marks an important geological/geophysical boundary within Baltica/Scandinavia (Figures 1, 2).

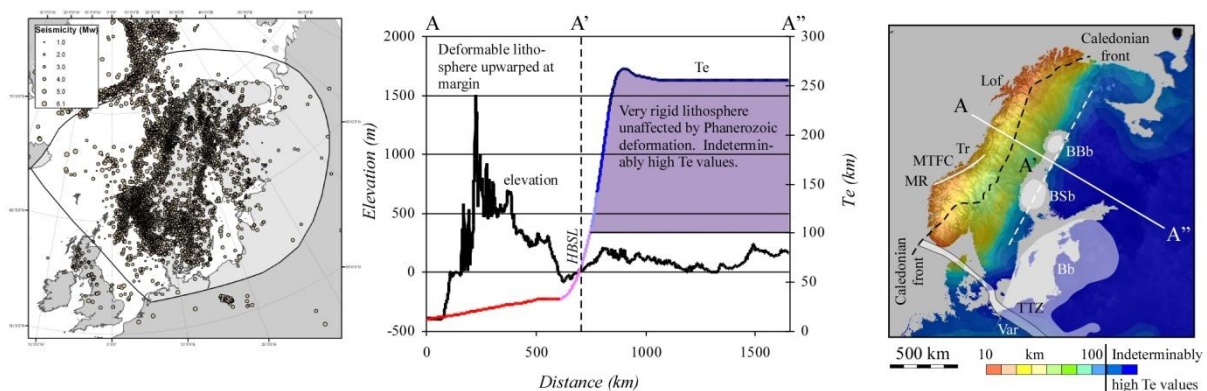


**Figure 1.** Relationship between seismicity, flexural rigidity ( $T_e$ , in km), the Hinterland Break in Slope (HBSL), and Fennoscandia's topographic envelope.  $T_e$  by Pérez-Gussinyé and Watts (2005). Seismic data from University of Helsinki catalogue.

Geological understanding of how continents undergo thinning leading to breakup has been revolutionized throughout the past decade (see Péron-Pinvidic and Manatschal et al., 2009). One very important concept is that, during large magnitude stretching, the brittle ductile transition can migrate out of the crust and into the underlying mantle. This can occur

at around 10 km thickness (Pérez-Gussinyé and Reston, 2001). Such margins have been called "hyperextended" (see Lundin and Doré, 2011). One result of hyperextension is that large detachment faults can penetrate the mantle, causing it to undergo serpentinization or other structural and rheological changes. Following large magnitude stretching the lithosphere must cool, resulting in subsidence and allowing the formation of a "sag" basin. It has been commonly assumed that lithospheric cooling also causes its strength to increase. However, serpentinization and structural damage may extend to surprising depths (see geoseismic interpretations in Zalán et al., 2011). It is possible that within certain zones at hyperextended margins, the lithosphere can remain weak for a long, long time (see previous work by Péron-Pinvidic et al. 2008, Mohn et al., 2010; Lundin and Doré, 2011).

These studies have generated much new terminology for the extended margin (Figure 2). However, the impact of hyperextension on passive margin evolution has only very recently become a topic of research. The interaction of Scandinavia's hyperextended margin with the old, cold lithosphere of the Fennoscandian interior provides fertile ground for new geological and geophysical research.

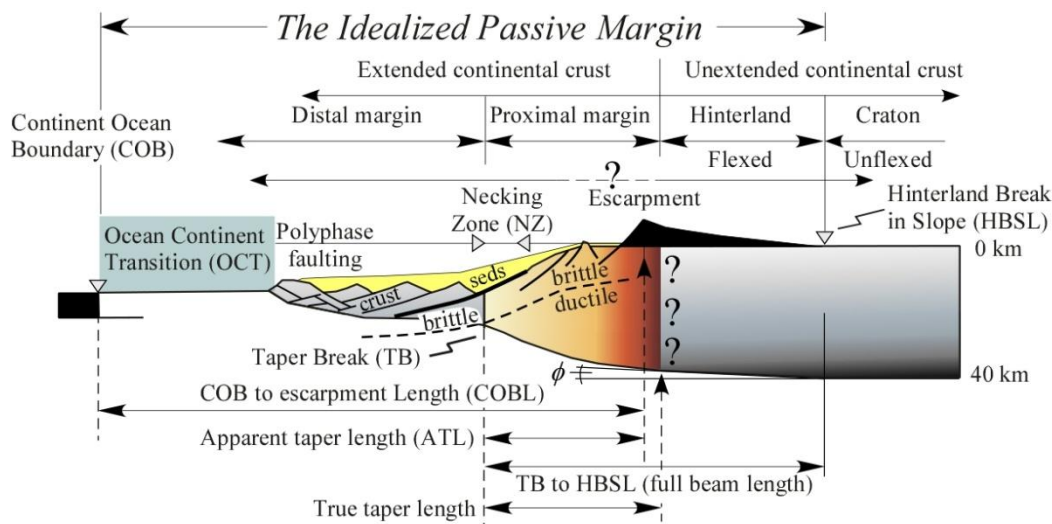


**Figure 2.** Some modern terminology applied to the passive margin.

Osmundsen and Redfield (2011) defined the Taper Break (TB) to be the landward point where the crystalline continental crust of the extended margin was thinned to 10 km. Commonly marked by large magnitude detachment faults, the TB is a fundamental benchmark. Osmundsen and Redfield (2011) showed that the distance between the TB and the escarpment crest (the Apparent Taper Length, or ATL) scales directly to the elevation of the escarpment (Figure 3). Redfield and Osmundsen (in press) showed that, in Scandinavia, the distance between the TB and the HBSL also scales directly to the escarpment elevation (Figure 4). The TB and the HBSL constitute fundamentally important markers for the Scandinavian passive margin.

Redfield and Osmundsen (in press) suggested that the hinterland of Sweden should be considered part of the Scandinavian passive margin because it has almost certainly been uplifted as part of an accommodation phase that took place after the main stretching and thinning phases were completed. This is in part evident from the patterns of Apatite Fission Track (AFT) apparent ages that have been determined for Fennoscandia (Hendriks et al.,

2007). Central Baltica's land surface is among the world's oldest: many of the Finnish AFT data have lost much (or even all!) of their thermal information to radiation enhanced annealing (Hendriks and Redfield, 2005). These AFT data rank are spatially associated with a nearly horizontal erosion surface named the sub Cambrian Peneplain. This peneplain has a relief of a few tens of meters, is exposed in many places, and probably once covered major parts of the Fennoscandian Shield. Not greatly incised, it has likely never been uplifted (Lidmar-Bergström et al., 2007 and citations therein). Similarly, although some thin sedimentary cover is likely, it has likely never been deeply buried (Hendriks and Redfield, 2005; 2006). Plus or minus some few hundred meters, Finland's part of the sub Cambrian Peneplain constitutes a marker horizon approximating sea level from the late Proterozoic to present-day times.

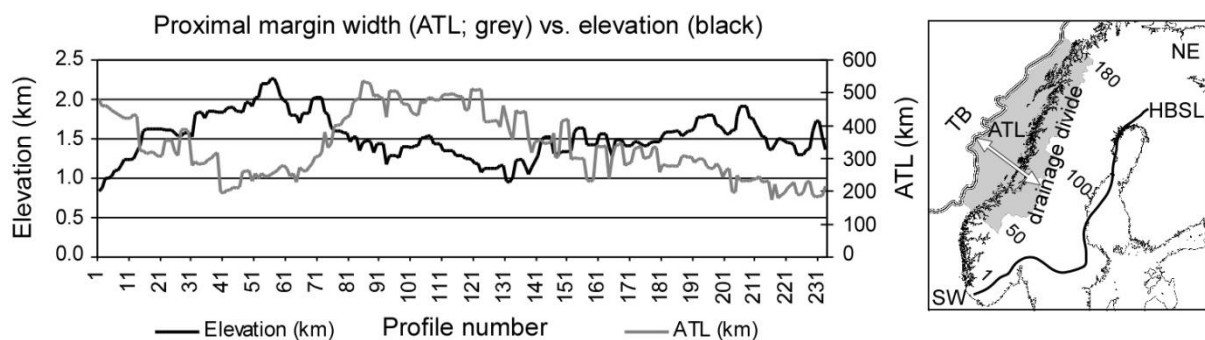


**Figure 3.** Relationship between the Taper Break (TB), the Apparent Taper Length (ATL), and the elevation of the Scandinavian Mountains. The 233 profiles were oriented parallel to the white arrow, also parallel to the direction of stretching (see Figure 4).

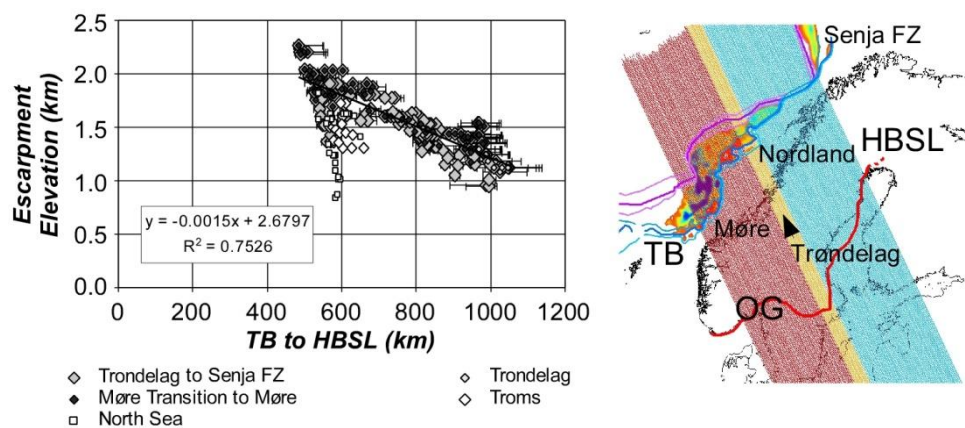


**Figure 4.** Relationship between the Taper Break (TB), the Hinterland Break in Slope (HBSL), and the elevation of the Scandinavian Mountains (after Redfield and Osmundsen, in press).

In Sweden, the sub Cambrian Peneplain has been tilted, and in parts of Norway it has been uplifted to high elevation. However, in other places west of the HBSL, it has been completely obliterated by younger landforms. Lidmar-Bergström et al (2007) described a series of younger paleosurfaces that rise with the hinterland and fan gently westward. Preliminary K/Ar data from basement saprolite rocks drilled on the offshore Utsira High

yielded Triassic ages (Fredin et al., 2012). These data suggest some of the Swedish paleosurfaces may also be quite old.

We suggest that a self-reinforcing feedback between erosion, deposition, rift inheritance, and cratonic rigidity may have helped generate and shape post breakup Fennoscandia. The relative location of the first landward occurrence of total crustal embrittlement or deformation coupling ~ the Taper Break ~ controlled and continues to control Scandinavia's post-thinning geomorphic evolution. Marking the innermost limit that accommodation phase deformation can penetrate, the HBSL functions as a tectonic hinge. From the dark, rigid heart of cratonic Baltica to her structurally eviscerated, hyperextended continental edge, the landscapes and lithosphere of Fennoscandia are systematically linked.

### References:

- Fredin, O., Sørli, R., Knies, J., Zwingmann, H., Müller, A., Vogt, C., Grandal, E.M., and Lie, J.E. 2012. Weathered basement saprolite, at southern Utsira High – with examples from PL 501 (Johan Sverdrup discovery) and PL 338 areas (Edvard Grieg discovery). Is the saprolite a possible origin of the Draupne sandstone (Johan Sverdrup discovery)? NGF Abstracts and Proceedings, 2, 22-23.
- Hendriks, B.W.H. and Redfield, T.F., 2006. Reply to: Comment on 'Apatite Fission Track and (U--Th)/He data from Fennoscandia: An example of underestimation of fission track annealing in apatite.' Earth and Planetary Science Letters. 248. 1-2. 568-576. .
- Hendriks, B.W.H. and Redfield, T.F., 2005. Apatite fission track and (U-Th)/He data from Fennoscandia: An example of underestimation of fission track annealing in apatite. Earth and Planetary Science Letters 236. 443- 458. .
- Hendriks, B. W. H., Andriessen, P. A. M., Huigen, Y., Leighton, C., Redfield, T. F., Murrell., G., Gallagher, K. & Soren Nielsen. A Fission Track Data Compilation for Fennoscandia. Norwegian Journal of Geology. 87, 143-155.
- Lidmar-Bergström, K. et al. 2007. Cenozoic landscape development on the passive margin of northern Scandinavia. Norwegian Journal of Geology, 87, 181-196.
- Lundin, E.R. and Doré, A.G., 2011, Hyperextension, serpentinitization, and weakening: A new paradigm for rifted margin compressional deformation: Geology, v. 39, p. 347-350.
- Mohn, G., Manatschal, G., Müntener, O., Beltrando, M., and Masini, E., 2010, Unravelling the interaction between tectonic and sedimentary processes during lithospheric thinning in the Alpine Tethys margins: Int. J. Earth Sci.. v. 99 (Suppl. 1), p. 75–101.
- Osmundsen, P. T. and Redfield, T.F., 2011, Crustal taper and topography at passive continental margins: Terra Nova, v. 23, p. 349-361.
- Pérez-Gussinyé M. and Watts, A. B., 2005, The long-term strength of Europe and its implications for plate-forming processes: Nature, v. 436, doi:10.1038/nature03854.
- Peréz-Gussinyé, M. and Reston. T. J., 2001, Rheological evolution during extension at passive, non-volcanic margins: Onset of serpentinitization and development of detachments to continental breakup: J. Geophys. Res., v. 106, p. 3961-3975.
- Péron-Pinvidic, G., Manatschal, G., Dean, S. M. and Minshull, T. A., 2008, Compressional structures on the West Iberia rifted margin: controls on their distribution in Johnson, H., Doré, A.G., Gatliff, R.W., Holdsworth, R., Lundin, E.R., and Ritchie, J.D., eds., The Nature and Origin of Compression in Passive Margins: Geological Society, London, Special Publications, London. No. 306, p. 169–183. DOI: 10.1144/SP306.8. .
- Péron-Pinvidic and Manatschal, G., 2009, The final rifting evolution at deep magma-poor passive margins from Iberia-Newfoundland: a new point of view: Int. J. Earth Sci. (Geol. Rundsch.), v. 98, p. 1581–1597.
- Redfield and Osmundsen. The long-term topographic response of a continent adjacent to a hyperextended margin: a case study from Scandinavia. In press, GSA Bulletin.
- Zalán, P.V., Severino, M.C.G., Rigoti, C., Magnavita, L.P., Oliveira, J.A.B., Viana, A.R., 2011, An entirely new 3D-view of the crustal and mantle structure of a ruptured South Atlantic passive margin – Santos, Campos and Espírito Santo Basins, Brazil [abs]: AAPG Annual Convention and Exhibition Abstracts Volume CD-ROM, Paper 986156 (Expanded Abstract), Houston, April 10-13.

## Magmatic evolution of the Vaasa granite complex, western Finland: Preliminary constraints from *in situ* geochemistry of alkali feldspar megacrysts

O.T. Rämö<sup>1</sup>, A. Kotilainen<sup>1</sup>, M.A. Barnes<sup>2</sup>, R. Michallik<sup>1</sup> and C.G. Barnes<sup>2</sup>

<sup>1</sup>Department of Geosciences and Geography, University of Helsinki, Finland

<sup>2</sup>Texas Tech University, Lubbock, Texas, U.S.A.

E-mail: tapani.ramo [at] helsinki.fi

A disk-shaped alkali feldspar megacryst (1.5 cm by 7 cm) from the south-central part of the granitic core of the Paleoproterozoic Vaasa complex has been examined for *in situ* major and trace element geochemistry along a 42-point profile from megacryst center to margin. The results show that the megacryst grew from the center outwards, imply growth from relatively homogeneous magma, and point to early garnet control followed by enhanced crystal-liquid fractionation.

**Keywords:** alkali feldspar, megacryst, *in situ* geochemistry, trace elements, granite, Paleoproterozoic, Vaasa, Finland

### 1. Introduction

The overall age-associated structure of the Paleoproterozoic Svecofennian crust in Finland has been delineated by seismic, lithologic, and geochemical means (e.g., Lahtinen et al., 2005 and references therein). Salient processes include mantle-crust differentiation to juvenile crust (e.g., Huhma, 1986) and accretion of distinct crustal blocks (e.g., Lahtinen and Huhma, 1997; Rämö et al., 2001), probably during several successive orogenic events. Little attention has thusfar been paid to model the dynamic processes associated with the growth of the Svecofennian orogen. An on-going Academy of Finland project (PI: Annakaisa Korja, Seismological Institute, University of Helsinki) entitled “Three-dimensional evolution of the middle crust in central Fennoscandia” is in pursuit of a generic model for the Svecofennian orogen, focusing on dynamic processes in upper and middle crust during orogenic tectonothermal peaks. Important targets in dynamic modelling are metamorphic core complexes (e.g., Rey et al., 2009) that expose deep (middle) crust as a result of intracratonic mass movement within crustal domains undergoing gross extension and anatexis.

A key area from the perspective of dynamic modelling of the Svecofennian orogen is the Vaasa complex in western Finland (Fig. 1). The Vaasa complex consists of an oval granite/granodiorite core (the Vaasa batholith) surrounded by migmatites (diatexite, metatexite) and metasedimentary rocks (Mäkitie et al., 2012). The metamorphic grade of the metasedimentary rocks increases towards the migmatites and the granitic core. The granitic rocks in the central part of the complex are characterised by alkali feldspar megacrysts ( $\geq 10$  cm in diameter) as well as garnet, an almost ubiquitous minor mineral. In order to examine the evolution and origin of the Vaasa granite, we have launched an *in situ* geochemical study of the alkali feldspar megacrysts hosted by the granites. Here we report preliminary results of a pilot major and trace element study of a megacryst recovered from the Vaasa granite.

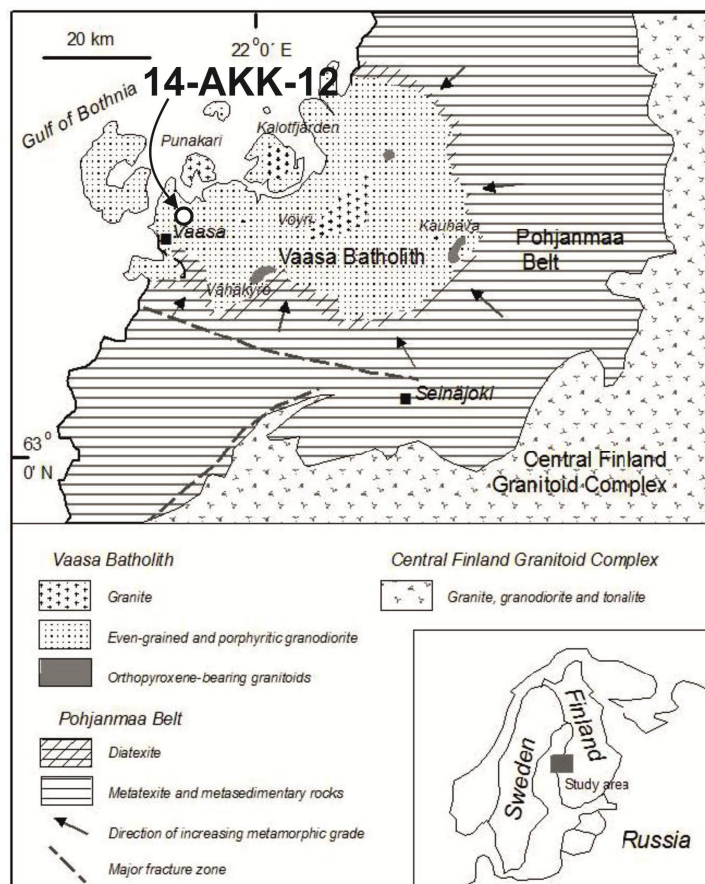


**Figure 1.** Geological sketch map of the Vaasa complex (modified from Mäkitie et al., 2012). The Vaasa complex is surrounded in the east and south by the Central Finland granitoid complex. The Vaasa complex forms a concentric structure across the Gulf of Bothnia; approximately half of this structure is exposed on the Finnish mainland. The metamorphic grade of the meta-sedimentary rocks increases toward the center of the complex where a granitoid core (the Vaasa batholith) is flanked by a zone of diatexitic and metatexitic migmatites. Location of the pilot sample (14-AKK-12) is shown.

## 2. Sample preparation

The pilot sample (14-AKK-12; 63°08'03.9" N, 21°45'11.2" E) comes from a macadam quarry (Rudus Oy) in the southern part of the Vaasa granite area northeast of Vaasa (Fig. 1). The megacryst is disk-shaped, ~7 cm in diameter and ~1.5 cm in thickness, and is enclosed in a coarse-grained garnet-bearing biotite granite host. The megacryst was sawn in half along the plane of the disk and a polished section (280  $\mu\text{m}$ ) was made from the projected center of the megacryst to the rim of it. A linear 35 mm long traverse of 42 points from the projected core to the edge of the megacryst and into the granite host was marked for *in situ* spot analysis.

## 3. Methods

The major element composition of alkali feldspar was measured using the electron microprobe at the Department of Geosciences and Geography, University of Helsinki. The diameter of the (defocused) electron beam was 75  $\mu\text{m}$ , beam current measured at the Faraday cup 15 nA, and accelerating voltage 20 kV. After EPMA major element work, the spots were analysed for trace elements using the LA-QICP/MS at the Department of Geosciences, Texas Tech University. The laser beam diameter was 100  $\mu\text{m}$ . With repetition frequency of 13 Hz, energy output of 55%, and dwell time of 46 seconds, an overall fluency of 20-21 J/cm<sup>2</sup> was acquired and the vertical ablation holes (~250  $\mu\text{m}$ ) almost penetrated the thick section. This high-energy ablation secured measurement of, e.g., most of the rare earth elements to the ~10 ppb level. The NIST612 glass was run as an external standard, SiO<sub>2</sub> values determined by EPMA were used as the internal standard. The results are shown in Fig. 2 and described below.

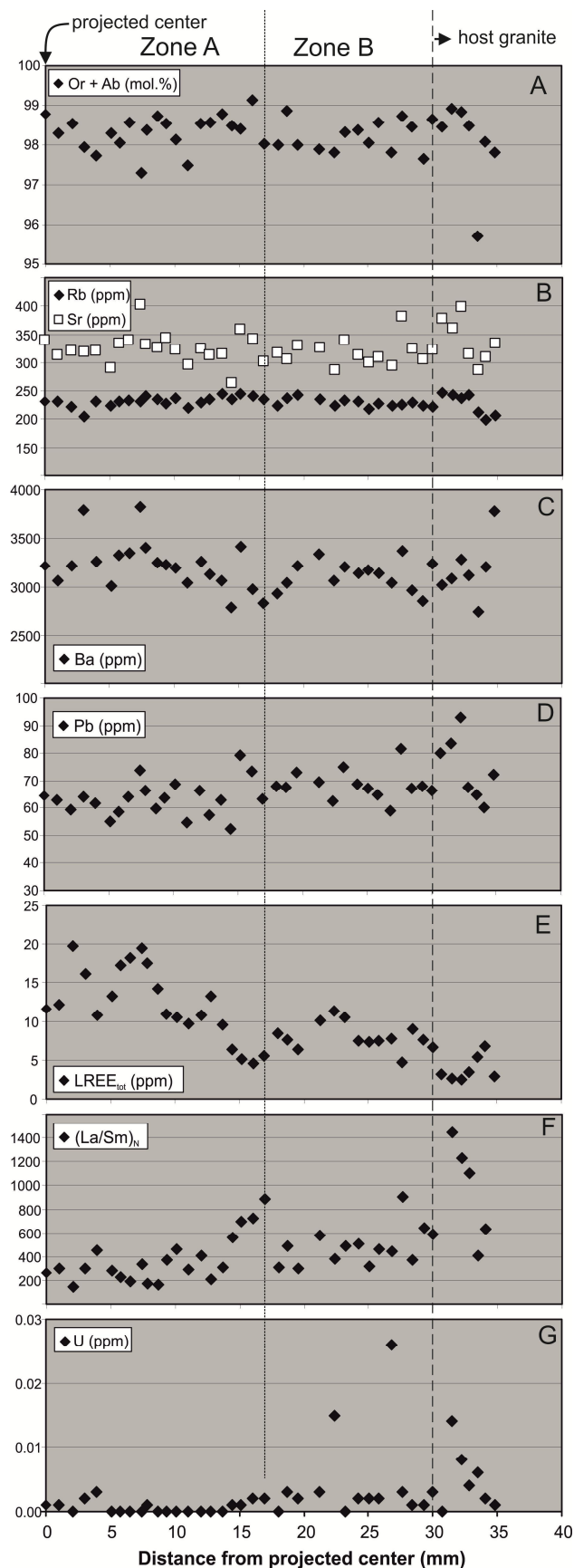


**Figure 2.** Geochemical variations along a linear profile in a Vaasa granite alkali feldspar megacryst (sample 14-AKK-12). The megacryst is ~7 cm in diameter, ~1.5 cm thick and disk-shaped. The 42 spots analysed extend from the projected center to the host granite, and the profile covers 30 mm of the megacryst and 3.5 mm of the surrounding biotite granite. Panels are as follows: A: molar Or + Ab; B: Rb and Sr; C: Ba; D: Pb; E: total LREE (La through Sm); F: Chondrite-normalized La/Sm; G: U. Feldspar-incompatible trace element concentration profiles (E, F, G) divide the megacryst into two domains, core (Zone A) and mantle (Zone B).

#### 4. Petrography and mineralogy

The alkali feldspar of the examined megacryst is relatively homogeneous and only sparsely perthitic with flame-shaped up to 10  $\mu\text{m}$  thick and, on the average, 50  $\mu\text{m}$  long albite exolutions. Quartz is present as anhedral 1-3 mm wide and up to 5 mm long rods aligned obliquely or concentrically around the projected center of the megacrysts. The megacryst has been partly sericitized along albite exolutions, yet not to the extent that would have compromised the laser analysis. Further mineral inclusions in the megacryst comprise euhedral biotite (length  $\leq 1.5$  mm), pyrope-almandine (diameter  $\leq 2$  mm), cordierite, monazite, zircon, ilmenite, titanite, apatite, albite, fluorite, rutile, pyrrhotite, and pyrite.

#### 5. Major and trace element composition of the examined alkali feldspar megacryst

Along the examined profile, the alkali feldspar is quite homogeneous in major element composition, averaging  $84.9 \pm 3.1\%$  Or,  $13.4 \pm 2.9\%$  Ab, and  $0.9 \pm 2.6\%$  An. From the projected core to the rim (30 mm), the megacryst alkali feldspar has about  $98 \pm 1\%$  Or + Ab and shows no trends relative to position, whereas the host granite is more varying in this respect (Fig. 2a). Feldspar-compatible trace elements Ba (~3000-3500 ppm), Rb (~200-250 ppm), and Sr (~300-350 ppm) are quite constant throughout the examined profile (Fig. 2b, c). Pb, however, shows a slight overall increase (~60 ppm to 70 ppm) from the center to the margin (Fig. 2d). In contrast feldspar-incompatible trace elements reveal two distinct compositional segments in the megacryst – from the projected center to a distance of 17 mm (Zone A; Fig. 2) and from 17 mm to the margin of the megacryst at 30 mm (Zone B). Zone A shows a decline in total LREE (La-Sm) from ~20 ppm to 5 ppm, whereas in Zone B the LREE are ~constant between ~5 ppm and 10 ppm (Fig. 2e). This also shows in the relative enrichment of LREE with  $(\text{La}/\text{Sm})_N$  increasing from ~200 to ~800 in Zone A and from ~250 to ~700 in Zone B (Fig. 2f). A salient difference between Zone A and Zone B is also demonstrated by U that straddles along the detection limit (~1 ppb) in Zone A and is clearly higher (up to 25 ppb) and more varying in Zone B (Fig. 2g).

#### 6. Conclusions

The non-varying major components and compatible trace elements of the alkali feldspar megacryst show that, during the crystallization of the megacryst, the magmatic system was probably not refurbished with primary melts. The chemical zoning observed shows that the megacryst grew from the center outwards in a magmatic environment. The REE patterns may imply garnet control in the outset (Zone A), whereas the enrichment in U points to enhanced (magmatic) fractionation at the later stage (Zone B). Common-Pb composition along the traverse will be determined in search of possible isotopic changes during megacryst growth.

#### References:

- Huhma, H., 1986. Sm-Nd, U-Pb and Pb-Pb isotopic evidence for the origin of the Early Proterozoic Svecokarelian crust in Finland. *Geol. Surv. Finland Bull.* 337
- Lahtinen, R. and Huhma, H., 1997. Isotopic and geochemical constraints on the evolution of the 1.93-1.79 Ga Svecofennian crust and mantle in Finland. *Precambrian Res.*, 82, 13-34.
- Lahtinen, R., Korja, A., and Nironen, M., 2005. Paleoproterozoic tectonic evolution. In: Lehtinen, M., Nurmi, P.A., Rämö, O.T. (Eds.), *Precambrian Geology of Finland – Key to the Evolution of the Fennoscandian Shield*. Developments in Precambrian Geology, Volume 14. Elsevier, Amsterdam, 481-531.
- Mäkitie, H., Sipilä, P., Kujala, H., and Kotilainen, A., 2012. The diatexitic Vaasa batholith in the Fennoscandian shield: petrography and geochemistry. *Bull. Geol. Soc. Finland*, in press.
- Rämö, O.T., Vaasjoki, M., Mänttari, I., Elliott, B. A., and Nironen, M., 2001. Petrogenesis of the post-kinematic magmatism of the Central Finland Granitoid Complex I: radiogenic isotope constraints and implications for crustal evolution. *J. Petr.*, 42, 1971-1993.
- Rey, P.F., Teyssier, C., and Whitney, D.L., 2009. Extension rates, crustal melting, and core complex dynamics. *Geology*, 37, 391-394.

# Paleomagnetic and geochemical studies of the Subjotnian Satakunta diabase dykes – implications to Mesoproterozoic supercontinent Nuna

J. Salminen<sup>1</sup>, S. Mertanen<sup>2</sup>, D. Evans<sup>3</sup> and Z. Wang<sup>3</sup>

<sup>1</sup>Division of Geophysics and Astronomy, Physics Department, University of Helsinki, P.O. Box 64, FIN-00014 University of Helsinki, Finland

<sup>2</sup>Geological Survey of Finland, South Finland Unit, P.O. Box 96, FI-02151 Espoo, Finland

<sup>3</sup>Department of Geology and Geophysics, Yale University, 301 Kline Geology Laboratory, P.O. Box 208109, New Haven, CT 06520-8109, USA

E-mail: Johanna.m.salminen [at] helsinki.fi

Paleoproterozoic supercontinent Nuna (Columbia, Hudsonland) has been suggested by several studies. Many recent reconstructions of this supercontinent are based on the assumption that the core of Nuna was composed of united Baltica and Laurentia cratons forming the NENA (Northern Europe – North America) configuration that lasted from 1.8 Ga to at least 1.26 Ga. Our new paleomagnetic results from the Mesoproterozoic (1565–1590 Ma) diabase dyke swarm in Satakunta, western Finland, provides new paleomagnetic evidence to support the NENA configuration.

**Keywords:** Subjotnian, dykes, supercontinent, Nuna

## 1. Introduction

The concept of supercontinent cycles is mainly based on the global peaks in distribution of U-Pb ages in zircon and Nd-model ages in whole rock samples (Condie, 1998). Reddy and Evans (2009) summarized recently the secular evolution of the Earth from the Neoproterozoic to the Mesoproterozoic eras, revealing intriguing temporal relationships of supercontinent cycles with early evolution of core, mantle, crust, oceans, atmosphere and life.

Paleoproterozoic supercontinent Nuna (Columbia, Hudsonland) has been suggested by several authors (e.g. Williams et al., 1991; Pesonen et al., 2003; Zhao et al., 2004; Condie, 2004). Baltica (East European craton) and east Laurentia (North America and Greenland) are some of the most important building blocks of this supercontinent. The temporal and compositional overlap between the anorogenic and orogenic magmatism in west Baltica and east Laurentia, together with the paleomagnetic data available from these two cratons, suggest that these continents coexisted for more than 600 million years (from ca. 1.8 to ca. 1.2 Ga), constituting the juxtaposition named NENA (Northern Europe – North America; Gower et al., 1990). However, a recent study from Greenland were purported to challenge this fit (Halls et al., 2011). In this paper we present new Subjotnian (1.565–1.59 Ga) paleomagnetic and geochemical data to support the NENA fit.

## 2. Geology and sampling

In Satakunta, the Svecofennian crust consists of Paleoproterozoic granitoids, paragneisses and felsic and intermediate metavolcanic rocks. This assemblage is cut by mafic dyke swarms of three different age groups. The oldest one consists of metamorphosed amphibolite dykes of Svecofennian age. The rest of the dykes are unmetamorphosed and can be further divided to two groups; Subjotnian diabases and Postjotnian olivine diabases. Based on petrography, mode of occurrence and field relations, it has been suggested that the Subjotnian dykes in Satakunta are continuations of both Häme (1665 Ma: Vaasjoki and Sakko, 1989 and  $1646 \pm 6$  Ma: U-Pb (zr), Laitakari, 1987) and Föglö ( $1577 \pm 12$  Ma: U-Pb and  $1540 \pm 12$  Ma, Suominen, 1991) dyke swarms. The width of the Subjotnian swarm is tens of kilometers, and the length

is likely ca. 300 km, from Pori to Åland. These dykes trend N-S, E-W, and NE/NNE-SW/SSW and dip vertically/subvertically. Dyke widths vary from a few centimetres to over one hundred metres. There is a U-Pb age (baddeleyite) of 1565-1590 Ma for one N-S trending dyke (Lehtonen et al., 2003) supporting the suggestion that it belongs to the same system as the Föglö dykes.

Altogether, 41 diabase dyke sites were sampled at Satakunta, Finland. The distance from the northernmost sampling site to the southernmost sampling site is ca. 100 km. In 31 of the sites we sampled baked host rocks, and in 22 of them also unbaked host rock was sampled for baked contact tests to study the age of magnetic remanence.

### 3. Results

Whole-rock geochemical data show that concentrations of REE are high (e.g. La ca. 35 ppm). The chondrite-normalized REE patterns of E-W trending dykes are nearly linear and show enrichment of light REE relative to heavy REE. N-S and NE-SW trending dykes show wider range of values also with enrichment of light REE. Magma from Satakunta N-S and NE-SW trending dykes is characterised by similar Nb/Y values compared to Föglö (1.54-1.58 Ga) dykes and magma from Satakunta E-W trending dykes similar with Häme (1.64-1.67 Ga) dykes (e.g. Luttinen and Kosunen, 2006). Based on these correlations we divide the paleomagnetic data into two groups.

From all Satakunta dykes with different trends, a dual-polarity, high-stability magnetic remanence component was obtained, and it was confirmed to be primary by several baked contact tests. A suite of rock-magnetic analyses demonstrates that pseudo-single domain magnetite is the remanence carrier.

For N-S and NE-SW trending dykes the combined mean remanence direction for both polarities is  $D = 8.3^\circ$ ,  $I = 6.5^\circ$  ( $\alpha_{95} = 5.9^\circ$ ), yielding a new key paleomagnetic pole (SK1) for Baltica at  $32.7^\circ\text{N}$ ,  $188.7^\circ\text{E}$  with  $A_{95} = 4.2^\circ$ . This pole fulfills six out of seven Van der Voo (1990) factors (failing only the criterion of similarity to younger poles from Baltica). For E-W trending dykes the combined mean remanence direction for both polarities is  $D = 356.9^\circ$ ,  $I = 8.3^\circ$  ( $\alpha_{95} = 15.9^\circ$ ), yielding a paleomagnetic pole (SK2) for Baltica at  $32.6^\circ\text{N}$ ,  $205.5^\circ\text{E}$  with  $A_{95} = 14.3^\circ$ . This pole fulfills four out of seven Van der Voo (1990) factors.

### 4. Discussion

Based on the reconstruction using the new Satakunta pole and the nearly coeval ( $1592 \pm 3$  Ma) Western Channel Diabase pole from Laurentia (Irving, 1972; Hamilton and Buchan, 2010), the NENA fit could have existed at 1.57-1.59 Ga. Consequently, coeval paleomagnetic data coupled with correlations of geochronology and basement geology of Baltica and Laurentia validates the NENA fit at 1.77-1.75 Ga, 1.59-1.57 Ga, 1.46 Ga, and 1.27 Ga (Fig. 1).

Using the same NENA reconstruction, the dual-polarity 1.63 Ga paleomagnetic poles from Greenland (Melville Bugt, Halls et al., 2011) and Finland (Sipoo, Mertanen and Pesonen, 1995) are offset by about  $30^\circ$  (Fig. 1). However, when using the whole range of the fairly scattered data from individual sites, the NENA fit can be allowed. In Sipoo dykes, as well as in several other similar aged formations in Fennoscandia, the reversed polarity data are more scattered than normal polarity data, possibly due to transition of the Earth's magnetic field during remanence acquisition. Other reasons for scattered Subjotnian data could include rock magnetic effects, unrecognized secondary components, unrecognized tilting of the granites, enhanced secular variation or non-dipolarity of the geomagnetic field, continent drift, or oscillatory true polar wander at 1.6-1.5 Ga (e.g. Evans and Mitchell, 2011).

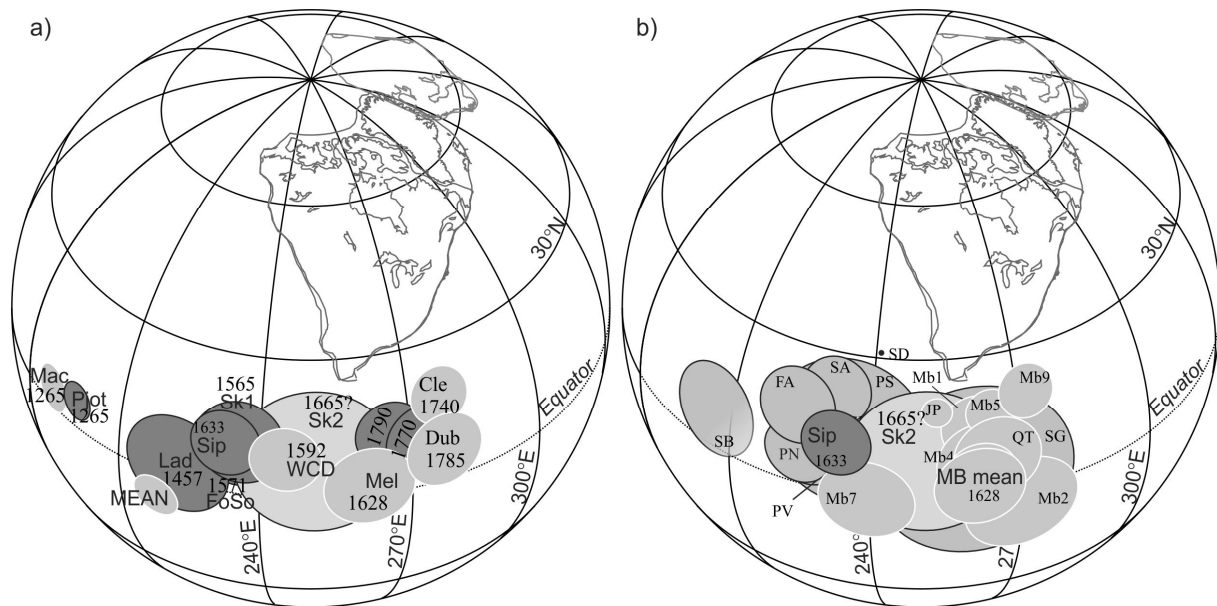


**Figure 1.** Testing the NENA fit. (a) Key poles of Laurentia (light grey with white circles) and Baltica (dark grey with black circles) and pole from Satakunta E-W dykes (SK2) rotated to NENA configuration in the North American reference frame. (b) Site-mean virtual geomagnetic poles for Melville Bugt dykes, Greenland (normal polarity is used; Halls et al., 2011; grey with white circles) and for Sipoo dykes, Finland (Mertanen and Pesonen, 1995; grey with black circles). Additionally, the SK2 pole of this study is plotted. Baltica and its poles are rotated to the reference frame of North America by Euler pole: Plat = 47°, Plong = 1.5°, angle = 49° (Evans and Pisarevsky, 2008). Poles from Greenland are rotated to reference frame of North America by Euler pole: Plat = 67.5°, Plong = 241.5°, angle = -13.8° (Roest and Sirvastava, 1989).

## 5. Conclusions

The paleomagnetic study of Satakunta diabase dykes in southwest Finland, associated to rapakivi magmatism, provides a new key pole (SK1: Plat = 29°, Plong = 188°, A95 = 7°) for Baltica. This pole is derived from N-S and NE-SW trending dykes, where the former have the age of 1565-1590 Ma (U-Pb, baddeleyite; Lehtonen et al., 2003). Rock magnetic analyses and positive baked contact tests suggest that the Satakunta pole SK1 represents a primary thermoremanent magnetization, which fulfils the first six quality criteria for paleomagnetic poles (Van der Voo, 1990). E-W trending dykes provided primary paleomagnetic pole (SK2: Plat = 33°, Plong = 206°, A95 = 14°) that fulfils four quality criteria for paleomagnetic pole.

Analyses of previous Subjotnian paleomagnetic data for Baltica, and comparison of the new Satakunta poles with the present Mesoproterozoic paleomagnetic data and correlations of geochronology and basement geology for Baltica and Laurentia suggest that NENA configuration is valid during the whole time period between 1.77 and 1.27 Ga forming the core of Nuna supercontinent.

## References:

Condie, K.C., 1998. Episodic continental growth and supercontinents: a mantle avalanche connection? *Earth. Plan. Sci. Lett.*, 163, 97-108.

- Condie, K. C., 2004. Supercontinents and superplume events: distinguishing signals in the geologic record. *Phys. Earth Planet. Sci.* 146, 319-332.
- Evans, D.A.D., Pisarevsky, S.A., 2008. Plate tectonics on early Earth? Weighing the paleomagnetic evidence. *Geol. Soc. Am. Spec. Pap.* 440, 249-263.
- Evans, D.A.D., Mitchell, R.N., 2011. Assembly and breakup of the core of Paleo-Mesoproterozoic supercontinent Nuna. *Geology* 39, 443-446.
- Gower, C.F., Ryan, A.B., Rivers, T., 1990. Mid-Proterozoic Laurentia–Baltica: an overview of its geological evolution and a summary of the contributions made by this volume. In: Gower, C.F., Rivers, T., Ryan, B. (Eds.), *Mid-Proterozoic Laurentia–Baltica*. *Geol. Ass. Can. Spec. Pap.* 38, 1–20.
- Halls, H. C., Hamilton, M., Denyszyn, S. W., 2011. The Melville Bugt dyke swarm of Greenland: A connection to the 1.5 - 1.6 Ga Fennoscandian rapakivi granite province? In: Srivastava (ed.) *Dyke Swarms: keys for Geodynamic Interpretation*, 509-535. doi 10.1007/987-3-642-12496-9\_27.
- Hamilton, M., A.; Buchan, K.L., 2010. U–Pb geochronology of the Western Channel Diabase, northwestern Laurentia: Implications for a large 1.59 Ga magmatic province, Laurentia’s APWP and paleocontinental reconstructions of Laurentia, Baltica and Gawler craton of southern Australia. *Precambrian Res.* 183, 463–473.
- Irving, E., Donaldson, J. A., Park, J. K., 1972. Paleomagnetism of the Western Channel Diabase and Associated Rocks, Northwest Territories. *Can. J. Earth Sci.* 9, 960-971.
- Laitakari, I., 1987. The Subjotnian diabase dyke swarm of Hame. In: Aro, K., and Laitakari, I., (eds.) *Suomen diabaasit ja muut mafiset kivilajit*. *Geol. Surv. Finl. Report of investigation* 76, 99-116.
- Lehtonen, M.I., Kujala, H., Kärkkäinen, N., Lehtonen, A., Mäkitie, H., Mänttari, I., Virransalo, P., Vuokko, J., 2003. Etelä-Pohjanmaan liuskealueen kallioperä. Summary: Pre-Quaternary rocks of the South Ostrobothnian Schist Belt. *Geol. Surv. Finl. Report of Investigation* 158, pp. 125.
- Luttinen, A.V., Kosunen, P.J., 2006. The Kopparnäs dyke swarm in Inkoo, southern Finland: new evidence for Jotnian magmatism in the SE Fennoscandian Shield. In: Hanski, E., Mertanen, S., Rämö, T., Vuollo, J. (Eds.) *Dyke Swarms – Time markers of Crustal Evolution. Selected papers of the Fifth International Dyke Conference in Finland, Rovaniemi, Finland, 31 July – 3 Aug. 2005*. Taylor & Francis Group, London, 85-97.
- Mertanen, S., Pesonen, L. J., 1995. Paleomagnetic and rock magnetic investigations of the Sipoo Subjotnian quartz porphyry and diabase dykes, southern Fennoscandia. *Phys. Earth Planet. Int.* 88, 145-175.
- Pesonen, L. J., Elming, S.-Å., Mertanen, S., Pisarevsky, S., D’Agrella-Filho, M. S., Meert, J. G., Schmidt, P.W., Abrahamsen, N., Bylund, G. 2003. Paleomagnetic configuration of continents during the Proterozoic. *Tectonophysics* 375, 289-324.
- Reddy, S.M., Evans, D.A.D., 2009. Palaeoproterozoic supercontinents and global evolution: Correlations from core to atmosphere. In: Reddy, S.M., Mazumder, R., Evans, D.A.D., Collins, A.S., eds., *Palaeoproterozoic Supercontinents and Global Evolution*. *Geol. Soc. Lond. Spec. Publ.*, 323, 1-26.
- Roest, E.R., Srivastava, S.P., 1989. Sea floor spreading in the Labrador Sea: a new reconstruction. *Geology* 17, 1000-1003.
- Vaasjoki and Sakko, 1989. The radiometric age of the Virmaila diabase dyke: Evidence for 20 Ma continental rifting in Padasjoki, southern Finland. In: Autio, S. (ed.) *Current Research 1988*, *Geol. Surv. Fin. Spec. Pap.* 10, 43-44.
- Van der Voo, R., 1990. The reliability of paleomagnetic data. *Tectonophysics* 184, 1-9.
- Williams, H., Hoffman, P.F., Lewry, J.F., Monger, J.W.H., Rivers, T., 1991. Anatomy of North America: thematic portrayals of the continent. *Tectonophysics* 187, 117–134.
- Zhao, G., Sun, M., Wilde, S. A., Li, S., 2004. A Paleo-mesoproterozoic supercontinent: assembly, growth and breakup. *Earth Sci. Rev.*, 67, 91-123.

# Structure of the upper mantle beneath the northern Fennoscandian Shield revealed by high-resolution teleseismic P-wave traveltimes tomography

H. Silvennoinen<sup>1,2</sup>, E. Kozlovskaya<sup>1</sup>, E. Kissling<sup>3</sup>, and POLENET/LAPNET Working Group

<sup>1</sup>Sodankylä geophysical observatory, PoB 3000, 90014 University of Oulu, Finland

<sup>2</sup>Department of Physics, PoB 3000, 90014 University of Oulu, Finland

<sup>3</sup>Institute of Geophysics, ETH Zürich, Sonneggstrasse 5, 8092 Zürich, Switzerland  
E-mail: hanna.silvennoinen [at] oulu.fi

In this article we describe the data set for our teleseismic tomography study of the upper mantle below northern Fennoscandian Shield based on passive seismic data of POLENET/LAPNET project. We also show the initial results on our inversion.

**Keywords:** lithosphere, upper mantle, teleseismic tomography, Fennoscandia

## 1. POLENET/LAPNET project

POLENET/LAPNET project is a passive seismic array experiment in northern Finland with some stations also in northern Sweden, Norway and Russia. The study area extends between 18° and 31° E and 64° and 70° N. The experiment was a part of International Polar Year (IPY) 2007-2009. The data acquisition period of POLENET/LAPNET experiment was May 2007 – September 2009. The array contained 21 permanent broad band stations and 35 temporary stations, of which 30 were broad band the whole data acquisition period and 3 were broad band for a significant portion of the period. The average distance between stations was 60 km.

The main targets of POLENET/LAPNET project are collecting waveforms of seismic phases travelling through the core and recordings of glacial earthquakes from Greenland. The research also aims to obtain a 3D seismic model of the upper mantle down to 670 km (P- and S-wave velocity models, position of major boundaries in the crust and upper mantle and estimates of seismic anisotropy strength and orientation) in northern Fennoscandian Shield and, in particular, beneath its Achaean domain. This study is one of the first steps in our project to obtain a model of the upper mantle in our study area.

## 2. Available data

The P-wave traveltimes dataset is based on 103 high quality teleseismic events with magnitudes larger than 5.8 and epicentral distances between 30° and 90° chosen from the bulletin of International Seismological Centre (<http://www.isc.ac.uk/>) and recorded by POLENET/LAPNET array. The events were manually picked from the data and the total amount of picked P-wave travel times is 3275. With these events we got a good azimuthal coverage. The largest gap in our azimuthal coverage is 15°.

We used IASP91 model (Kennett and Engdahl, 1991) as our 1D global reference model. The reference model is used on one hand to estimate seismic P-wave velocity outside our study area and on other hand as a starting model for travel time inversion.

## 3. The method and first results

In teleseismic tomography the magnitude and the spatial extension of the velocity anomalies are estimated by tracing the path of the seismic wave front back towards the epicentre through a 3D model. As the aim of this study is to obtain a model of seismic velocities at upper mantle, the effect of the crust above needs to be removed from the data. This crustal

correction has been calculated using a 3D crustal model build for POLENET/LAPNET study area (Silvennoinen et al., 2012). The model is based on previous controlled source seismic profiles and receiver function results in the area. Moho depth on our study area varies between 40 km and almost 60 km and most of the variations on crustal correction are caused by the variations in the Moho depth.

The initial model of the inversion extends between approximately 18° and 31° E and 64° and 70° N and to the depth of 600 km and it is formed of 60 km x 60 km x 30 km cells, respectively. For the inversion we used Telinv code.

Our resolution analysis demonstrated that the resolution of POLENET/LAPNET data is reasonably good between depths of 75 km and 300 km. The structure of the upper mantle beneath the LAPNET array appears to be heterogeneous down to the depth of about 200 km, with a number of positive and negative anomalies relative to the IASP91 standard velocity model. The velocities beneath the depth of 200 km are close to the IASP91 velocities.

The most pronounced features are positive anomaly (about 2%) with respect to the IASP91 model beneath the Achaean Karelian Craton in southeastern part of the study area and negative anomaly (-2%) in central part of the study area located below the Central Lapland Granitoid Complex. Both these anomalies extend down to the depth of about 200 km.

While our model of the upper mantle may be regarded as a northward extension of the 3D tomography model of SVEKALAPKO project by Sandoval et al. (2004), the structure of the upper mantle in the northern Fennoscandian Shield revealed in our study is generally different from the structure of the southeastern part of the Fennoscandian Shield revealed by the previous SVEKALAPKO experiment that revealed a high-velocity lithospheric "keel" stretching down to the depth of 300 km.

### References:

- Kennett, B.L.N. and Engdahl, E.R. 1991. Travel times for global earthquake location and phase association. *Geophysical Journal International*, 105:429-465.
- S. Sandoval, E. Kissling, J. Ansorge, SVEKALAPKO Seismic Tomography Working Group, High-resolution body wave tomography beneath the SVEKALAPKO array: II. Anomalous upper mantle structure beneath the central Baltic Shield. *Geophysical Journal International*, 157:200– 214.
- Silvennoinen, H., Kozlovskaya, E., Kissling, E., and POLENET/LAPNET working group. Compilation of Moho boundary map for northern Fennoscandian shield. *Geophysical Journal International*. (Submitted.)

## 3-D structural model of the Slave craton mantle lithosphere, Northwest Territories, Canada

D. B. Snyder<sup>1</sup>, M. Hillier<sup>1</sup> and B.A. Kjarsgaard<sup>1</sup>

<sup>1</sup>Geological Survey of Canada, Ottawa, Ontario  
Email: dsnyder [at] NRCan.gc.ca

After over ten years of acquiring and analyzing geophysical, geochemical and geological observations, we are able to compile a fully 3-dimensional model of the subcontinental mantle lithosphere of the Slave craton in northwestern Canada. This modelling supports future diamond exploration in northern Canada, but also benefits from the wealth of information derived from the numerous kimberlites, diamonds, mantle xenoliths and xenocrysts produced by exploration to date.

**Keywords:** Seismic wave velocity models, diamond deposits, kimberlites, subcontinental mantle lithosphere structure

### 1. Multiple knowledge layers

For the past five years, a collaborative research project oriented at enhancing diamond exploration in Canada's North has brought together geologists, geochemists and geophysicists to study the subcontinental mantle lithosphere of several key cratons within the Canadian Shield of North America. Because the Slave and Rae cratons now have undergone over a decade of relatively intense diamond exploration, these cratons have superior collections of mantle xenoliths, xenocrysts and derivative observations and models. The Slave craton hosts four diamond mines and its exploration-driven petrologic database is now comparable with the Kaapvaal, Zimbabwe and Siberia cratons.

Our 3-D model of the Slave craton mantle lithosphere incorporates ten geographically co-referenced knowledge layers that can be viewed together or separately. These knowledge layers include:

- continuous seismic P- and Rayleigh-wave velocity 3-D models;
- 3-D model of conductivity from MT recordings;
- seismic anisotropy or velocity discontinuity surfaces contoured from multi-azimuthal receiver functions;
- rock type "drill cores" constructed from xenoliths and xenocrysts;
- paleogeotherms modelled from xenolith suites recovered from kimberlite pipes;
- large-scale estimates of mantle rock fabric orientation from SKS splitting models;
- surface maps (2D) of elevation, gravity, magnetics and geology.

Many of these products are derived from recent Geomapping for Energy & Minerals program activities within Natural Resources Canada.

The P-wave and Rayleigh-wave velocity models are greatly improved by the increase in coverage by 3-component broadband stations deployed by the POLARIS consortium over the past decade (Bedle and van der Lee, 2009; Yuan et al., 2011). This station coverage is not as uniform or dense as that of USArray further south in North America, but is sufficient to provide new insights within focus areas such as the Slave and Rae cratons. These spatially continuous seismic models include P- and S-wave speeds as well as radial and azimuthal anisotropy.

Conductivity is being modelled in 3-D on a regional scale for the first time using newly developed algorithms and scattered or linear arrays of magnetotelluric soundings acquired over the past two decades (e.g., Jones et al., 2001; Spratt et al., 2009).

In addition to their use as arrays, the POLARIS stations have been active for sufficient periods (3–8 years) to enable their recordings of earthquakes at multiple azimuths to be used in impulse response or receiver functions studies (Bostock, 1989; Snyder, 2008). The resulting 3-dimensional ‘cones’ demarcate local discontinuity surfaces which can then be contoured over much of the craton. The Moho is the most prominent discontinuity surface, but several intra-lithosphere surfaces are also observed.

A number of kimberlite pipes or clusters have yielded sufficient mantle xenoliths for which pressure-temperature determinations can be made to allow construction of vertical ‘cores’ of mantle rock types and paleotemperatures. The lithosphere-asthenosphere boundary can thus be estimated in some locations. In some pipes, diamonds, garnets and other indicator minerals provide additional geochemical information such as age, REEs (e.g., Aulbach et al. 2007; Mather et al., 2011). These 1-D “drill hole” arrays provide critical localized calibration for the regional 3-D models.

Very low-resolution, but important structural fabric information is also derived from analysis of clear SKS-wave birefringence (splitting) observed at individual POLARIS stations. Seismic anisotropy observed in receiver functions and Rayleigh waves helps calibrate SKS-derived fast polarization directions.

Finally, new compilations of surface geology, improved digital elevation models, and regional magnetic and gravity potential field maps all provide very detailed 2-D knowledge at the surface and near-surface with which to relate the deeper knowledge layers. This surface information can only be extrapolated to the mantle structures that are of primary interest to our project with great care, but is invaluable because of its continuous and higher spatial resolution.

## **2. Structural analysis**

The primary focus of the analysis to date has been depth correlation of major regional discontinuities, such as the Moho or mid-lithosphere discontinuity, with significant gradients in seismic velocities or conductivity. Intriguing corrugated structure (about 20-km wavelength) on these deep discontinuity surfaces is observed and possibly correlates with NE-SW seismic anisotropy polarizations or mapped regional D2 crustal fold structures and orogenic trends along the margins of the Slave craton (e.g., Bleeker et al., 1999). The mid-lithosphere discontinuity within the central Slave craton correlates well with gradients in the surface wave velocity models across most of North America. The Moho is doubled along the southeast margin of the Slave craton where the Slave crust and uppermost mantle lithosphere are separated from the Rae craton by the Taltson magmatic arc and possibly the Queen Maud tectonic block.

Broad-scale lateral changes in mantle geochemical properties first identified by geochemical studies of xenoliths and garnet xenocrysts from kimberlites appear to match subtle lateral velocity variations in the surface-wave models. Both of these changes occur near mapped surface geology domain boundaries, in particular the limits of the Central Slave Basement Complex or edges of the Slave craton. Interestingly, along the northwest margin of the Slave craton the higher velocities that typify the Slave mantle continue about 100 km to the west and beneath rocks mapped as the Paleoproterozoic Wopmay Orogen. Mantle-derived diamonds have been discovered here and led to a hypothesized McKenzie craton underlying the much younger crustal rocks.

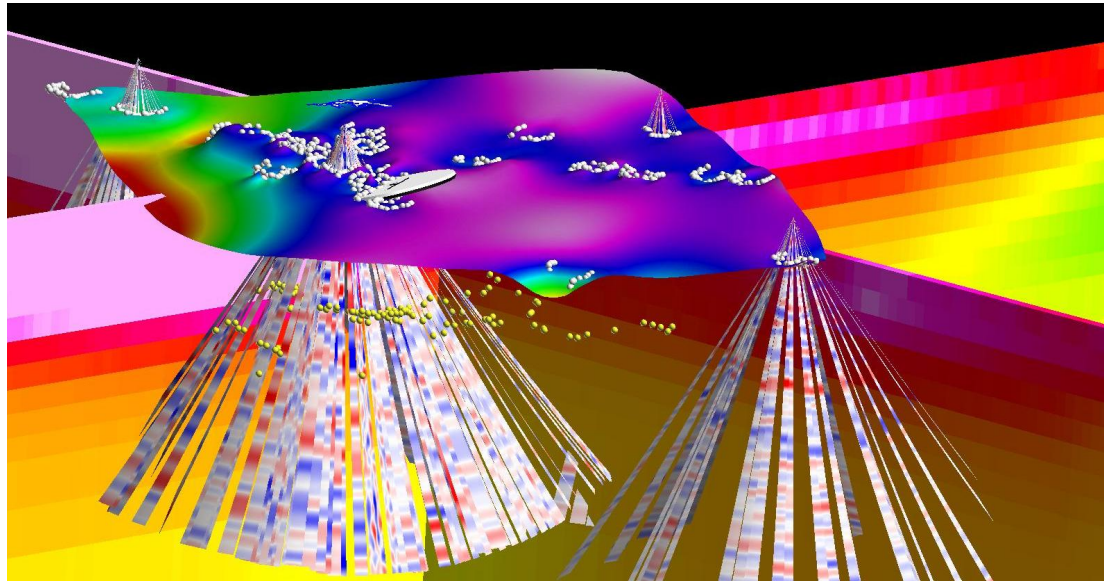


**Figure 1.** A snapshot of the 3-D knowledge cube of the Slave craton lithosphere, as viewed from the northeast. Vertical planes are cross sections from the Rayleigh wave model; near-horizontal surface is the Moho discontinuity (38-42 km depth); “ribbon cones” are receiver functions; white & yellow balls mark discontinuity picks on receiver functions. Apex of cones marks surface and the cones bottom at about 400 km depth.

### References:

- Aulbach, S., Pearson, N.J., O'Reilly, S.Y., and Doyle, B.J., 2007. Origins of xenolithic eclogites and pyroxenites from the central Slave craton, Canada, *J. Petrology*, 48, 1843–1873.
- Bedle, H., and van der Lee, S., 2009. S velocity variations beneath North America, *J. Geophys. Res.*, 114, B07308, doi:10.1029/2008JB005949.
- Bleeker, W.J., W.F. Ketchum, V.A. Jackson, and M. Villeneuve, 1999. The Central Slave Basement Complex, Part I: its structural topology and autochthonous cover, *Can. Journal of Earth Sciences*, 36, 1083–1109.
- Bostock, M.G., 1998. Mantle stratigraphy and evolution of the Slave Province, *J. Geophys. Res.*, 103, 21183–121200.
- Jones, A.G., Ferguson, I.J., Chave, A.D., Evans, R.L., and McNeice, G.W., 2001. Electrical lithosphere of the Slave craton, *Geology*, 29, 423–426.
- Mather, K.A., Pearson, D.G., McKenzie, D., Kjarsgaard, B.A., and Priestley, K., 2011. Constraints on the depth and thermal history of cratonic lithosphere from peridotite xenoliths, xenocrysts and seismology, *Lithos*, 125, 729–742.
- Snyder, D.B., 2008. Stacked uppermost mantle layers within the Slave craton of NW Canada as defined by anisotropic seismic discontinuities, *Tectonics*, 27, TC4006, doi:10.1029/2007TC002132.
- Spratt, J., Jones, A.G., Jackson, V., Collins, L., and Avdeeva, A., 2009. A magnetotelluric transect from the Slave craton to the Bear Province across the Wopmay Orogen, *J. Geophys. Res.*, 114, B01318, doi:10.1029/2008JB005326.



## Geochemistry and age of some A-type granitoid rocks of Estonia

A. Soesoo<sup>1</sup> and S. Hade<sup>1</sup>

<sup>1</sup>Institute of Geology, Tallinn University of Technology, Ehitajate tee 5, Tallinn 19086 Estonia  
E-mail: alvar [at] gi.ee

In this abstract we describe geochemical and geochronological features of some Estonian granitoid rocks with A-type chemical characteristics.

**Keywords:** geochemistry, age, granitoids, rapakivi-type rocks, Estonia

### 1. Introduction

An “alphabetic” granite classification into S-I-M-C-A has been in vogue for several decades. Specific chemical features distinguish a group of felsic rocks into A-type granitoids. These include high LILE and HFSE concentrations, usually, alkaline-calcic to alkaline affinities, and iron-rich mafic mineralogy. Although the original concept of A-type granites was fairly clear, it has been obscured during the last decade (Bonin, 2007).

In Fennoscandia, there is a large population of A-type granitoids differing in age and tectonic settings. After the Fennoscandian convergence with megablocks of Volga-Uralia, Sarmatia, Amazonia around 1.80 Ga ago, Fennoscandia underwent a major stabilization period incorporated with rapid uplift and thermal resetting.

A specific spectrum of “post-orogenic” and “anorogenic” igneous formations from the time span of 1.83-1.45 Ga has well survived at plutonic level. They formed specifically in the areas of the juvenile crust of the Svecofennian Domain, including the present Estonian territory (Soesoo et al., 2004). We provide an overview of the Estonian Orosirian, Statherian, and Calymmian granitoids in respect of their A-type geochemical features.

### 2. The Estonian Precambrian basement

The Estonian basement can be considered as a southern continuation of the Fennoscandian shield of the East European craton. This basement comprises two major units: amphibolite facies rocks of northern Estonia, which are similar to the rocks of southern Finland; and mostly granulite facies rocks of southern Estonia, which form a part of the Belarus-Baltic granulite belt (Soesoo et al., 2006). On the basis of geophysical and petrological studies, six structural-geological zones can be distinguished within these major units: the Tallinn, Alutaguse and Jõhvi Zones in northern Estonia, and the West Estonian, Tapa and South Estonian zones in southern Estonia (Soesoo et al., 2004; Figure 1).

### 3. The Estonian Orosirian and Statherian granitoids

Granitic rocks are widespread in the basement of Estonia. However, as the crystalline rocks are covered by 100-700 m thick sedimentary cover, geological information on the granitic rocks in Estonia comes mostly from studies of drill core material. As a consequence of that, only large granitic bodies have been drilled and studied, while very little is known about smaller granitic intrusions.

The postorogenic magmatism is represented by small monzonite-type mafic to felsic intrusions of shoshonitic geochemical affinity, originating possibly from enriched lithospheric mantle, and having been emplaced within the Estonian crust at 1.83-1.63 Ga. Partly gneissic rock of the Muhu quartz-monzonite and Taadikvere granodiorite plutons of the Estonian basement show a U-Pb isotope age about 1.83 Ga.

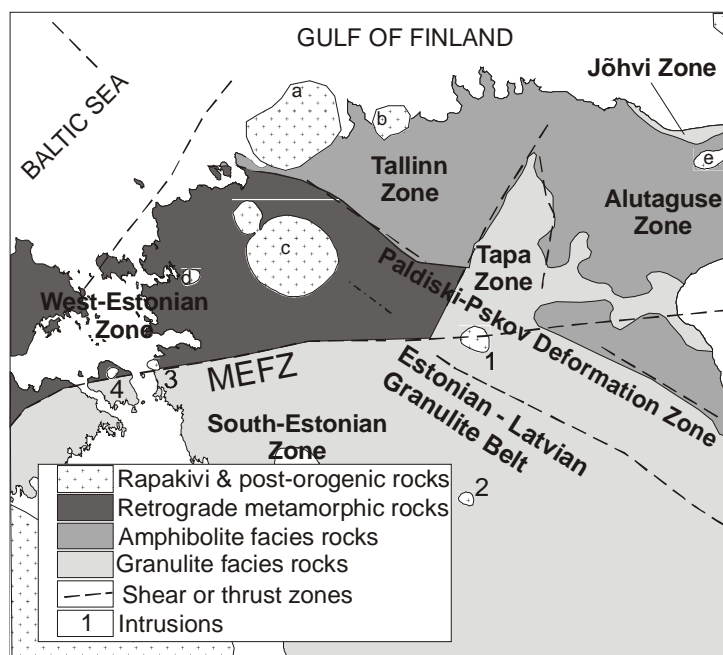


**Figure 1.** Structural units of Estonian Precambrian basement rocks. Key to rapakivi-type granitoid intrusions: a – Naissaare, b – Neeme, c – Märjamaa, d – Taebbla, e – Ereda. Key to shoshonitic intrusions: 1 – Taadikvere, 2 – Abja, 3 – Virtsu, 4 – Muhu.

The shoshonitic Virtsu pluton yields, however, a U-Pb age about 1.61 Ga (Figure 2; Soesoo, unpublished data). The quartz-monzonite of the Abja pluton shows a similar zircon U-Pb age – 1.638 Ga. The rocks of Virtsu, Muhu, and Abja plutons are shoshonitic and fall on the typical A-type granite field (Figure 3). In spite of age differences between the Muhu (1.83 Ga) and Abja-Virtsu (1.606 and 1.638 Ga) shoshonites, they all show similar chemical affinities. It is interesting that some of the Virtsu and Muhu rock types (high-K varieties) are chemically similar to the Finnish rapakivi granites, while others are similar to shoshonites.

In the South Estonian and Tapa zones, there are populations of granitoids derived from the melting of granulite facies rocks (Soesoo et al., 2006). Those rocks are usually charnockites and tonalities. The charnockites from the Tapa zone show both A-type and unfractionated granitic geochemistry, while the South Estonian charnockites show mainly I-type granitic features (Figure 3).

#### 4. The rapakivi-type rocks

The Fennoscandian anorogenic anorthosite-rapakivi plutons developed in the time span of 1.67-1.45 Ga within the Svecofennian juvenile crust. Several igneous rapakivi subprovinces of complex association of mafic to felsic rocks from deep infracrustal intrusive to supracrustal volcanic facies have been distinguished in the region. They can be divided into two large units: the Wiborg subprovince of 1.67-1.62 Ga and the Calymmian Riga-Åland subprovince of 1.59-1.54 Ga. As Estonia is located in the central part of the Fennoscandian rapakivi province, granitoids temporally similar to both rapakivi subprovinces are found here. Geophysical studies and drilling has revealed five stock-like granite plutons (Naissaare, Neeme, Märjamaa, Taebbla, Ereda) under the 150 to 300 m thick late Neoproterozoic and Palaeozoic sedimentary cover (Soesoo & Niin, 1992; Soesoo, 1993; Kirs et al., 2009). Granodiorite of the Märjamaa pluton yields a U-Pb zircon age of 1.65-1.63 Ga (Rämö et al., 1996; Soesoo, unpublished data). The Neeme granitoids yield a U-Pb zircon age of 1.634 Ga and the Taebbla rocks 1.648 Ga, whereas the Ereda rocks show two age groups of 1.642 and 1.627 Ga (Soesoo, unpublished data). All the Estonian “rapakivi-type” granitoids show

distinct A-type geochemical characteristics and are by this criterion similar to the Finnish proper rapakivi (Figure 2).

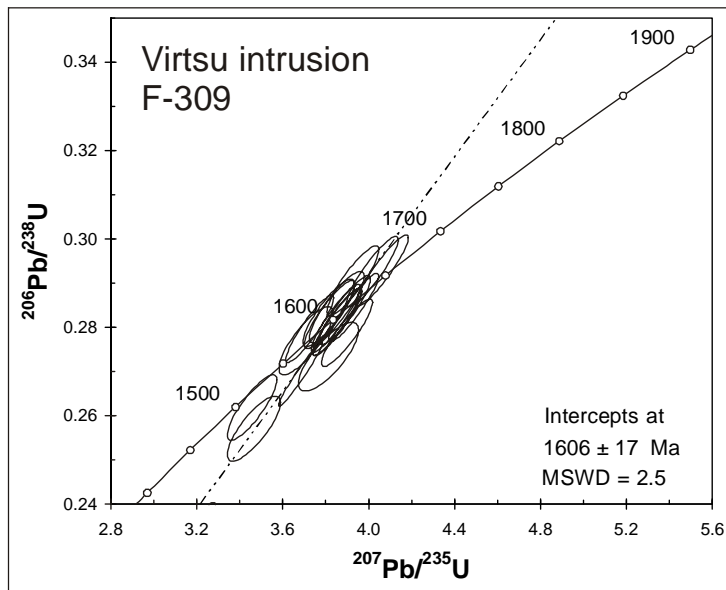


**Figure 2.** New zircon  $^{207}\text{Pb}/^{235}\text{U}$  vs.  $^{206}\text{Pb}/^{238}\text{U}$  age data on the shoshonitic rock of the Virtsu intrusion (Western Estonia).

### 5. The Estonian Calymmian granitoids

The Calymmian granitoids in Estonia are so far known only from the Riga-Åland rapakivi subprovince, which are located on islands of Saaremaa and Ruhnu. The basement beneath the Gulf of Riga as well as on Ruhnu Island and western Saaremaa Island is represented by the northern portion of the Riga batholith. Zircons from leucogabbro-norite and biotite-hornblende granite from the Riga batholith (NW Latvia) show U-Pb ages of 1.59 and 1.58 Ga (Rämö et al., 1996), respectively. The rapakivi-related volcanic rocks from plagioclase porphyrites to quartz porphyries were penetrated by drilling (Undva 580 drill hole) on NW Saaremaa Island. The drill hole is located near the northern border of the Riga pluton and its age is conventionally assumed to be similar to the age of the Riga and Åland plutons.

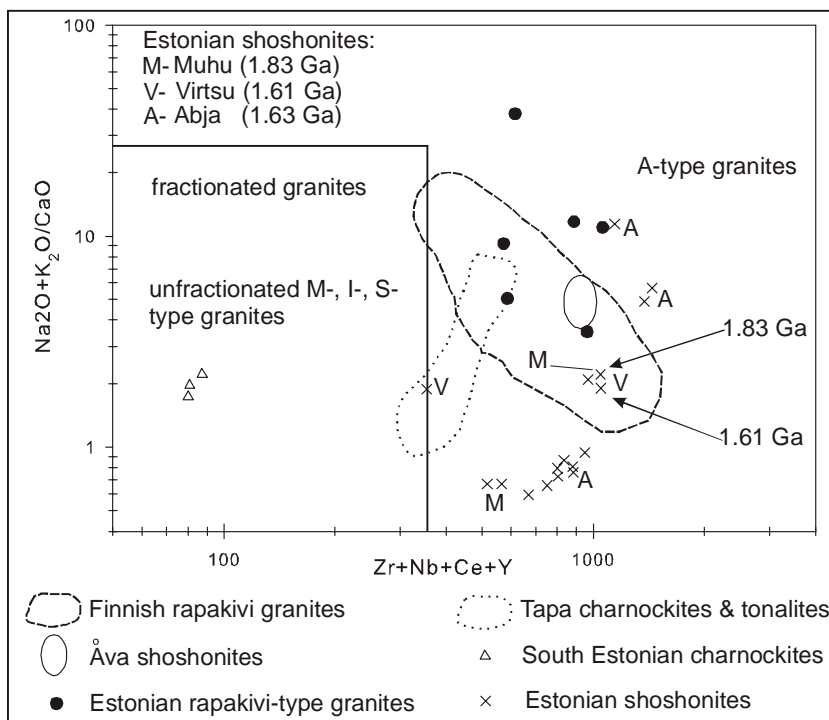


**Figure 3.** Composition of Estonian granitoids shown on granitoid classification diagram of  $\text{Zr}+\text{Nb}+\text{Ce}+\text{Y}$  (ppm) vs.  $\text{Na}_2\text{O}+\text{K}_2\text{O}/\text{CaO}$  (wt.%). Finnish rapakivi granites (Kirs et al., 2004) and Åva shoshonites (Jurvanen et al., 2005) are shown for reference.

A new study on a few zircon grains found from the Undva basaltic rocks of the Riga batholith's volcanic counterpart yield U-Pb age of 1.669 Ga (Soesoo, unpublished). As the age of the Riga batholith is 1.576-1.584 Ga (Rämö et al. 1996), these older ages may reflect the source age or illustrate a long-living magmatic system. Zircons from a subvolcanic biotite granite porphyry unit in Ruhnu Island (Riga batholith) yield an age of 1.595 Ga (Soesoo, unpublished data), being thus just slightly older than "classical" Riga rocks.

## 6. Discussion and conclusions

In Estonia, A-type granitoids are present within different age groups and different structural zones. The oldest known granitoids with A-type characteristics are 1.83-1.82 Ga tonalites derived by partial melting of mafic granulite facies gneisses in Tapa zone, but probably also elsewhere. The Muhu and possibly Taadikvere intrusions show a similar emplacement age (1.83 Ga) and shoshonitic chemistry. The youngest A-type rocks are shoshonites and rapakivi-type granitoids, which all form small undeformed rock bodies. By several geochemical characteristics, the 1.8 Ga and 1.6 Ga granitoids are sometimes indistinguishable. Recent geochronological studies show another melting event at 1.78 to 1.76 Ga both in the South Estonian and Tapa zones. This event has produced a range of granitoids with charnockitic, tonalitic, and other compositions. Some of these granitoids yield A-type characteristics.

In conclusion, the large time span – ca. 200 Ma – of A-type granitoid evolution may hint at similarities in melting conditions and source. However, it seems that during every melting event where A-type compositions were produced, there were also different granitoids formed close in space. Due to sedimentary cover and lack of proper field data, the genesis of the Estonian granitic rocks is difficult to establish. In order to understand the large chemical spectrum and formation specifics of granitic rocks, a large-scale modeling incorporating tectonical, physical, and chemical parameters is needed.

## References:

- Bonin, B., 2007. A-type granites and related rocks: Evolution of a concept, problems and prospects. *Lithos*, 97, 1-29.
- Jurvanen, T., Eklund, O., and Väisänen, M., 2005. Generation of A-type granitic melts during the late Svecofennian metamorphism in southern Finland. *GFF*, 127, 139-147.
- Kirs, J., Puura, V., Soesoo, A., Klein, V., Konsa, M., Koppelmaa, H., Niin, M., and Urtson, K., 2009. The crystalline basement of Estonia: rock complexes of the Paleoproterozoic Orosirian and Statherian and Mesoproterozoic Calymmian Periods, and regional correlations. *Estonian Journal of Earth Sciences*, 58, 219-228.
- Kirs, J., Haapala, I., and Rämö, T., 2004. Anorogenic magmatic rocks in the Estonian crystalline basement. *Proceedings of Estonian Academy of Sciences. Geology*, 53, 210-225.
- Petersell, V. and Levchenkov, O., 1994. On the geological structure of the crystalline basement of the southern slope of the Baltic Shield. *Acta et Commentationes Universitatis Tartuensis*, 972, 16-39.
- Rämö, O.T., Huhma, H., and Kirs, J., 1996. Radiogenic isotopes of the Estonian and Latvian rapakivi suites: new data from the concealed Precambrian of the East European Craton. *Precambrian Research*, 79, 209-226.
- Soesoo, A., Kosler, J., and Kuldkepp, R., 2006. Age and geochemical constraints for partial melting of granulites in Estonia. *Mineralogy and Petrology*, 86, 277-300.
- Soesoo, A., Puura, V., Kirs, J., Petersell, V., Niin, M., and All, T., 2004. Outlines of the Precambrian basement of Estonia. *Proceedings of the Estonian Academy of Sciences. Geology*, 53, 149-164.
- Soesoo, A., 1993. Estonian porphyreous potassium granites: petrochemical subdivision and petrogenetical interpretation. *Proceedings of the Estonian Academy of Sciences. Geology*, 42, 97-109.
- Soesoo, A., and Niin, M., 1992. Petrographical and geochemical features of the Estonian porphyritic potassium granites. *Proceedings of the Estonian Academy of Sciences. Geology*, 41, 93-107.

## Contrasting orogenic systems in the Fennoscandian Shield, southern Sweden

M.B. Stephens<sup>1</sup> and J. Andersson<sup>1</sup>

<sup>1</sup>Geological Survey of Sweden, Box 670, SE-751 28 Uppsala, Sweden  
E-mail: michael.stephens [at] sgu.se

SIMS U-Th-Pb zircon data have provided constraints on the timing of anatexis and high-grade metamorphism inside the Svecokarelian and Sveconorwegian orogens in southern Sweden. An evaluation of these data in the context of the regional geological setting suggests contrasting heat sources and contrasting orogenic systems. Advection of heat into the crust from a basic igneous source gave rise to anatexis and high-grade metamorphism in the low pressure Svecokarelian orogen and can explain at least some of the high crustal thickness anomalies. Accretionary tectonics involving a continental, extensional back-arc setting in an overriding plate is inferred, where slab retreat away from the Fennoscandian continental nucleus prevailed. By contrast, crustal thickening and decompression melting during exhumation of deeply rooted crust accounted for anatexis and high-grade metamorphism in the high pressure Eastern Segment in the Sveconorwegian orogen. Subduction of Fennoscandian continental lithosphere in a downgoing plate setting is inferred.

**Keywords:** U-Th-Pb zircon data, Svecokarelian orogen, Sveconorwegian orogen, anatexis, heat supply, palaeotectonic setting, crustal thickness

### 1. Background and aims of study

Two major orogenic belts dominate the Fennoscandian Shield in the southern part of Sweden, the 1.9 to 1.8 Ga Svecokarelian orogen in the south-eastern part of the country and the 1.1 to 0.9 Ga Sveconorwegian orogen to the south-west (Figure 1). The metamorphosed rocks in the Svecokarelian orogen in this part of the shield are characterized by low pressure/variable temperature metamorphism, extending locally to high temperature conditions with the formation of granulites (see synthesis in Stephens et al., 2009). By contrast, the Eastern Segment in the Sveconorwegian orogen is characterized, in large areas, by high pressure/high temperature metamorphism (Möller, 1998, Johansson et al., 2001; Möller et al., 2007). Furthermore, a large part of the crustal segment inside the Svecokarelian orogen is anomalously thick, in several areas more than 50 km, with a significant, dense lower crustal component, in sharp contrast to the crustal segment to the west inside the Sveconorwegian orogen (Kuusisto et al., 2006; Stratford and Thybo, 2011).

This study presents SIMS U-Th-Pb zircon data that provide constraints on the timing of anatexis and high-grade metamorphism inside the lithotectonic unit between the complex Singö deformation belt in the north (immediately north of Figure 1) and the Loftahammar-Linköping deformation zone in the south (Figure 1) in the Svecokarelian orogen, and inside the northern part of the Eastern Segment in the Sveconorwegian orogen (Figure 1). These data have been acquired in order to evaluate the mechanisms for the generation of heat that resulted in the formation of the migmatites in these areas and, thereby, improve our understanding of the palaeotectonic setting of each orogenic system. All analyses were carried out using the secondary ion mass spectrometry (SIMS) technique at the Swedish Museum of Natural History, Stockholm (NORDSIM facility).

### 2. U-Th-Pb zircon data from the Svecokarelian orogen

Crystallization of igneous zircons in two samples of migmatitic orthogneiss directly north of the Loftahammar-Linköping deformation zone (Figure 1) occurred at 1.88 Ga. Inferred metamorphic events occurred at 1.87 to 1.83 Ga and resulted in younger zircon domains

showing bright, backscattered electron (BSE) images and lower Th/U ratios. A single zircon grain showing similar secondary textural and Th/U characteristics also yielded an age of 1.81 Ga. A pegmatitic leucosome concordant to the planar fabric in an augen-bearing orthogneiss, occurring further to the north-west in the Svecokarelian high-grade belt (Figure 1), crystallized at 1.83 to 1.82 Ga. However, the majority of the zircons in the pegmatitic leucosome yield an age of  $1852 \pm 10$  Ma and are inferred to be xenocrysts derived from the host, augen-bearing rock, which shows an igneous crystallization age of  $1855 \pm 6$  Ma (Andersson et al. 2006).

Detrital zircons derived from source rocks with ages of 2.1–2.0 Ga and 1.91–1.88 Ga are present in a sample of migmatized paragneiss and in two samples of anatectic leucogranite associated with a diatexitic migmatite of sedimentary origin in the Stockholm region (Figure 1). Crystallization of anatectic leucogranite occurred at 1.84 to 1.83 Ga. Furthermore, inferred metamorphic events occurring around 1.86 Ga and at 1.83 to 1.82 Ga gave rise to younger zircon domains showing bright BSE images and lower Th/U ratios. Uncertainties concerning the transported or in situ character of these events are currently being addressed in an ongoing, complementary study.

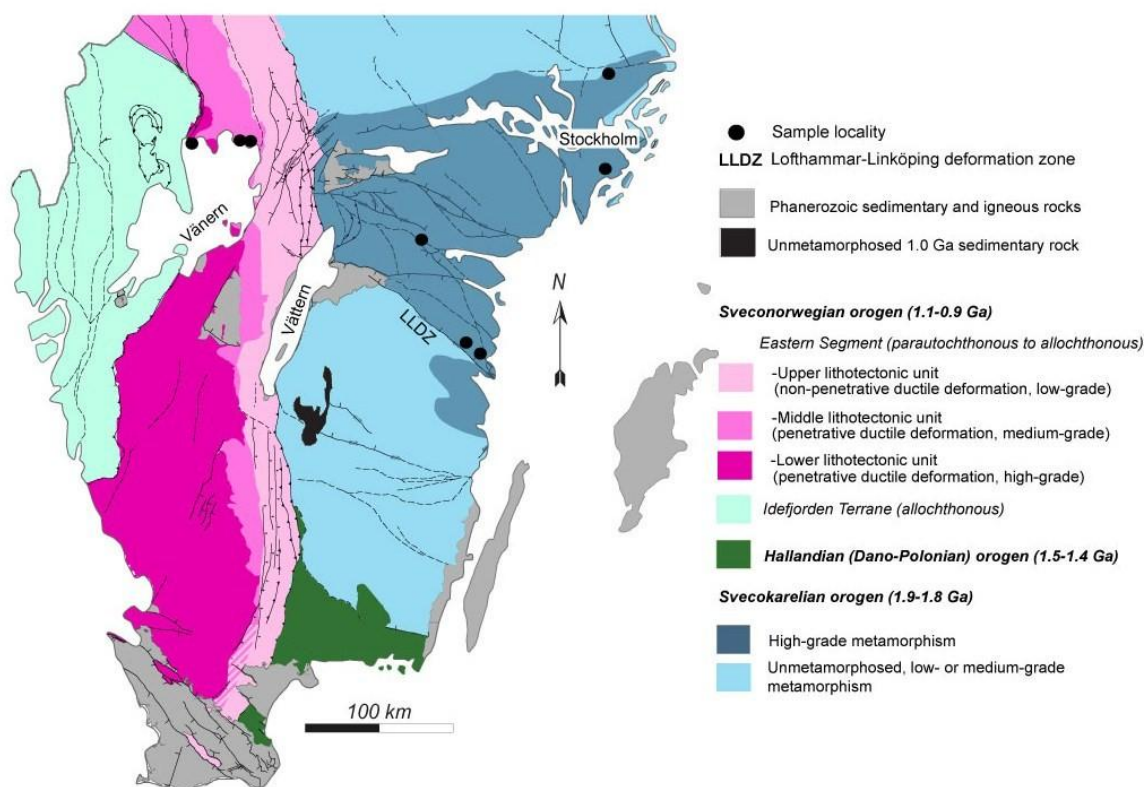


**Figure 1.** Major tectonic units and deformation zones in southern Sweden, and sample localities for U-Th-Pb analytical work. The deformation zones are shown as black lines. Continuous lines indicate zones where some kinematic data exist and are shown; dashed lines indicate zones where kinematic data are absent.

### 3. U-Th-Pb zircon data from the Eastern Segment in the Sveconorwegian orogen

Preliminary evaluation of the U-Th-Pb zircon data from the Eastern Segment north of Lake Vänern (Figure 1) indicates that the igneous protolith to the two samples of orthogneiss from the lower lithotectonic unit formed at 1.7 Ga. However, there is also an input of zircon from a bedrock source with an igneous crystallization age of 1.3 to 1.2 Ga in one of the samples. It is noteworthy that there is no input of material dated to 1.4 Ga, which is a common component further south in the Eastern Segment (Söderlund et al., 2002; Möller et al., 2007), supporting the results from earlier geochronological work (Söderlund et al., 1999).

Anatectic melting and formation of migmatite occurred around 1000 to 980 Ma, possibly a little earlier than that (980 to 960 Ma) identified further south in the lower lithotectonic unit (Möller et al., 2007). This would be consistent with the exhumation of deeper crustal levels in the southern part of the Eastern Segment (Möller et al., 2007) during a single tectonic event, as also inferred from the variation in structural features along the western boundary shear zone to this unit (Stephens et al., 1996). The majority of the zircons in a garnet-bearing amphibolite in the middle lithotectonic unit show a preliminary  $^{206}\text{Pb}/^{238}\text{U}$  age of  $960\pm 12$  Ma, inferred to represent the timing of metamorphism. U-Pb baddeleyite data from an equivalent, unmetamorphosed dolerite in the same area yield an igneous crystallization age of  $1569\pm 3$  Ma (Söderlund et al., 2005).

### 4. Heat source and palaeotectonic setting

The ages dating anatexis and high-grade metamorphism in the Svecokarelian orogen in south-eastern Sweden (1.87 to 1.81 Ga) overlap with the timing of intrusion of batholithic igneous suites composed of granite, syenitoid, dioritoid and gabbroid at 1.87 to 1.84 Ga and, probably, even at 1.81 to 1.78 Ga (Högdahl et al., 2004; Stephens et al., 2009). The dates also overlap with the timing of an inferred extensional tectonic realm between 1.86 and 1.83 Ga (Bergman et al., 2008) that both followed and preceded shorter, transpressional tectonic events (Stephens et al., 2009). Mingling and mixing between mantle- and crustal-derived melts is a conspicuous feature of these batholithic rocks (Högdahl et al., 2004; Stephens et al., 2009). It is inferred that the anatexis and high-grade metamorphism in this orogenic system was related to the emplacement of significant volumes of basic material into the lower part of the crust, resulting in advection of heat into the crust from a basic magmatic source. This mechanism would also account for the anomalous crustal thickness observed inside the Svecokarelian orogen. It is also inferred that this anatexis and high-grade metamorphism formed in a continental back-arc setting in an overriding plate, where slab retreat away from the Fennoscandian continental nucleus prevailed. The orogenic system was accretionary in character with a lack of medium- or high-pressure metamorphism and resulted neither in significant crustal thickening nor extensional collapse.

Anatexis and high-grade metamorphism in the Sveconorwegian orogen in south-western Sweden took place during or shortly after extensive high-pressure metamorphism (Möller et al., 2007), which, inside a discrete tectonic sub-unit in the lower lithotectonic unit, reached eclogite facies (Möller, 1998; Johansson et al., 2001). Heat supply related to igneous activity is not apparent and a heating mechanism related to crustal thickening in combination with decompression melting during exhumation of deeply rooted crust has been inferred (Möller et al., 2007). Thus, in contrast to the Svecokarelian orogen, the Eastern Segment in the Sveconorwegian orogenic system formed by subduction of continental crust in a downgoing plate setting, with significant crustal thickening and with a strong potential for later extensional collapse and crustal delamination. These considerations open the possibility that the character of the crust beneath south-western Sweden and southern Norway is also

steered by the Sveconorwegian and not only by the Phanerozoic tectonic evolution (cf. Startford and Thybo, 2011).

### References:

- Andersson, U.B., Högdahl, K., Sjöström, H., and Bergman, S., 2006. Multistage growth and reworking of the Palaeoproterozoic crust in the Bergslagen area, southern Sweden: evidence from U-Pb geochronology. *Geol. Mag.*, 143, 679–697.
- Bergman, S., Högdahl, K., Nironen, M., Ogenhall, E., Sjöström, H., Lundqvist, L., and Lahtinen, R., 2008. Timing of Palaeoproterozoic intra-orogenic sedimentation in the central Fennoscandian Shield; evidence from detrital zircon in metasandstone. *Prec. Res.*, 161, 231–249.
- Högdahl, K., Andersson, U.B., and Eklund, O., 2004 (Eds.). *The Transscandinavian Igneous Belt (TIB) in Sweden: a review of its character and evolution*. Geological Survey of Finland, Special Paper 37, 125 pp.
- Johansson, L., Möller, C., and Söderlund, U., 2001. Geochronology of eclogite facies metamorphism in the Sveconorwegian province of SW Sweden. *Prec. Res.*, 106, 261–275.
- Kuusisto, M., Kukkonen, I.T., Heikkinen, P., and Pesonen, L.J., 2006. Lithological interpretation of crustal composition in the Fennoscandian Shield with seismic velocity data. *Tectonophysics*, 420, 283–299.
- Möller, C., 1998. Decompressed eclogites in the Sveconorwegian (-Grenvillian) orogen of SW Sweden: petrology and tectonic implications. *J. Metamorphic Geol.*, 16, 641–656.
- Möller, C., Andersson, J., Lundqvist, I., and Hellström, F., 2007. Linking deformation, migmatite formation and zircon U-Pb geochronology in polymetamorphic orthogneisses, Sveconorwegian Province, Sweden. *J. Metamorphic Geol.*, 25, 727–750.
- Söderlund, U., Jarl, L.-G., Persson, P.-O., Stephens, M.B., and Wahlgren, C.-H., 1999. Protolith ages and timing of deformation in the eastern, marginal part of the Sveconorwegian orogen, southwestern Sweden. *Prec. Res.*, 94, 29–48.
- Söderlund, U., Möller, C., Andersson, J., Johansson, L., and Whitehouse, M., 2002. Zircon geochronology in polymetamorphic gneisses in the Sveconorwegian orogen, SW Sweden: ion microprobe evidence for 1.46–1.42 and 0.98–0.96 Ga reworking. *Prec. Res.*, 113, 193–225.
- Söderlund, U., Isachsen, C., Bylund, G., Heaman, L., Patchett, P.J., Vervoort, J.D., and Andersson, U.B., 2005. U-Pb baddeleyite ages and Hf, Nd isotope chemistry constraining repeated mafic magmatism in the Fennoscandian Shield from 1.6 to 0.9 Ga. *Contr. Mineral. Petrol.*, 150, 174–194.
- Stephens, M.B., Ripa, M., Lundström, I., Persson, L., Bergman, T., Ahl, M., Wahlgren, C.-H., Persson, P.-O., and Wickström, L., 2009. Synthesis of the bedrock geology in the Bergslagen region, Fennoscandian Shield, south-central Sweden. *Geological Survey of Sweden, SGU Ba 58*, 249 pp.
- Stephens, M.B., Wahlgren, C.-H., Weijermars, R., and Cruden, A.R., 1996. Left-lateral transpressive deformation and its tectonic implications, Sveconorwegian orogen, Baltic Shield, southwestern Sweden. *Prec. Res.*, 79, 261–279.
- Stratford, W., and Thybo, H., 2011. Seismic structure and composition of the crust beneath the southern Scandes, Norway. *Tectonophysics*, 502, 364–382.

## Vintage and retro conductivity models of the Bothnian Bay region: implications for the crustal structure and processes of the Svecofennian orogen

Katri Vaittinen<sup>1,2</sup>, Toivo Korja<sup>1</sup>, Mohamed Mahmoud<sup>1</sup>, Markku Pirttijärvi<sup>1</sup>, Maxim Smirnov<sup>1</sup>, Ilkka Lahti<sup>3</sup> and Pertti Kaikkonen<sup>1</sup>

<sup>1</sup> Department of Physics, University of Oulu, Finland

<sup>2</sup> Boliden Mineral AB, Boliden, Sweden

<sup>3</sup> Geological Survey of Finland, Rovaniemi, Finland  
E-mail: toivo.korja [at] oulu.fi

We have combined all existing broad-band magnetotelluric data from the extended Bothnian region, from the Ylikiiminki Schist Belt in north to the Bothnian Belt and Vaasa Complex in south. In the east, the study area extends to the Central Finland Granitoid Complex. Older data from 1980's were inverted as only 2-D forward models were available. The new inversion models of the old data together with old inversions of newer data revealed a set of successive, eastward/southeastwardly dipping conductors to the east of the Vaasa Complex whereas a conductor associated with the Ylikiiminki Schist Belt dips south/southeastward under the Savo Belt.

**Keywords:** electrical conductivity, crust, magnetotellurics, collision, extension, Bothnian region, Fennoscandian Shield

The orogenic evolution has three distinct phases: (1) a collisional phase, i.e., the accretion of crustal fragments and a subsequent continent-continent collision, (2) development of a continental plateau, and (3) a gravitational (extensional) collapse - each of which will leave distinct geological markers and affects the final geophysical structure. We use magnetotelluric data, i.e., electrical conductivity data, to explore various geological markers on the tectonic evolution of the area.

The studies of crustal conductivity by the Oulu magnetotelluric team started in the early 80's (e.g. Pajunpää, 1987). Several profiles were measured in the Palaeoproterozoic Svecofennian orogen with a main focus on the Bothnian Bay region (Oulu 1 and 2 profiles, Korja et al., 1986; Oulu 4, Hjelt et al., 1992; SVEKA, Korja and Koivukoski, 1994) (Fig. 1 and 2). The data were modelled at that time with a 2-D forward modelling technique. The 2-D model of the Oulu 1 is reproduced in Fig. 3. In the new millennium, we visited the region again in the MT-FIRE project, where new magnetotelluric data were acquired from several profiles. In the Bothnian region, the profile E coincides with the FIRE 3 profile (Kukkonen et al., 2006) The results from the new studies and an earlier experiment to invert GGTSVEKA data (Lahti et al., 2002), inspired us to return to the older Bothnian datasets: (a) to invert the old data with modern techniques, (b) to compare old models with new models (see Fig 3) and (c) to add electrical conductivity models to an on-going project (MIDCRUST; Fig. 4) investigating the properties of the crust after the extensional processes.

The 2-D determinant inversions models show that a successive set of conductors dips to the east/southeast extending from the western coast of Finland to the Archaean-Proterozoic boundary zone ca. 250 km to the east. In the middle crustal levels, the conductors form a sub-horizontal continuous layer, which, according to the seismic interpretations, may represent a crustal scale detachment zone. Collisions have squeezed the carbon bearing sediments of the ocean basins into narrow zones, where conducting material were transported to deeper crustal levels (50 km). Post-collisional processes, however, may have extended the structures and consequently the conductors become wider. They form ramp-like structures in the upper crust while a sub-horizontal detachment zone at deeper levels. Comparison of the conductivity

models with airborne electromagnetic data (Airo, 2005) suggests that deeper conductors are composed of graphite-bearing metasedimentary rocks.

### **Acknowledgements:**

This is a contribution to the Academy of Finland grants 201548 (MT-FIRE) and 139516 (MIDCRUST).

### **References and sources of data**

- Airo, M.-L. (ed.), 2005. Aerogeophysics in Finland 1972-2004: Methods, System Characteristics and Applications. Geological Survey of Finland, Special Paper 39, 197 pages, 115 figures, 12 table and 8 appendices.
- Hjelt, S.-E., Korja, T., and Vaaraniemi, E. (Compilers), 1992. Magnetovariational and magnetotelluric results. Map 11, in Freeman, R. and Mueller, St. (eds.): A Continent Revealed: The European Geotraverse. Cambridge University Press. Cambridge.
- Hjelt, S.-E., Korja, T., Kozlovskaya, E., Lahti, I., Yliniemi, J., and BEAR and SVEKALAPKO Seismic Tomography Working Groups, 2006. Electrical conductivity and seismic velocity structures of the lithosphere beneath the Fennoscandian Shield. Pp 541-559 in: Gee, D. G. & Stephenson, R. A. (eds) 2006. European Lithosphere Dynamics. Geological Society, London, Memoirs, 32. The Geological Society of London 2006.
- Koistinen, T., Stephens, M. B., Bogatchev, V., Nordgulen, Ø., Wennerström, M., and Korhonen, J. (Comps.), 2001. Geological map of the Fennoscandian Shield, scale 1:2 000 000. Espoo : Trondheim : Uppsala : Moscow: Geological Survey of Finland : Geological Survey of Norway : Geological Survey of Sweden : Ministry of Natural Resources of Russia.
- Korja, T., Zhang, P., and Pajunpää, K., 1986. Magnetovariational and magnetotelluric studies of the Oulu-anomaly on the Baltic Shield Finland. *Journal of Geophysics*, 59, 32-41.
- Korja, T. and Koivukoski, K., 1994. Magnetotelluric investigations along the SVEKA profile in central Fennoscandian Shield, Finland. *Geophys. J. Int.*, 116, 173-197.
- Kukkonen, I.T. and Lahtinen, R. (eds), 2006. Finnish Reflection Experiment FIRE 2001-2005. Geological Survey of Finland, Special paper 43, 247 pp.
- Lahti, I., Korja, T., Pedersen, L. B., and the BEAR Working Group, 2002. Lithospheric conductivity along GGT/SVEKA Transect: implications from the 2-D inversion of magnetotelluric data. In: Lahtinen, R. et al (eds). *Lithosphere 2002, Second Symposium on the Structure, Composition and Evolution of the Lithosphere in Finland*. Institute of Seismology, University of Helsinki, Report S- 42, 75-78.
- Lahtinen, R., Korja, A., and Nironen, M., 2005. Paleoproterozoic tectonic evolution. In: Lehtinen, M., Nurmi, P.A., and Rämö, O.T. (Eds.), *Precambrian Geology of Finland – Key to the Evolution of the Fennoscandian Shield*. Elsevier B.V., Amsterdam, pp. 481–532.
- Pajunpää, K., 1987. Conductivity anomalies in the Baltic Shield in Finland. *Geophys. J. R. astr. Soc.*, 91, 657-666.
- Vaittinen, K., Korja, T., Kaikkonen, P., Lahti, I., and Smirnov, M. Yu., 2012. High-resolution magnetotelluric studies of the Archaean-Proterozoic border zone in the Fennoscandian Shield, Finland. *Geophys. J. Int.*, 188, 908-924. doi: 10.1111/j.1365-246X.2011.05300.x

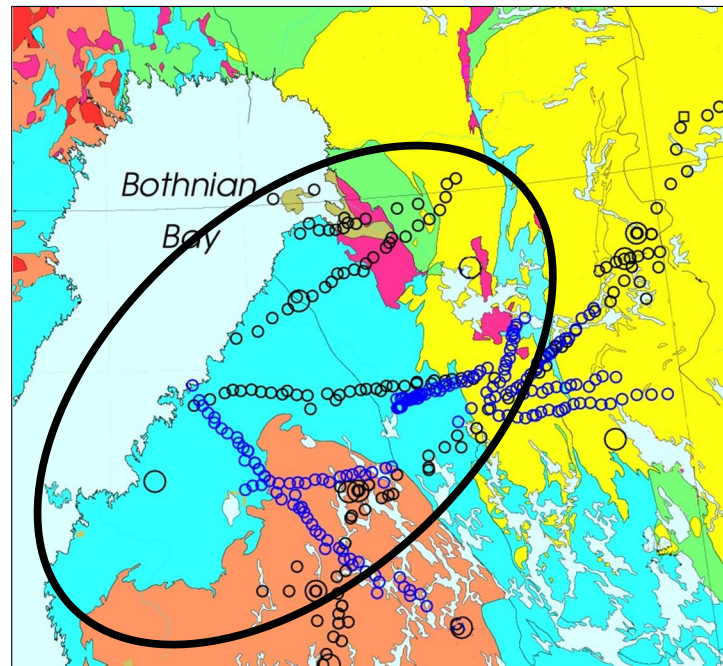


**Figure 1.** Location of the study region (black oval) and position of magnetotelluric sites: Small black circles = old data (Oulu 1, 2 and 4, SVEKA); blue circles = MT-FIRE sites in Pohjanmaa and Kainuu; large black circles = long period magnetotelluric sites (BEAR project). Geological map modified from Koistinen et al., 2001.

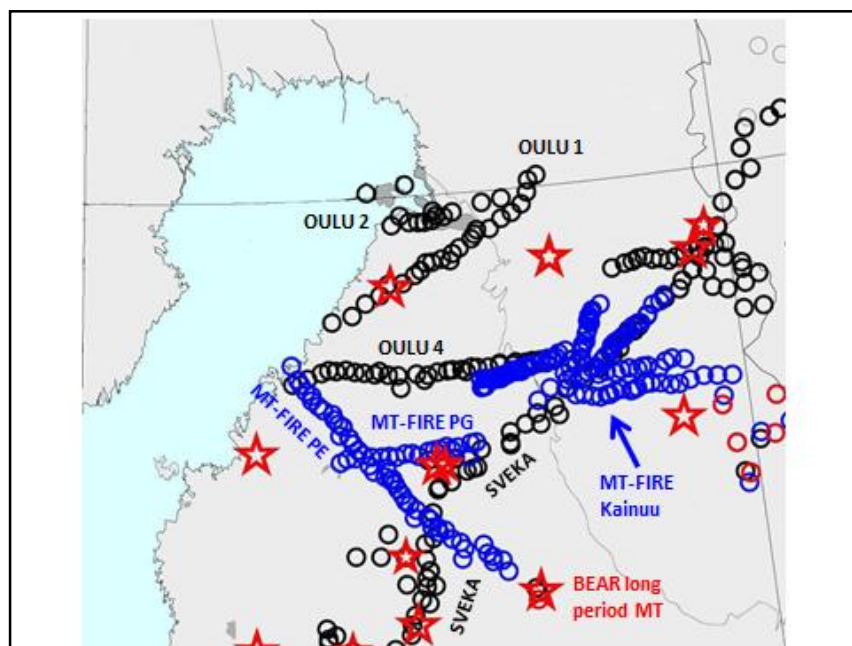


**Figure 2.** Magnetotelluric profiles in the “extended” Bothnian region. Black circles: older MT data from OULU 1 and 2 profiles (Korja et al., 1986), OULU 4 profile (Hjelt et al., 1992) and SVEKA (Korja and Koivukoski). Blue: MT-FIRE data in the Kainuu and Pohojammaa regions (Vaitinen et al., 2011). Red stars denote long period soundings (BEAR; Hjelt et al., 2006).

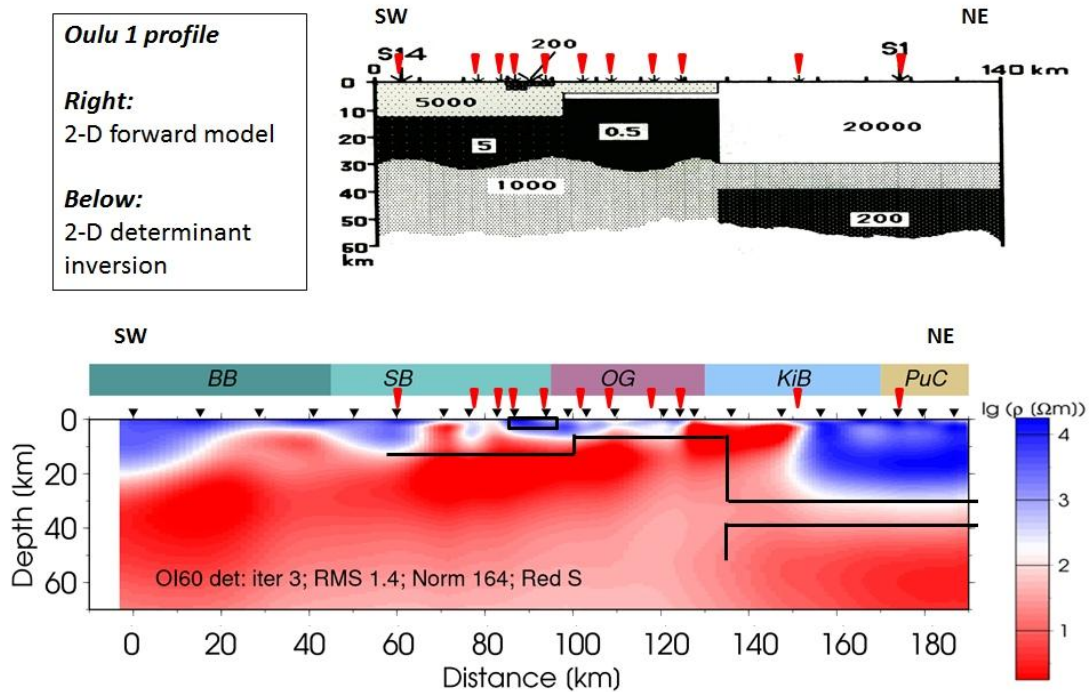


**Figure 3.** Two-dimensional conductivity models of the OULU 1 profile. Top: 2-D forward model (Korja et al., 1986), bottom: new determinant inversion of the old data. Note that in new inversion, additional data have been added at both ends of the profile and between the sites.

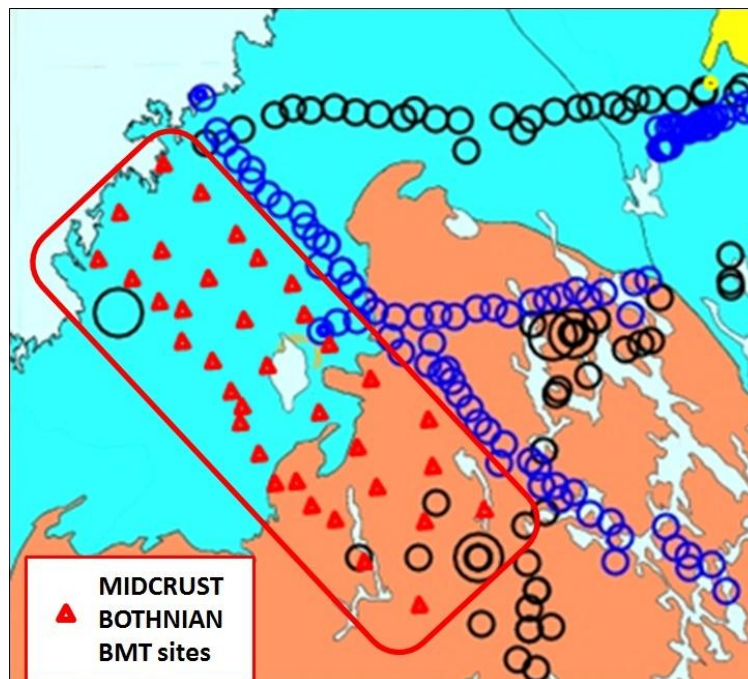


**Figure 4.** Broad-band magnetotelluric measurements (red triangles) in Pohojammaa on summer 2012. Other sites as in Figure 2.

# Method of joint inversion of velocity model and gravity data based on mineralogical composition

I. Virshylo<sup>1</sup>, G. Prodaivoda<sup>1</sup> and E. Kozlovskaya<sup>2</sup>

<sup>1</sup> National Taras Shevchenko University of Kyiv, Faculty of Geology  
90 Vasyl'kivs'ka str., Kyiv, Ukraine, 03022

<sup>2</sup>Sodankyla Geophysical Observatory/Oulu Unit, University of Oulu  
POB 3000 FIN-90014 University of Oulu, FINLAND  
E-mail: ivvir [at] univ.kiev.ua

Herein we describe a method of quantitative interpretation of results of deep seismic sounding (DSS) jointly with the data of other methods, preferably gravimetric. This approach is based on numerical modeling of elastic properties of polycrystalline composite influenced by pressure and temperature. We use a multi-component model of generally porous and anisotropic geological medium. In our study we apply this method to results of selected DSS profiles in Fennoscandia, in order to estimate mineralogical and petrochemical composition of the lithosphere composition along these profiles.

**Keywords:** joint inversion, deep seismic sounding, gravity, mineral composition, lithosphere

## 1. Introduction

Traditional way to interpret lithosphere velocity models obtained from deep seismic sounding (DSS) is based on calculation of petrophysical properties of major types of rocks under high pressure and temperature condition. Elastic properties of main rock types are usually obtained by averaging data of ultrasonic experiments. In this case, DSS velocity models are interpreted using either deterministic (Christensen & Mooney, 1995) or stochastic (c.f. Janik, Kozlovskaya, & Yliniemi, 2007) methods. In the case of joint inversion with gravimetric data, correlation of bulk velocity versus density is usually used.

There are some shortcomings in those approaches. Firstly, there exist an inconsistency between velocities in low-frequency seismological and high-frequency ultrasonic range. We couldn't apply laboratory velocity measurements directly to huge massif of rocks due to significant non-linearity of this relation. Furthermore, cracks and pores influence significantly elastic parameters of rocks, which led to many acoustic effects: dispersion, scattering, attenuation of elastic wave. The second shortcoming is related to different influence of temperature on elastic parameters and density. As known, the last one is used for velocity and gravity anomaly's calculation. But if one uses any pre-defined correlation between velocity and density, then one also introduces uncertainty from velocity data into the gravity modeling. In this case a regression analysis, even a non-linear one, is insufficient to consider all factors influencing the density-velocity relation. In addition, regression analysis required a representative amount of sample measurements from modeled region, which is not possible in the case of weakly investigated regions.

## 2. Brief description of modeling theory. Required conditions and data

To solve the problem described above we developed the method of numerical modeling of elastic properties and phase velocity for composite model of a geological medium. We use an hierarchical scaled system where the volume of the model is significantly greater than characteristic size of structural elements: mineral grains and porosity. Component shape is approximates by ellipsoid of revolution, and their orientation is defined by a special distribution function. Effective elastic properties of such medium are calculated by integration

elastic properties of components, depending on its shape and orientation, and also on temperature and pressure.

The calculation method is based on stochastic conditional moment function method related to a problem of geological medium stress-strain state (due to Duhamell-Neumann equation). The method has been used earlier for modeling of generalized velocity data of continental and oceanic Earth crust and uppermost mantle (Prodaivoda, Khoroshun, Nazarenko, & Vyzhva, 2000). In general case this method allows calculating a complete elasticity tensor. There are many references to measurements of mineral elastic properties under high pressure and temperature conditions (Anderson, Isaak, & Oda, 1992). But mainly the bulk and shear modulus derivatives are measured. As a result, an isotropic approach is used in practice.

In isotropic case we calculate effective bulk (K) and shear (G) modulus using hydrostatic pressure P, temperature T and correspondent derivatives. Grain orientation function is appropriated spherical, shape set to isometric. Exception could be made for shape of pores due to their significant influence on elasticity (Prodaivoda, Maslov & Prodaivoda, 2003).

Density value of model's cells is calculated from the same composite poly-mineral model as used for estimating of elastic modulus. In density calculation algorithm we include influence of compression due to hydrostatic pressure (using previously calculated bulk module K) and expansion due to heating (calculating previously thermo-expansion module which also related to pressure and temperature). For velocity calculation we use a well-known Green-Christoffel equation.

It is clear that each modeled cell should represent a mix of different rocks. Forward gravity modeling is based on integration of anomalous gravity effect from prismatic cells of a grid defined on the velocity model. Estimation of normal values of density and gravity for anomaly calculation depends on the method of gravity data processing. In the present study the curvature of the Earth's geoid is not taken into consideration, but generally, the latter should be taken into account in large areas. Cell size might be selected depending on seismic wave length. Also temperature and pressure conditions might be evaluated for each cell. Generally, it would be desirable to include a thermometry task into the calculation algorithm. We are still working in this direction, but at the moment we follow the results of depth pressure and temperature distribution obtained by other authors.

### **3. Inversion methodology. Task resolved, data and results**

We use decompositional least-square method (LMS) to estimate misfit between measured and calculated values of velocity and anomalous gravity. If the thermometry task is included into the inversion algorithm, then the LMS regression equation would have a third summand (square of heat flow density difference) in the right part. Minimization of the misfit is achieved by optimization of mineralogical parameter vector consisting of volume concentration of minerals, porosity and pores shape (Figure 1). Solution is restricted by some physical and geological constraints, mainly concerning mineral concentration. In the future it would be interesting to develop a mineral paragenesis control tool, which can limit solution region additionally. Our inversion algorithm has been realized as the Windows application including several methods of non-linear global and local optimization. To create a priori model and inverse problem job setting we integrate a local database into application.

As a result of forward modeling we gain geometrically matched models of P- and S-waves, density and temperature distribution. As an inversion result, we obtain distribution of main rock-forming minerals and porosity parameters. To reduce uncertainty it is reasonable to include results of gravity and heat flow surveys into inversion. For lithosphere modeling we usually use the following set of components, representing minerals and mineral groups:

quartz, albite and anorthite independently (its ratio allow to estimate plagioclase number), feldspar (representing mix of orthoclase and microcline), biotite, amphibole group (average composition), monopyroxene group (average composition), orthopyroxene group (average composition), olivine (average composition), garnet group (average composition). Additionally we use porosity (crack) component with properties depended on filling fluid (melt also possible).

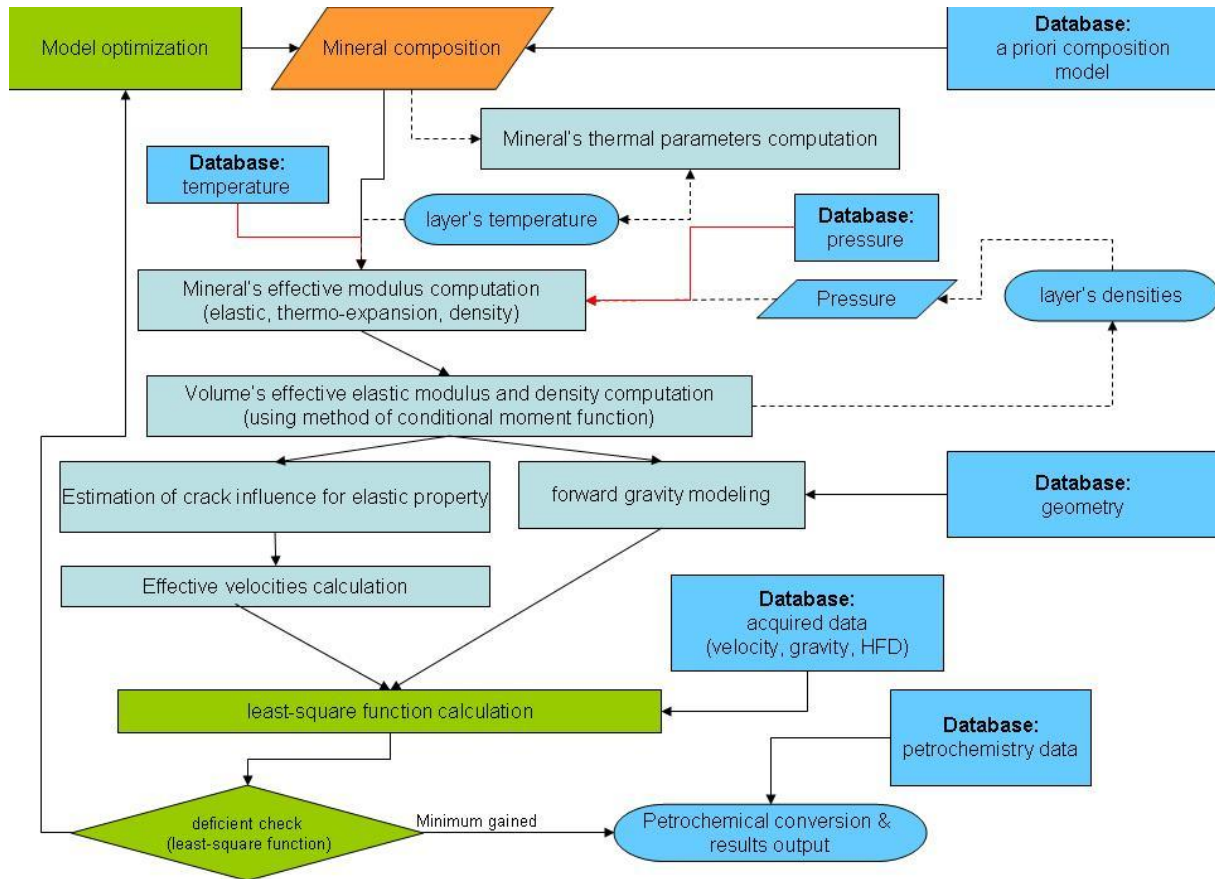


**Figure 1.** Principal scheme of the computation algorithm. Solid lines correspond to present procedure, dashed line will be realized soon.

The database consists of estimated (usually averaged) chemical composition of minerals. It allows to calculate model of main petrochemical oxides set and petrochemical classification factors. Huge dataset of petrochemical data (has been compiled for the Ukrainian shield (Prodaivoda, Zinchenko & Kozionova., 2005). It can be used partially (with correction) for Fennoscandia region. We try to interpret velocity models results proceeded by DSS profile in Finland (FENNIA Working Group, 1998; Grad & Luosto, 1994; Luosto, U., et al., 1989). For these profiles there exists a large amount of complementary high-quality geophysical and geological data. This makes it possible to compare our results of geological interpretation with previously published models (Janik, Kozlovskaya, Heikkinen, Yliniemi, & Silvennoinen, 2009; Janik et al., 2007; Silvennoinen & Kozlovskaya, 2010).

#### 4. Conclusion and discussion

Our inverse problem is ill-posed, like any other inverse problem in geophysics. As a result, we gain a set of equivalent solutions. However, if one has several independently acquired datasets

(for example, P- and S-wave velocities) then the solution region get narrow. Additionally, this region is cut by geological restrictions. Surely the optimization process met some difficulties in the vicinity of the restriction edge. As our experience has shown, these difficulties could be minimized by proper selection of geologically correct a priori model. We suggest that we can use generalized models of Earth's crust or mantle converted to mineralogical composition, if necessary. If good geological mapping results exist, it is recommended to modify composition for uppermost layers of the model. In our opinion, the method is developed just for numerical checking how any geological hypothesis is relevant to acquired surveys data.

The next aim of this method will be joint inversion of experimental travel times data with gravity and heat flow data. This would reduce uncertainty in velocity obtained from inversion of travel time data.

### Acknowledgments:

This work is associated to agreement between National Taras Shevchenko University of Kyiv and Sodankyla Geophysical Observatory, University of Oulu. We thank Ritta Hurskainen and Hanna Silvennoinen from Laboratory of Applied Seismology (Sodankyla Geophysical Observatory) for preparation of the data and glorious help. This work becomes feasible due to financial support of Ministry of Education and Science, Youth and Sport of Ukraine.

### References:

- Anderson, O., Isaak, D., & Oda, H. (1992). High-Temperature Elastic-Constant Data on Minerals Relevant to Geophysics. *Reviews of Geophysics*, 30(1), 57–90.
- Christensen, N. I., & Mooney, W. D. (1995). Seismic velocity structure and composition of the continental crust: A global view. *Journal of Geophysical Research*, 100(B6), 9761. doi:10.1029/95JB00259
- FENNIA Working Group (1998), P- and S-velocity structure of the Baltic Shield beneath the FENNIA profile in southern Finland, Rep. S-38, Univ. of Helsinki, Helsinki.
- Grad, M., and U. Luosto (1994), Seismic velocities and Q-factors in the uppermost crust beneath the SVEKA profile in Finland, *Tectonophysics*, 230, 1–18, doi:10.1016/0040-1951(94)90144-9.
- Janik, T., E. Kozlovskaya, P. Heikkinen, J. Yliniemi, and H. Silvennoinen (2009) Evidence for preservation of crustal root beneath the Proterozoic Lapland-Kola orogen (northern Fennoscandian shield) derived from P and S wave velocity models of POLAR and HUKKA wide-angle reflection and refraction profiles and FIRE4 reflection transect *J. Geophys. Res.*, 114, B06308, doi:10.1029/2008JB005689
- Janik, T., Kozlovskaya, E., & Yliniemi, J. (2007). Crust-mantle boundary in the central Fennoscandian shield: Constraints from wide-angle P and S wave velocity models and new results of reflection profiling in Finland. *Journal of Geophysical Research*, 112(B4), 1–28. doi:10.1029/2006JB004681
- Kozlovskaya, E., S. Elo, S.-E. Hjelt, J. Yliniemi, M. Pirrtijärvi and SVEKALAPKO STWG (2004) 3D density model of the crust of southern and central Finland obtained from joint interpretation of SVEKALAPKO crustal P-wave velocity model and gravity data. *Geoph. J. Int.*, 158, 827–848.
- Luosto, U., et al. (1989), The crustal structure along the POLAR Profile from seismic refraction investigation, *Tectonophysics*, 162, 51–85, doi:10.1016/0040-1951(89)90356-9
- Maslov B.P., Prodaivoda G.T. (1998) Dispersion and scatter of elastic waves in a jointed geological medium // *Geophysycal Journal (Ukraine)*, 18 (32), 303-316. (in Russian)
- Prodaivoda, G. T., Khoroshun, L. P., Nazarenko, L. V., & Vyzhva, S. A. (2000). Mathematical modeling of the azimuthal anisotropy in thermoelastic properties of the oceanic upper mantle. *Izvestiya Physics of the Solid Earth*, 36(5), 394–405.
- Prodaivoda G.T., Maslov B.P. & Prodaivoda T.G. (2003) Seismomineralogical model of uppermost mantle. *Physics of Earth*, 2, 3-14 (in Russian)
- Prodaivoda G., Zinchenko O., Kozionova O. (2005) Methodological principle of formation of main lithotypes database for determination Earth crust composition of north-west region of Ukrainian shield by seismogravitational method. *Vysnyk of Kyiv University. Geology*. 34, 11-18 (in Ukrainian)
- Silvennoinen, H., & Kozlovskaya, E. (2010). Upper Crustal Velocity and Density Models Along FIRE4 Profile ., *Geophysica*, 46(1-2), 21–46.

## Feeding the ‘aneurysm’: Orogen-parallel mass transport into Nanga Parbat and the western Himalayan syntaxis

D. M. Whipp, Jr.<sup>1,2</sup>, C. Beaumont<sup>1</sup> and J. Braun<sup>2</sup>

<sup>1</sup>Department of Oceanography, Dalhousie University, Halifax, NS, Canada

<sup>2</sup>ISTerre, Université Joseph Fourier de Grenoble, Grenoble, France

E-mail: dwhipp [at] dal.ca

Extreme rates of Plio-Quaternary erosional exhumation of the western Himalayan syntaxis region require a local crustal mass flux exceeding that found elsewhere in the Himalaya. 3D mechanical models of a generic oblique convergent orogen with a syntaxis demonstrate strain partitioning across the thrust front, which can provide an orogen-parallel mass flux into the syntaxis region that compensates very rapid exhumation.

**Keywords:** strain partitioning, geodynamic modelling, obliquely convergent orogens, Himalayas, Tibetan Plateau

### 1. Introduction

Mountain peak elevations of the Nanga Parbat-Haramosh massif (NPHM) in the western Himalayan syntaxis region are comparable to elsewhere in the Himalaya, but Plio-Quaternary rock exhumation rates are ~2-3 times faster than those from the central Himalaya (~3-13 vs. ~1-5 mm/a; Whittington, 1996; Whipp et al., 2007; Crowley et al., 2009; Herman et al., 2010). This disparity suggests an additional crustal mass flux into base of the NPHM is required to balance extreme rates of erosional exhumation. The ‘tectonic aneurysm’ model (Zeitler et al., 2001) can account for the localized nature of this upward flow of rock, but lacks quantitative constraints on the source of this excess mass flux. One potential source of crustal mass is orogen-parallel mass transport owing to strain partitioning across the range-bounding thrusts, which results in orogen-parallel shortening and crustal thickening in the syntaxis region (Figure 1a; McCaffrey and Nabelek, 1998; Seeber and Pecher, 1998). When strain is partitioned, the orogen-normal and orogen-parallel components of convergence are accommodated by separate thrust and strike-slip shear zones rather than by a single oblique thrust (e.g., Fitch, 1972). The partitioning behaviour is thought to be controlled primarily by the convergence obliquity angle,  $\gamma$  (Figure 1a), and the respective strengths of the thrust and strike-slip shear zones bounding the orogenic wedge {e.g., McCaffrey:1992ja}. If rock cohesion is negligible, the strength of the shear zones in the frictional plastic rheology often used for modelling crustal rock deformation is controlled by the respective angles of internal friction,  $\phi$ , of the basal thrust and rear strike-slip shear zones. We present 3D mechanical models of an obliquely convergent orogen with a syntaxis to explore the rheological controls on strain partitioning and whether translation of the orogenic wedge into the syntaxes can supply the additional crustal mass flux required to compensate extreme erosional exhumation rates and sustain high topography.

### 2. Numerical model design

We simulate strain partitioning and the resulting orogen-parallel mass transport using a 3D mechanical model of a generic oblique convergent orogen with a central oblique segment bounded by two regions of orogen-normal convergence. The model is designed to simulate a mature orogen, where crustal thickening has led to the formation of a plateau underlain by a low-viscosity ( $10^{19}$  Pa s) mid-lower crust and a neighbouring orogenic wedge. The orogenic

wedge geometry is defined by weak zones at the base and rear of the wedge. Deformation within the model is driven by velocity boundary conditions that provide an influx of mass to the orogen at a fixed rate (20 mm/a). The within the oblique segment, the orogen topography and defined weak zones are oblique to the mass influx direction, producing oblique convergence at an angle of  $\gamma=45^\circ$ . The influx of mantle lithosphere along the lateral margin of the model is balanced by a subduction outflux, leading to crustal thickening.

Strain partitioning behaviour and the magnitude of orogen-parallel mass transport are explored by varying the strength of the weak zone at the rear of the orogenic wedge, and the strength of the wedge itself. Crustal materials, other than the viscous region beneath the plateau, use a Mohr-Coulomb frictional plastic rheology with cohesion of 1 MPa. The basal shear zone is weak ( $\phi_b=2.5^\circ$ ) and dips at  $10^\circ$ . The respective ranges of the angles of internal friction for the near-vertical rear shear zone and wedge are  $\phi_r=2-5^\circ$  and  $\phi_w=15-5^\circ$ . Reduction of the strength of the rear shear zone and orogenic wedge is simulated via strain rate softening, where the angle of internal friction is linearly reduced over a defined strain rate range. Elsewhere the crust has a constant angle of internal friction of  $\phi_c=15^\circ$ , equivalent to conditions under which the crustal strength has been reduced by pore fluid pressure.

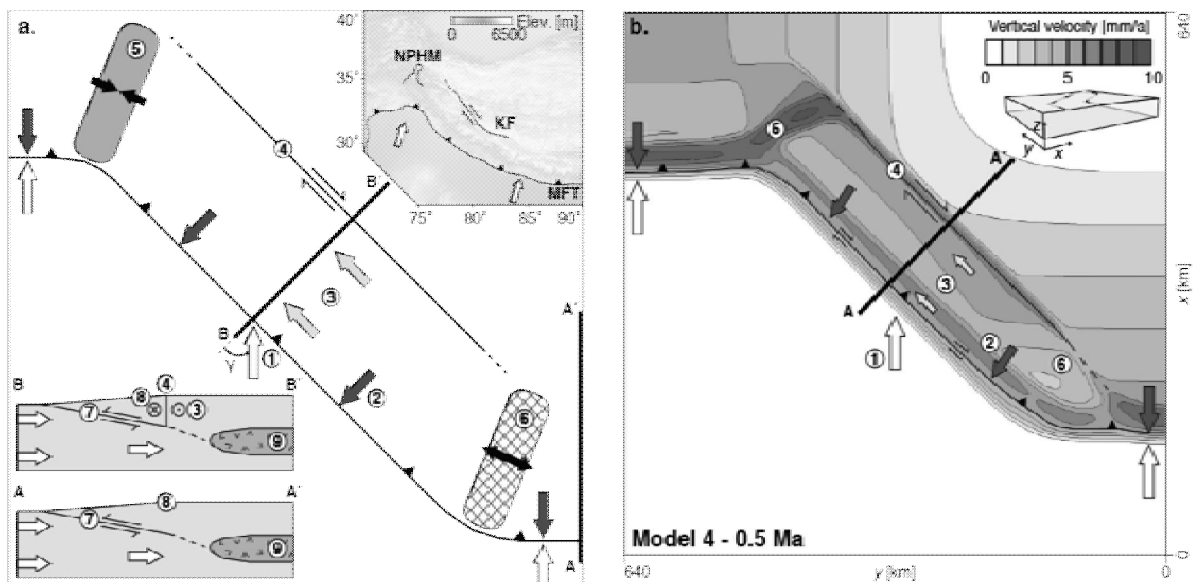


**Figure 1.** (a) Common features of an oblique convergent orogen with a syntaxis. In planform, features include: (1) Obliquity,  $\gamma$ , between the normal to the orogen-bounding structure and the convergence direction (white arrows), (2) orogen-normal (ON) thrust vergence (large dark gray arrows), (3) orogen-parallel (OP) mass transport owing to strain partitioning where convergence is oblique (light gray arrows), (4) a strike-slip structure at the rear of the orogenic wedge, (5) a shortening structure in the syntaxis region (gray region), and (6) a region accommodating OP extension (crosshatched region). Lower inset: Common features of a large orogen with neighboring plateau include (7) a shallowly dipping basal detachment ( $\sim 10^\circ$ ), (8) topography of an orogenic wedge topography and adjacent plateau, and (9) a region of weak, viscous middle-to-lower crust. Upper inset: Topography of the western Himalaya, Tibetan Plateau and Pamirs with major tectonic features and approximate Indian plate motion vectors (white arrows). KF: Karakoram fault, MFT: Main Frontal thrust, and NPHM: Nanga Parbat-Haramosh massif. (b) Surface uplift rates (background contours) and major features of Model 5 after 0.5 Ma. OP mass transport leads to uplift within the model syntaxis region at rates comparable to the NPHM.

### 3. Model results

We find that the partitioning behaviour is strongly controlled by the strength of the rear shear zone and strain rate softening of the orogenic wedge localizes uplift within the model syntaxis region. With  $\phi_r=5^\circ$  and no strain rate softening, a critical orogenic wedge develops with underplating and accretion of the incoming crust. In this case, however, the angle of internal friction on the rear shear zone is relatively high, preventing significant strain partitioning and orogen-parallel mass transport. Reducing  $\phi_r$  to  $2^\circ$  produces clear strain partitioning and with a lateral translation velocity of the wedge of 5-6 mm/a toward the model syntaxis. This crustal flux into the syntaxis region, however, produces distributed shortening and uplift within the syntaxis region due to the relative strength of the orogenic wedge ( $\phi_w=15^\circ$ ). With strain rate softening of the orogenic wedge,  $\phi_w$  is reduced from  $15^\circ$  to  $5^\circ$  in zones of high strain rate ( $>10^{-15} \text{ s}^{-1}$ ), facilitating formation of a shortening structure in the syntaxis region that produces localized uplift rates of  $\sim 10$  mm/a (5 in Figure 1b).

### 4. Implications and conclusions

We find that the model behaviour is quite sensitive to the strength of the defined weak zones bounding the wedge and the wedge material itself. Increasing the basal shear zone angle of friction from  $\phi_b=2.5^\circ$  leads to shortening on the rear shear zone, whereas decreasing  $\phi_b$  fails to transmit the orogen-parallel stresses from the basal shear zone to the rear. Likewise, if  $\phi_r=5^\circ$ , strain will not be partitioned, while decreasing  $\phi_r$  to  $<2^\circ$  leads again to shortening on the rear shear zone. In addition, uplift does not tend to be localized unless the orogenic wedge can dynamically weaken itself via strain rate softening.

Although the model geometry is only an approximation of the Himalaya and adjacent Tibetan plateau, the models produce comparable structural geometries and uplift patterns. Thrust vergence on the basal fault is generally orogen-normal similar to the pattern of slip vectors derived from earthquake focal mechanisms along the Himalayan front {Molnar:1989hk}, and the dextral slip on the rear shear zone and across the orogenic wedge is similar to the Karakoram fault system and segmented dextral faults crossing the wedge near the central Himalaya (Figure 1b; Taylor and Yin, 2009). In addition, the mass flux from strain partitioning can locally increase rates crustal uplift by a factor of  $\sim 2$ -3, producing local uplift rates of  $\sim 10$  mm/a, compared to average rates of 2-4 mm/a in most of the orogenic wedge (Figure 1b). The similarity of these rates to the Plio-Quaternary rates of exhumation from both the NPHM and central Himalaya (Whittington, 1996; Whipp et al., 2007; Crowley et al., 2009; Herman et al., 2010) suggests the additional orogen-parallel mass flux resulting from strain partitioning in an oblique convergent orogen with a syntaxis can compensate rapid surface erosion and exhumation.

### References:

- Crowley, J., Waters, D., Searle, M., Bowring, S., 2009. Pleistocene melting and rapid exhumation of the Nanga Parbat massif, Pakistan: Age and P-T conditions of accessory mineral growth in migmatite and leucogranite. *Earth and Planetary Science Letters* 288, 408–420.
- Fitch, T., 1972. Plate Convergence, Transcurrent Faults, and Internal Deformation Adjacent to Southeast Asia and the Western Pacific. *Journal of Geophysical Research* 77, 4432–4460.
- Herman, F., Copeland, P., Avouac, J.-P., Bollinger, L., Mahéo, G., Le Fort, P., Rai, S., Foster, D., Pecher, A., Stüwe, K., Henry, P., 2010. Exhumation, crustal deformation, and thermal structure of the Nepal Himalaya derived from the inversion of thermochronological and thermobarometric data and modeling of the topography. *Journal of Geophysical Research, B, Solid Earth and Planets* 115, B06407.
- McCaffrey, R., 1992. Oblique Plate Convergence, Slip Vectors, and Forearc Deformation. *Journal of Geophysical Research, B, Solid Earth* 97, 8905–8915.
- McCaffrey, R., Nabelek, J., 1998. Role of oblique convergence in the active deformation of the Himalayas and

- 
- southern Tibet plateau. *Geology* 26, 691–694.
- Molnar, P., Lyon-Caen, H., 1989. Fault plane solutions of earthquakes and active tectonics of the Tibetan Plateau and its margins. *Geophysical Journal International* 99, 123–154.
- Seeber, L., Pecher, A., 1998. Strain partitioning along the Himalayan Arc and the Nanga Parbat Antiform. *Geology* 26, 791–794.
- Taylor, M., Yin, A., 2009. Active structures of the Himalayan-Tibetan orogen and their relationships to earthquake distribution, contemporary strain field, and Cenozoic volcanism. *Geosphere* 5, 199–214.
- Whipp, D.M., Jr, Ehlers, T.A., Blythe, A.E., Huntington, K.W., Hodges, K.V., Burbank, D.W., 2007. Plio-Quaternary exhumation history of the central Nepalese Himalaya: 2. Thermo-kinematic and thermochronometer age prediction model. *Tectonics* 26.
- Whittington, A., 1996. Exhumation overrated at Nanga Parbat, northern Pakistan. *Tectonophysics* 260, 215–226.
- Zeitler, P., Meltzer, A., Koons, P., Craw, D., Hallet, B., Chamberlain, C., Kidd, W., Park, S., Seeber, L., Bishop, M., others, 2001. Erosion, Himalayan Geodynamics, and the Geomorphology of Metamorphism. *GSA Today* 11, 4–9.